Diarylethene derivatives and their applications

Salen derivatives in molecular recognition

Dissertation

Zur Erlangung des Doktorgrades der Naturwissenschaften
(Dr. rer. nat.)
an der Fakultät für Chemie und Pharmazie
der Universität Regensburg

vorgelegt von
Daniel Vomasta
aus Regensburg
2009

Diarylethene derivatives and their applications

Salen derivatives in molecular recognition

Dissertation

Zur Erlangung des Doktorgrades der Naturwissenschaften
(Dr. rer. nat.)
an der Fakultät für Chemie und Pharmazie
der Universität Regensburg

vorgelegt von

Daniel Vomasta

aus Regensburg

2009

The experimental part of this work was carried out between October 2005 and December 2008 at the Institute for Organic Chemistry at the University of Regensburg under the supervision of Prof. Dr. B. König.

The PhD – thesis was submitted on:	30. January 2009
The colloquium took place on:	23.02.2009

Board of Examiners:	Prof. Dr. F.-M. Matysik	(Chairman)
	Prof. Dr. B. König	(1st Referee)
	Prof. Dr. H.-A. Wagenknecht	(2nd Referee)
	Prof. Dr. S. Elz	(Examiner)

Danksagung

Mein besonderer Dank gilt Herrn Prof. Dr. B. König für die Überlassung des überaus interessanten und vielseitigen Themas, sowie für die Förderung und die mit Anregungen und Diskussionen verbundene Unterstützung dieser Arbeit.

Für die Möglichkeit eines dreimonatigen Aufenthaltes an der Simon Fraser University (SFU) in Vancouver/Kanada bedanke ich mich bei Dr. Neil R. Branda, sowie für seine Unterstützung und Tipps. Ein besonderer Dank gilt hierbei allen Mitgliedern dieses Arbeitskreises für die Unterstützung, die gute Zusammenarbeit in sehr freundschaftlicher Arbeitsatmosphäre. Spezieller Dank geht auch and Muriel und Fred, die mir Untermiete gewährten und viele kulinarische Abende.

Den Mitarbeitern der Zentralen Analytik der Fakultät für Chemie und Pharmazie danke ich für die schnelle und gewissenhafte Durchführung der analytischen Messungen. Insbesondere Herrn Dr. T. Burgemeister, Herrn F. Kastner, Frau N. Pustet, Frau A. Schramm und Frau G. Stühler für die Aufnahme der NMR-Spektren, ebenso wie Herrn J. Kiermaier und Herrn W. Söllner für die Messung und Auswertung der Massenspektren.

Des Weiteren danke ich dem Arbeitskreis von Prof. Dr. O. Reiser für die Möglichkeit der Benutzung des IR-Spektrometers.

Für die gute Zusammenarbeit im Rahmen gemeinsamer Forschungsprojekte danke ich Herrn Dr. Claudiu Supuran und Alession Innocenti (Universität von Florenz).

Allen aktuellen wie ehemaligen Mitarbeitern des Lehrstuhls danke ich für die gute Zusammenarbeit und das sehr angenehme Arbeitsklima – vor und nach Feierabend. Besonderer Dank gilt dabei:

Stefan (Toni) Stadlbauer und Michael Egger für unvergessliche Abende nach Feierabend innerhalb und außerhalb der Universität, sowie für die zahlreichen Diskussion.

Meinem Laborkollegen Florian Ilgen danke ich für unzählige magische Momente („zieh mal eine Karte“), die super Atmosphäre im Labor und die vielen Diskussionen, sowie für den Weimarer Aufenthalt.

Harald Schmaderer für die unzähligen Lauftreffs/Badminton-Matches und die lustigen Abende im Kölner Nachtleben bei einer gemeinsamen Tagung.

Dr. Stefan Ritter für die sehr entspannende und lustige Zeit in Bad Hofgastein sowie seiner Zwiebelkuchen-abende.

Florian Sahr und Ina Rosnizeck für amüsante kulinarische Abende außerhalb der Universität.

Dr. Giovanni Imperato danke ich für Rat und Tat bei Fragen und für die Unterstützung.

Dr. Michael Kruppa danke ich für die Unterstützung während des Studiums und der Diplomarbeit.

Herzlicher Dank geht an Stefan Stadlbauer und Michael Egger für das Korrekturlesen dieser Arbeit.

Herrn Dr. W. Braig, Frau Dr. C. Braig, Frau E. Liebl, Frau S. Graetz, Simone Strauß, Ernst Lautenschlager und Herrn Dr. R. Vasold und Frau Dr. C. Wanninger-Weiss danke ich für ihre Unterstützung.

Meinem sehr guten Freund Stephan Rauner für die Unterstützung und die unzähligen gemeinsamen Abende.

Mein persönlicher großer Dank gilt meiner Verlobten Eva für ihre Liebe, ihre Unterstützung und ihr Verständnis zu jeder Zeit. Ebenso danke ich ihrer Familie, die mir ein zweites Zuhause bot.

Zuletzt, aber vor allem, danke ich meiner Familie für ihre großartige Unterstützung, ihre Aufmunterungen und den großen Rückhalt während meines gesamten Studiums.

Wer nichts als die Chemie versteht, versteht auch die nicht recht.

Georg Christoph Lichtenberg
(dt. Schriftsteller, Künstler und Physiker)

Für Eva und

meine Familie

Table of Contents

I. GENERAL INTRODUCTION - DIARYLETHENES FOR PHOTOCHROMISM 10

I.1 History 10

I.2 Photochromic Molecular Switches 10

I.3 Light as a Stimulus[7] 13

I.4 Dithienylethenes 14

I.5 Quantum Yield and Photostationary State[7] 16

I.6 References 17

II. REGULATION OF HUMAN CARBONIC ANHYDRASE I (HCAI) ACTIVITY BY USING A PHOTOCHROMIC INHIBITOR 20

II.1 Introduction 20

II.2 Results and discussion 22

II.3 Conclusion 30

II.4 References 31

II.5 Supporting information 33

III. CARBONIC ANHYDRASE INHIBITORS: TWO-PRONG VERSUS MONO-PRONG INHIBITORS OF ISOFORMS I, II, IX, XII AND XIV EXEMPLIFIED BY PHOTOCHROMIC 1,2-DITHIENYLETHENE DERIVATIVES 53

III.1 Introduction 54

III.2 Results and discussion 56

III.3 Conclusion 61

III.4 References and notes 62

IV. BINDING OF PHOSPHATES USING A PHOTOCHROMIC BIS-ZN(II)-CYCLEN DERIVATIVE 66

IV.1 Introduction 66

IV.2 Results and discussion 67
IV.3 Conclusion 80
IV.4 Experimental Part 82
IV.5 References 107

V. BIS-INDOLYLETHENE - REVISITED 110

V.1. Introduction 110
V.2 Results and discussion 112
V.3 Conclusion 124
V.4 Experimental Part 125
V.5 References 130

VI. SALEN METAL COMPLEXES AND THEIR USE IN AMINO ACID RECOGNITION 133

VI.1 Introduction 133
VI.2 Results and disucussion 135
VI.3 Conclusion 150
VI.4 Experimental Part 152
VI.5 References 157

VII. SUMMARY 159

VIII. ABBREVIATIONS 161

XI. APPENDIX 163

I. General introduction - Diarylethenes for Photochromism

I.1 History

Probably, *Alexander the Great* (356 – 323 B. C.) used already colour changes of a photochromic dye to coordinate his troop attacks.[1] His macedonian warriors used wristbands treated with an unknown photochromic dye. Upon appropriate irradiation of the sunlight colour changes occurred, telling the troops the right time of attack.[2]

The term photochromism was introduced by *Hirshberg* in 1950.[3] However, *TerMeer* described this effect already in the year 1876. Since then photochromism was observed in a couple of organic and inorganic compounds.

I.2 Photochromic Molecular Switches

Molecular switches are defined as compounds that can be toggled between two isomers **A** and **B** (Figure 11) by an external stimulus.[5] Each isomer shows particular properties such as absorption spectra and emission. The used stimuli that trigger the toggling of the compound can be light, heat, electrons, and chemical reagents. Photochromism is described by the reversible conversion between two isomers having different absorption spectra. Therefore, the electrocyclization (switching) process can be followed by UV-VIS absorption spectroscopy. An example of the absorption spectra of a typical isomerization process between isomers **A** and **B** is shown in Figure **1**. As isomer **A** is irradiated in the UV region ($h\nu_1$), a new band is generated in the visible region as isomer **B** is originated. Cyclization back to **A** is accomplished by irradiating **B** with visible light ($h\nu_2$). During the isomerization process an isosbestic points should evolve to indicate that the photoisomerization is a clean process that means without degradation or formation of side products takes place. Separated absorption maxima allow addressing each isomer independently.

Irradiation with the appropriate wavelength will only affect one isomer. For example, if both isomers absorb within the energy range $h\nu_1$, stimulation of isomerisation of **A -> B** and **B -> A** can result. The transfer to the ring-closed isomer **B** is not complete; instead, **A** (ring-open) and **B** (ring-closed) are in a equilibrium (called the photostationary state).[6]

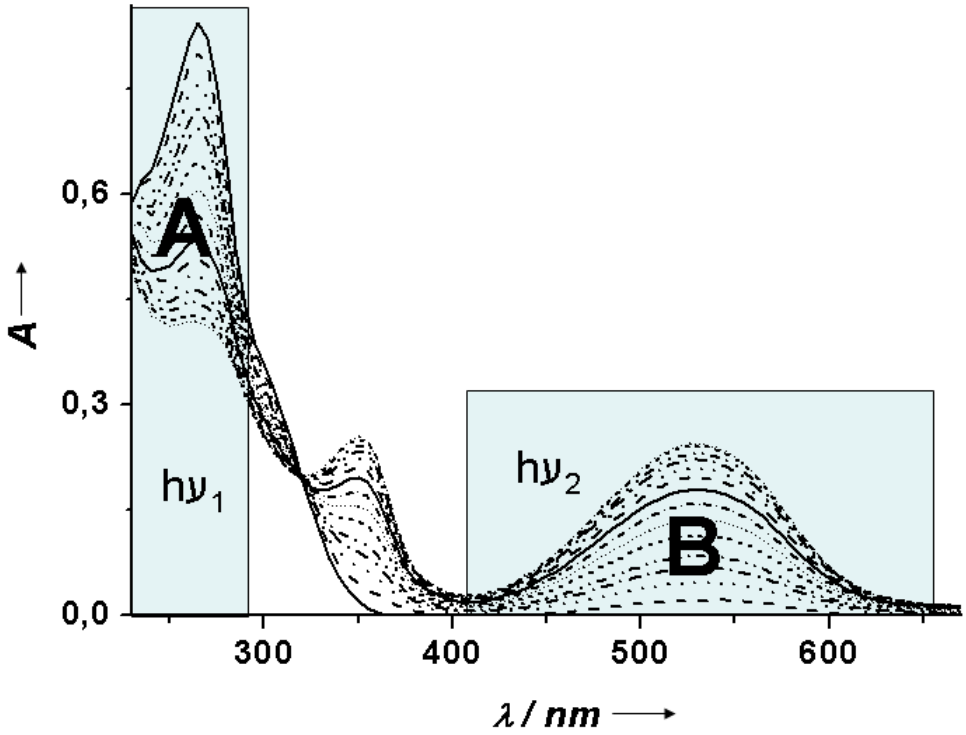

Figure 1. UV-Vis absorption spectra of a typical photoisomerization reaction between differently coloured isomers **A** and **B**.[6]

The ability to control the physical properties of molecular switches makes them appealing candidates for the use in a range of applications such as filters, sensors, information storage and medicinal chemistry. In particular, eyewears varying between dark and light lenses in response to changing light conditions are constructed from photoresponsive compounds or they are used to control biological systems by external stimuli. It has to be taken into account that according to the application, several specific properties are often necessary. For example, it is critical that a given system is able to interconvert between its isomers many times without significant degradation (fatigue resistance), which is important for the use as a device. Also, it is desirable that the photostationary

state is quantitative. It is also considered desirable for photoresponsive compounds to exhibit thermal stability of each form (bistability).[6, 7]

During the photoisomerization process sigma and pi bonds are formed or broken. If the isomerization process involves aromatic pi systems that are present in one isomer and destroyed in the other, a driving force for the thermal back reaction is created (as defined by the aromatic stabilization energy). From the different aromatic and heteroaromatic systems shown in Figure 2, thiophene having the smallest aromatic stabilization energy leads to the most thermally stable photochromic diarylethenes.

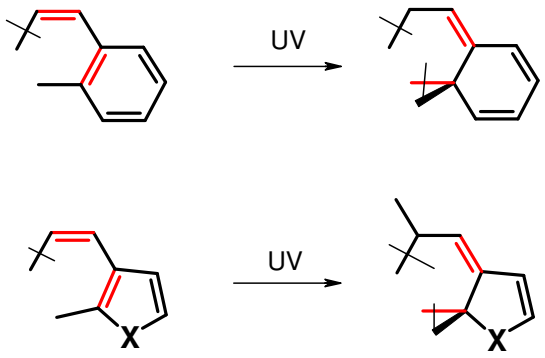

group	energy (kcal/mol)
phenyl	27.7
pyrrolyl	13.8
furyl	9.1
thienyl	4.7

Figure 2. Aromatic stabilization energies of different aryls.[4]

I.3 Light as a Stimulus[7]

Photons are a suitable stimulus for isomerization because modern lasers can be used to achieve fast response times and focus a fine-tuned light stimulus of a specific wavelength on small localized areas, e.g. in a film, without significant diffusion.[8] The alternations in the electronic structure of the molecules that are responsible for the dramatic changes in colour can also result in variations of other useful physical properties such as luminescence,[9] electrical conductance,[10] refractive index,[11] optical rotation[12] and conformation.[13] The photo-modulation of these properties has the potential to significantly positively influence optoelectronic technologies such as waveguides,[14] influencing biological actions [14] and read/write/erase optical information storage systems.[10a, 11c]

I.4 Dithienylethenes

A large number of photochromic compounds are known including azobenzenes, spiropyrans, dihydropyrans, fulgides, spirooxazines and dithienylethenes. The huge majority of these photoresponsive molecular switches are limited by their thermal stability of the electrocyclization reactions, and the difficulties during synthesis of functionalized derivatives.[5, 6, 8]

Dithienylethenes (DTEs) constitute a class of molecular switches that exhibit stability in the open and the closed isomer (bistability), high fatigue resistance and easy synthetic access. Due to these properties, DTEs have been the in the focues academic and industrial research. Dithienylethenes can be switched between the ring-open (**A**) and the ring-closed isomer (**B**) isomers, as shown in Scheme 1. The ring-open isomer is colourless, and exhibit rotation around two sigma bonds (connecting the central ring with the heterocycles) making it flexible. Irradiation of the open form with UV-light induces a conrotatory electrocyclization to the ring-closing isomer, generating a conjugation which gives the molecule its colour and is influenced the R substituents (Scheme 1). As the closed isomer is cyclized, it is more rigid than the open version. The DTE architecture contains few positions that can be changed, the easiest being the R substituent on each thiophene.[6]

For combination with biology the photoresponsive dithienylethene exhibits several attractive features. They display fatigue resistance and high quantum yields compared to other photoresponsive compounds. Secondly, many of these properties can be tuned by synthetic variation of the thiophene substituents, often without any loss of performance. Therefore these systems can be functionalized for either hydrophobic or hydrophilic conditions making them suitable for the biological environment. The small scaffold size relative to biological macromolecules such as nucleic acids and proteins allows use of these in such systems.[6]

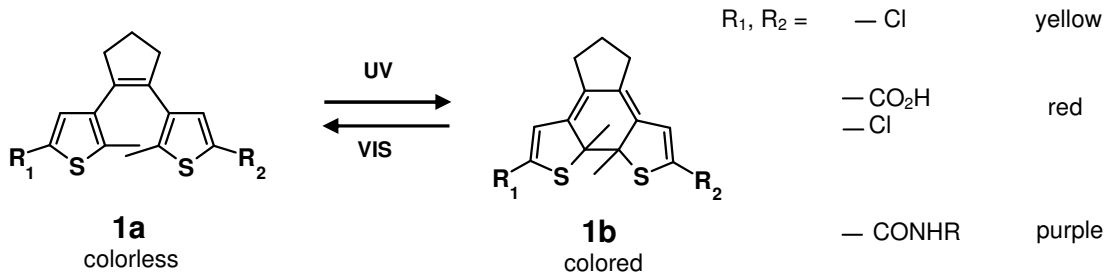

Figure 3. Photochemical reactions of the dithienylethene (DTE) architecture. The absorption properties attainable in the ring-closed forms **1b** can be fine-tuned by modifying the groups R_1 and R_2 at the ends of the π-conjugated backbone.[15]

I.5 Quantum Yield and Photostationary State[7]

For photochromic performance of DTEs two quantities should be known. The first is the quantum yield (Φ) which gives information about the efficiency of the electrocyclization reactions. It is defined as the ratio of the number of mcyclized olecules to the total number of absorbed photons.[16]

$$\Phi = \frac{\text{molecules that cyclize}}{\text{absorbed photons}}$$

$$PSS = \frac{\text{molecules that cyclize}}{\text{total number of molecules}} \text{ x } 100\%$$

Equation 1. Quantum yield and photostationary state.

The second quantity is the photostationary state (PSS), which describes the percentage of ring-open molecules that are converted to the ring-closed isomer.[16]

I.6 References

(1) Dessauer, R.; Paris, J. P. *Adv. Photchem.* **1963**, *1*, 275-278.

(2) Wöhrle, D; Tausch, M. W.; Stroher, W.-D. in: *Photochemie,* Wiley-VCH: Weinheim, 1998.

(3) Hirshberg, Y. *Comptes Rendus de l´Academie des Sciences*, **1950**, *231*, 903-904.

(4) Irie, M. *Chem. Rev.* **2000**, *100*, 1685-1716.

(5) Feringa, B.L. (editor). **2001**. Molecular Switches. Wiley-VCH, Weinheim.

(6) Master thesis of Kelly Elizabeth Chapple Cadieux, Simon Fraser University/ Vancouver (CA), **2001**.
http://ir.lib.sfu.ca/handle/1892/2317?mode=full

(7) Dissertation of Anthony James Wigglesworth, Simon Fraser University/ Vancouver (CA), **2006**.
http://ir.lib.sfu.ca/dspace/retrieve/2948/etd2257.pdf

(8) Organic Photochromic and Thermochromic Compounds; Crano, J. C., Guglielmetti, R. J., Eds.; Plenum Press: New York, **1999**; Vols. 1 and 2.

(9) (a) Matsuda, K.; Irie, M. J. *Photochem. Photobiol. C: Photochem. Rev.* **2004**, *5*, 170-182. (b) Tian, H.; Chen. B.; Tu, H.; Miillen, K. *Adv. Mater.* **2002**, *14*, 918-923. (c) Irie, M.; Fukaminato, T.; Sasaki, T.; Tamai, N.; Kawai, T. *Nature* **2002**, *420*, 759-760. (d) Norsten, T. B.; Branda, N. R. *J. Am. Chem. Soc.* **2001**, *123*, 1784-1785. (e) Norsten, T. B.; Branda, N. R. *Adv. Mater.* **2001**, *13*, 347-349.

(10) (a) Kawai, T.; Nakashima, Y.; Irie, M. *Adv. Mater.* **2005**, *17*, 309-314. (b) Li, J.; Speyer, G.; Sankey, 0. *Phys. Rev. Lett.* **2004**, *93*, 2483-2502 1 4 . (c) Guo, X.; Zhang, D.; Yu, G.; Wan, M.; Li, J.; Liu, Y.; Zhu, D. *Adv. Mater.* **2004**, *16*, 636-640. (d) Dulic, D.; Van der Molen, S . Kudernac, T.; Jonkrnan, H. T.; de Jong, J. J. D.; Bowden, T. N.; van Esch, J.; Fering,a, B. L. *Phys. Rev. Lett.* **2003**, *91*, 207402 1-4 . (e) Tsujioka, Y.; Hamada, K.; Shibata, K.; Taniguchi, A.; Fuyuki, T. *Appl. Phys. Lett.* **2001**, *78*, 2282-2284.

(11) (a) Bertarelli, C.; Bianco, A.; D'Amore, F.; Gallazzi, M. C.; Zerbi, G. *Adv. Funct. Mater.* **2004**, *14*, 357-363. (b) Kim,, M.-S.; Maruyama, H.; Kawai,

T.; Irie, M. *Chem. Mater.* **2003**, *15*, 4539-4543. (c) Kim, E.; Choi, Y.-K.; Lee, M.-H. *Macromolecules* **1999**, *32*, 4855-4860.

(12) (a) Wigglesworth, T. J.; Sud, D. Lekhi, V. S.; Norsten, T. B.; Branda, N. R. J. *Am. Chem. Soc.* **2005**, *127*, 7272-7273. (b) Kose, M.; Shinoura, M.; Yokoyama, Y.; Yokoyama, Y. *J. Org. Chem.* **2004**, *69*, 8403-8406. (c) de Jong, J. J. D.; Lucas, L. N.; Kellogg, R. M.; van Esch, J. H.; Feringa, B. L. *Science* **2004**, *304*, 278-301. (d) Yamamoto, S.; Matsuda, K.; Irie, M. *Org. Lett.* **2003**, *5*, 1769-1772. (e) Pieraccini, S.; Masiero, S.; Spada, G. P.; Golttarelli, G. *Chem. Commun.* **2003**, 598-599. *(f)* Murguly, E.; Norsten, T. B.; Brancla, N. R. *Angew. Chem. Int. Ed.* **2001**, *40*, 1752-1755.

(13) (a) Kang, J.-W.; Kim, J.-J.; Kim., E. *Appl. Phys. Lett.* **2002**, *80*, 1710-1713. (b)

Kang, J.-W.; Kim, J.-J.; Kim, E. *Optical Materials* **2002**, *21*, 543-548.

(14) Vomasta, D.; Högner, C.; Branda, N. R.; König, B. *Angew. Chem. Int. Ed.* **2008**, *47*, 7644.

(15) Lemieux, V.; Gauthier, S.; Branda, R. N. *Angew. Chem. Int. Ed.* **2006**, *45*, 6820-6824.

(16) (a) Irie, M. in Molecular Switches; Feringa, B. L., Ed.; Wiley-VCH: Weinheim, Germany, **2001**. pp 37-60. (b) Irie, M. in Organic Photochromic and Thermochromic Compounds; Crano, J. C., Guglielmetti, R. J., Eds.; Plenum Press: New York, **1999**; Vol. 1, pp 207-221. (c) Tian, H.; Yang, S. *Chem. Soc. Rev*. **2004**, *33*, 85-97. (d) Irie, M. *Chem. Rev*. **2000**,*100*, 1685-1716.

Regulation of Human Carbonic Anhydrase I (hCAI) Activity by Using a Photochromic Inhibitor[11]

This chapter deals with the use of photoresponsive 1, 2 dithienylethenes (DTE), decorated with a Cu(II)-ida complex and a sulphonamide, as an inhibitor for human carbonic anhydrase I. With the help of these molecules it is possible to influence biological actions, in this case enzyme activity, by light.

The knowledge of synthesis and handling of dithienylethenes was gained during a research stay at the Simon Fraser University (SFU) in Vancouver/Canada in the group of Prof. Dr. Neil Branda. The synthesis of the control compounds **7** and **8** was done by Christina Högner under the supervision of Daniel Vomasta (F-Praktikum). The synthesis of the other compounds as well as all the measurements was done by Daniel Vomasta.

[1] Vomasta, D.; Högner, C.; Branda, N.R.; König, B. *Angew. Chem.* **2008**, *120*, 7756-7759; *Angew. Chem., Int.Ed.Engl.* **2008**, *47*, 7644 – 7647

II. Regulation of Human Carbonic Anhydrase I (hCAI) Activity by Using a Photochromic Inhibitor

II.1 Introduction

The regulation of enzyme activity is crucial for the metabolism of every organism. In biology, enzymatic control is typically achieved through the use of allostery[1] or by covalently modifying the enzyme (by phosphorylation or dephosphorylation, for example).[2] Some of the origin attempts to artificially influence the activity of enzymes rely on chemical modifications of the enzyme structure,[3–6] an approach that is limited by the fact that the regulation is not reversible. The use of light as a stimulus offers a heightened level of control, and photoresponsive compounds would provide the reversibility needed for practical use. Existing examples of systems that take advantage of the beneficial properties of light include those that use azobenzene-based enzyme inhibitors[7] or use thiophenfulgide derivatives covalently linked to the enzyme's structure.[8] Photoinducing changes in the environment around the enzyme has also been used as a regulation mechanism by influencing the permeability of a photoisomerizable polymer containing the enzyme for the substrate, [8] by controlling the conformation of a specific domain of the enzyme with surfactants[9] and by changing the conditions of the medium (pH or viscosity, for example).[10]

Controlling the activity of carbonic anhydrase is of special interest as it is an enzyme central to both cellular transport and metabolic processes. It can be found in virtually every tissue and cell type, in many subcellular organelles, and in organisms ranging from unicellular cyanbacteria to mammals.[11] Recently, an azobenzene-based biolabel was used to photomodulate the activity of carbonic anhydrase (about twofold).[12] Although controlling enzyme activity with azobenzene derivatives is an elegant concept, the thermal reversibility that plagues these particular photoresponsive compounds significantly limits their use in practical applications. On the other hand, compounds constructed from the 1,2-dithienylethene (DTE) scaffold represent a significant improvement over most other photoresponsive structures,

primarily because they undergo thermally irreversible photochemical ring-closing and ring-opening reactions (see, for example, the substructures **1o** ⇆ **1c** in Scheme 1).[13]

In this communication, we describe how this versatile photoresponsive structure can be used to reversibly control the activity of carbonic anhydrase by decorating the DTE architecture with sulphonamide and copper(II)iminodiacetic acid (Cu•IDA) moieties. These two moieties were chosen in light of Mallik's recently reporting a significant increase in the activity of the weak enzyme inhibitor sulphanilamide (4-aminobenzenesulfonamide, **4**) when covalently combined with a Cu•IDA complex.[14]

II.2 Results and discussion

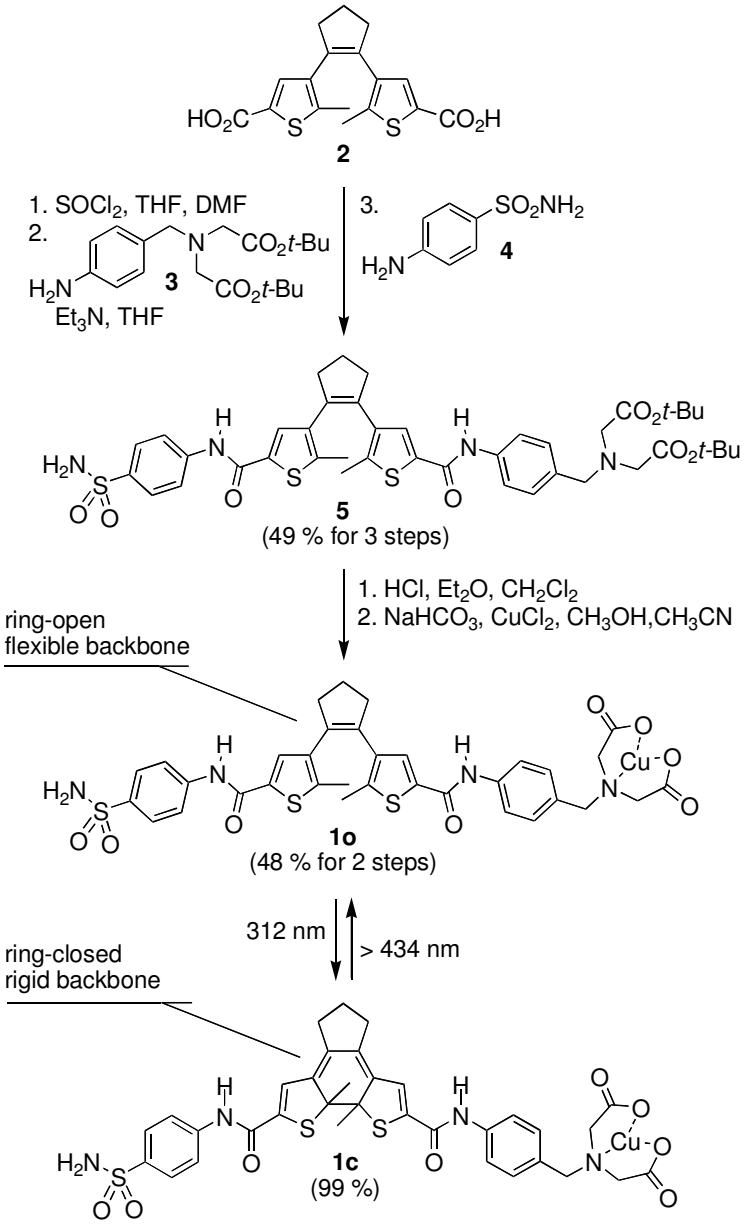

Scheme 1. Synthesis and the reversible photochemical ring-closing reaction of DTE inhibitor **1o**.

While the sulphonamide group in **1o** acts as the inhibitor, the role of the Cu•IDA component is to reversibly coordinate to the imidazole side-chains of the histidine amino acids exposed on the protein surface close to the Zn(II) active site of the enzyme and help dock the sulphonamide inhibitor group into the catalytic centre. Given the fact that the activity of any two-pronged enzyme inhibitor is directly dependent on the distance and relative orientation of the two groups (in this case, the Cu•IDA and the sulphonamide) and the fact that the DTE architecture can be toggled between a flexible, ring-open (**1o**) and rigid, ring-closed (**1c**) isomer,[15] we designed compound **1** to reversibly photoregulate enzyme activity without having to resort to chemical modifications or changes in the natural environment of the enzyme. How the structures of these two photoisomers affect carbonic anhydrase activity will be discussed in more detail after the results are presented.

The synthesis of compound **1o** is shown in Scheme 1[16] and starts by stepwise coupling the acid chloride of 1,2-bis(5-carboxy-2-methylthien-3-yl)cyclopentene **2**[17] with [(4-aminobenzyl)-*tert*-butoxycarbonylmethylamino]acetic acid tert-butyl ester (**3**) and sulphanilamide (**4**). After removing the two *tert*-butyl groups with acid, treatment with $CuCl_2$ under basic conditions affords the final compound, **1o** in good yield.

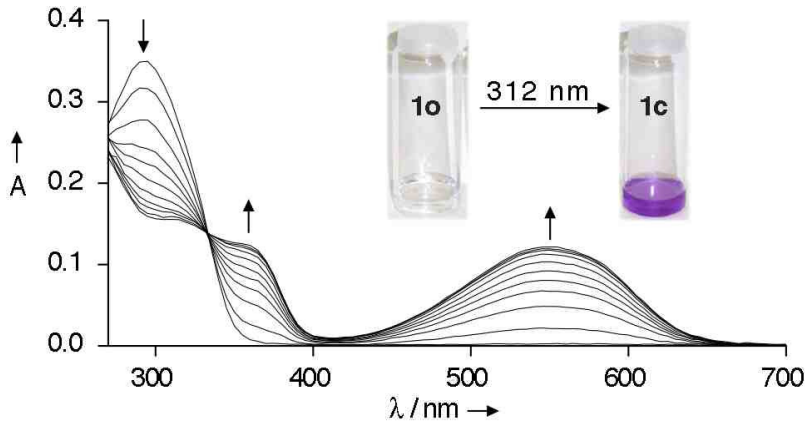

Figure 1. Changes in the UV–Vis absorption spectra of an aqueous DMSO (5 % v/v) solution (1.08×10^{-5} M) of **1o** when irradiated with 312 nm light. Irradiation periods are 0, 3, 5, 8, 10, 14, 17, 20 and 34 s. The solution also contains Tris sulphate buffer (20 mM, pH 8.3). The inset illustrates the change in colour of the solution from colourless to purple as the ring-closed isomer is generated.

Irradiating an aqueous 5% DMSO solution of **1o** (Tris sulphate buffer, 20 mM, pH = 8.3 at 25 °C) with 312 nm light[18] results in the immediate changes in the UV-Vis absorption spectra that are typical for photoresponsive DTE derivatives. The high-energy band (λ_{max} = 290 nm) decreases in intensity and an absorption band in the visible spectral region (λ_{max} = 545 nm) appears as the solution changes from colourless to purple due to the formation of the ring-closed isomer **1c** (a smaller band at λ_{max} ~ 360 nm also appears). These spectral changes are complete after 34 sec of irradiation (at a concentration of 1.08×10^{-5} M) and a photostationary state containing at least 99% of the ring-closed isomer is generated according to HPLC analysis of the reaction mixture. This effective photoconversion attests to the versatility of the dithienylethene backbone as a photoresponsive architecture on which to build practical devices. The high photostationary state is highly beneficial and a lower amount of **1c** in the photogenerated mixture would make the differences in enzyme inhibition significanlty less pronounced. The solution containing the ring-closed isomer is very stable at room temperature as long as it is kept in the dark, and the colored state did not revert back to its colorless form even after 6 months. Irradiation of the coloured solution with visible light (λ > 420 nm) converts the ring-closed isomer back to **1o** and regenerates the original absorption spectrum. This ring-closing/ring-opening cycle can be repeated at least seven times without any sign of degradation. [16]

$$CO_2 + H_2O \xrightarrow{\text{hCAI}} HCO_3^- + H^+ \qquad (1)$$

The human carbonic anhydrase I (hCAI)-catalyzed hydration of carbon dioxide (equation 1) is a convenient probe that can be used to investigate the inhibitory effect of the photoresponsive DTE compound in its ring-open (**1o**) and ring-closed (**1c**) states.[16] The known inhibitor, sulphanilamide **4**,[19] and photoresponsive compounds **7**–**9** provide excellent controls for comparison. All results are presented in Figure 2 and Table 1.

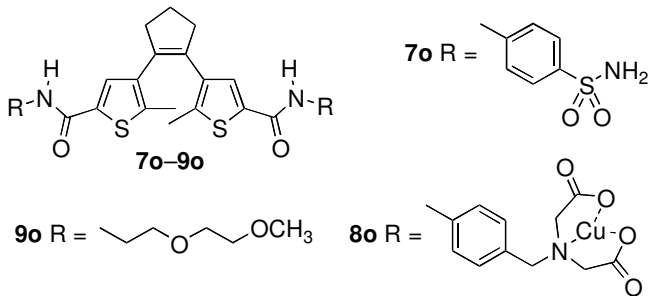

Sulphanilamide **4** has an IC_{50} value of 0.46 μM, which is in good agreement with that reported in the literature.[20] The ring-closed DTE isomer **1c** has a similar inhibition effect (IC_{50} = 0.4 μM) as that of sulphanilamide. The similarity of the inhibitor strength of **4** and **1c** suggests that only the sulphonamide component interacts with the active site of the enzyme in the latter compound. This is likely due to the planar and rigid backbone in **1c** preventing the simultaneous binding of the Cu•IDA and sulphonamide components as will be elaborated on later in this communication.

On the other hand, the ring-open counterpart (**1o**) inhibits the enzyme much more significantly and its inhibition activity is two orders of magnitude higher (IC_{50} = 8 nM) than both **4** and **1c**. This increase can be attributed to the structural flexibility of ring-open isomer **1o**, which allows both recognition components to bind to the enzyme and leads to a higher overall binding affinity. The photoresponsive bis(sulphonamide) **7** shows similar inhibition as sulphanilamide **4** and no difference between the activity of the ring-open (IC_{50} = 0.53 μM) and ring-closed isomers (IC_{50} = 0.57 μM) can be observed. [21] In the case of the photoresponsive bis(IDA) **8**, the IC_{50} values are lower than sulphanilamide **4** and but once again, no significant difference between the ring-open (IC_{50} = 1.55 μM) and the ring-closed isomers (IC_{50} = 1.46 μM) is measured. The photoresponsive bis(ethyleneglycol) DTE **9** was synthesized to investigate whether the dithienylethene unit itself has an influence on the enzyme activity. This compound shows no inhibition in the hCAI catalyzed hydration of carbon dioxide. All observed changes in the enzyme's activity can, therefore, be ascribed to the synergistic roles the sulphonamide and the Cu•IDA groups play as well as to their relative spatial orientation to each other. The binding affinities (K_i) of all compounds show similar trends (Table 1). The exception is ring-open isomer **1o**, which more

effectively binds to the enzyme (K_i = 0.005 μM for **1o** as compared to ~ 0.29–1.16 μM for **1c**, **4**, **7o**, **7c**, **8o** and **8c**). The reversible DTE ring-closing and ring

opening cycle, converting **1o** into **1c** and back, is also possible in the presence of the enzyme.[16]

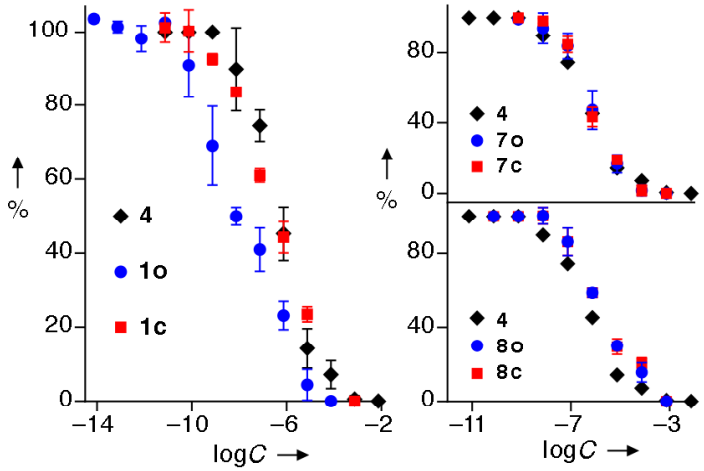

Figure 2. Change in % activity of hCAI when the concentrations of compounds **1**, **4** and **7**–**8** in their ring-open and ring-closed forms are varied.[16] The data were obtained in an enzymatic assay that monitored the reaction of carbon dioxide and water to generate hydrogen carbonate (equation 1). [22]

inhibitor	IC_{50} (μM)		K_i (μM)[a]	
	ring-open	ring-closed	ring-open	ring-closed
4	0.46 ± 0.01		0.29 ± 0.007	
1	0.008 ± 0.0003	0.40 ± 0.005	0.005 ± 0.0002	0.30 ± 0.003
7	0.53 ± 0.007	0.57 ± 0.01	0.34 ± 0.005	0.35 ± 0.008
8	1.55 ± 0.8	1.46 ± 0.15	1.16 ± 0.05	1.00 ± 0.01
9	none	none	none	none

[a] The values of K_i were obtained using the Cheng-Prusoff equation.[16]

Table 1. IC_{50} values and K_i binding affinities of compounds 1, 4 and 7–9 in their ring-open and ring-closed forms.

As eluded to throughout this communication, we can explain the differences in inhibition and binding affinity of the two photoisomers of DTE **1** by comparing the differences in their conformational flexibility. The flexible ring-open form **1o** was designed to allow the simultaneous docking of the sulphonamide and the Cu•IDA components onto the enzyme surface. This is possible due to the free rotation around the C–C single bonds joining the two thiophene heterocycles to the central cyclopentene ring, which allows the inhibitor to adopt a geometry appropriate for bivalent binding only when in its ring-open form. The structure of the enzyme active site (containing both sulphonamide and Cu•IDA components) illustrated in Figure 3 clearly reveals the need for geometric adaptation. The distance between the two binding components (~10 Å) and the way they project in space can only be satisfied by **1o**.

Although the distance between the sulphonamide and Cu•IDA components is the same when the anti-parallel conformation of **1o** is converted into its ring-closed counterpart (Figure 3), it is the parallel conformation of **1o** that is the likely candidate for bivalent binding to the enzyme. The planar, rigid backbone found in the ring-closed isomer **1c** forces the two components away from each other in a non-productive manner, allowing only one of the components to bind to the enzyme at a time. This reduces binding and inhibition.

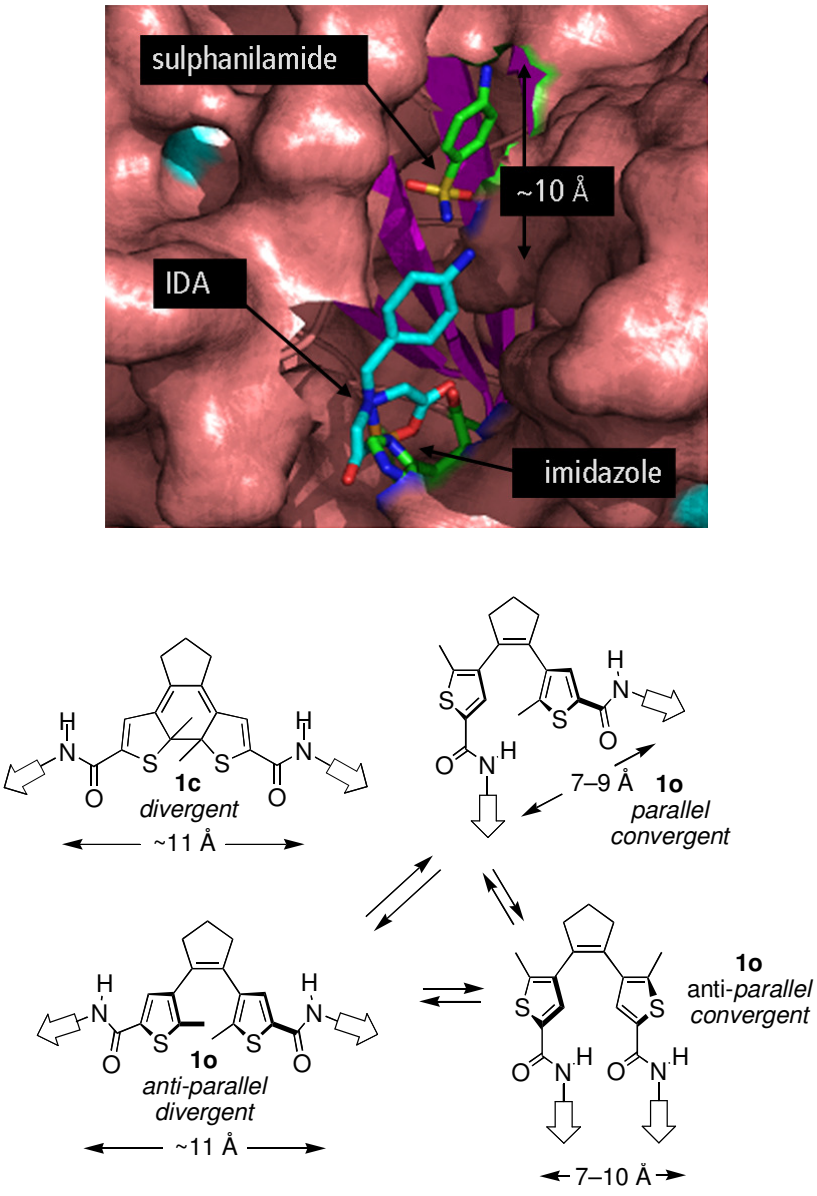

Figure 3. Illustration of the hCAI, catalytic centre containing a sulphanilamide, an IDA and one of the surface exposed imidazole groups. The distance between and relative positioning of the sulphanilamide and IDA groups can only

be satisfied by the ring-open form of compound **1**, which can adopt the productive *parallel* conformation. The structure of the enzyme with sulphanilamide in the active site was derived from crystal structure data, generated and rendered with the program PYMOL from Graph Pad. From Mallik's results[15] the length of the inhibitor to guarantee a high binding affinity is known.

II.3 Conclusion

We have demonstrated that by using a well-designed, two-pronged inhibitor and appropriate wavelengths of light, the enzyme activity can be reversibly and significantly enhanced by toggling the DTE between a high- and a low-affinity conformation. The thermal stability, nearly quantitative formation of each photoisomer and activation with visible light makes the system a suitable tool for the reversible regulation of enzyme activity by an external light input. The use of visible light to activate the inhibitor is particularly important as it will allow better penetration into tissue and reduce the amount of damage caused by higher energy UV light.

II.4 References

(1) Stadtman, E.R. *Adv. Enzymol. Relat. Areas Mol. Biol.* **1966**, *28*, 41 – 154.

(2) Corbett, A.H.; DeVore, R.F.; Osheroff, N. *J. Biol. Chem.* **1992**, *267*, 20 513 – 20518.

(3) Ybarra, J.; Prasad, A.R. ; Nishimura, J.S. *Biochemistry* **1986**, *25*, 7174 – 7178.

(4) Pavlenko, I.M.; Klyachko, N.L.; Levashov, A.V. *Russ. J. Bioorg. Chem.* **2005**, *31*, 535 – 542.

(5) Oda, T.; Tokushige, M. *J. Biochem.* **1988**, *104*, 178 – 183.

(6) Sadana, A.; Henley, J.P. *Biotechnol. Bioeng.* **1986**, *28*, 256 – 268.

(7) Fujita, D.; Murai, M.; Nishioka, T.; H. Miyoshi, H. *Biochemistry* **2006**, *45*, 6581 – 6586.

(8) Rubin, S.; Willner, I. *Mol. Cryst. Liq. Cryst.* **1994**, *246*, 201. For a review on the control of structure and function of biomaterials by light, see: Willner, I.; Rubin, S. *Angew. Chem.* **1996**, *108,* 419 – 439; *Angew. Chem. Int. Ed. Engl.* **1996**, *35*, 367 – 385.

(9) Wang, S.-C.; Lee, Jr., C. T. *Biochemistry* **2007**, *46*, 14557 – 14566.

(10) Varfolomeyev, S.D.; Kazanskaya, N.F.; Eremeev, N.L. *BioSystems* **1996**, *39*, 35 – 42.

(11) Henry, R. P. *Annu. Rev. Physiol.* **1996**, *58*, 523 – 538.

(12) Harvey Jessica, H.; Trauner, D. *ChemBioChem* **2008**, *9*, 191 – 193.

(13) Special issue on photochromism: Irie, M. *Chem. Rev.* **2000**, *100*, 1685 – 1716; M. Irie in Molecular Switches (Ed.: B. L. Feringa), Wiley-VCH, Weinheim, 2001, pp. 37 – 62; M. Irie in Photochromic and Thermochromic Compounds, Vol. 1 (Eds.: J. C. Crano, R. J. Guglielmetti), Plenum, New York, 1999, pp. 207 – 222; Tian, H.; Yang, S. *Chem. Soc. Rev.* 2004, 33, 85 – 97; Tian, H.; Wang, S. *Chem. Commun.* **2007**, 781 – 792.

(14) Banerjee, A.L.; Eiler, D.; Roy, B.C.; Jia, X.; Haldar, M.K.; Mallik, S.; Srivastava, D.K. *Biochemistry* **2005**, *44*, 3211 – 3224. Use of reversible

coordination in molecular recognition: Kruppa, M.; König, B. *Chem. Rev.* **2006**, *106*, 3520 – 3560.

(15) Two conformations (parallel and antiparallel)of the ring-open isomer of the DTE architecture coexist, typically in a 1:1 ratio, in solution (see the Supporting Information). The photoactive form is the antiparallel conformation.

(16) See the Supporting Information for details.

(17) Norsten, T.B.; Branda, N.R. *J. Am. Chem. Soc.* **2001**, *123*, 1784 – 1785.

(18) Standard hand-held lamps used for visualizing TLC plates (from Herolab, 6 W) were used to carry out the ring-closing reactions at 312 nm. The ring-opening reactions were carried out using the light of a 200W tungsten source that was passed through a 420 nm cutoff filter to eliminate higher energy light.

(19) Anderson, D.J.; Thomson, L.C. *J. Physiol.* **1948**, *107*, 203 – 210.

(20) Franchi, M.; Vullo, D.; Gallori, E.; Antel, J.; Wurl, M.; Scozzafava, A.; Supuran, C.T. *Bioorg. Med. Chem. Lett.* **2003**, *13*, 2857 – 2861.

(21) The photoreactions of compounds **6a**, **7a**, and **8a** are shown in the Supporting Information.

(22) During the enzyme-catalyzed reaction, the pH of a buffered solution (5% DMSO, Tris sulfate buffer, pH 8.3) containing a pH indicator (phenol red, 5×10^{-5} M) dropped from 8.3 to 6.3, which is the end point of the reaction. The time required for this change in color was recorded for each concentration of inhibitor, and from this data the enzyme activity was calculated.

II.5 Supporting information

Synthesis and characterization of new compounds

General. Thin layer chromatography (TLC) was performed on alumina plates coated with silica gel (Merck silica gel 60 F 254, layer thickness 0.2 mm). Column chromatography was performed on silica gel (70–230 mesh) from Merck. Starting materials were purchased from either Acros or Sigma-Aldrich and used without any further purification. Solvents were purchased from Aldrich and used without further purification except for dry THF, which was prepared by distillation from potassium. 1,2-Bis(5-carboxy-2-methylthien-3-yl)cyclopentene[1] and 2-(2-methoxyethoxy)-ethylamine[2] were prepared according to literature known procedures.

Techniques. Melting points (MP) were determined with a Büchi SMP 20. IR-spectra were recorded with a Bio-Rad FTS 2000 MX FT-IR spectrometer. NMR spectra were recorded on a Bruker Avance 400 (^{1}H: 400.1 MHz, ^{13}C: 100.6 MHz, T = 300 K) or a Bruker Avance 300 (^{1}H: 300.1 MHz, ^{13}C: 75.5 MHz, T = 300 K). The spectra are referenced against the NMR-solvent and chemical shifts are reported in ppm. The symbol "+" stands for an NMR signal with positive intensity in the DEPT 135 spectra indicating a CH or CH_3 carbon. The symbol "–" stands for an NMR signal with negative intensity in the DEPT 135 spectra indicating a CH_2 carbon. MS-Spectra were determined on a Varian CH-5 (EI), a Finnigan MAT 95 (CI; FAB and FD) or a Finnigan MAT TSQ 7000 (ESI). UV–Vis absorption spectroscopy was performed using a Cary 50 Bio spectrophotometer.

Photochemistry. Standard hand-held lamps used for visualizing TLC plates (Herolab, 6 W) were used to carry out the ring-closing reactions at 312 nm. The ring-opening reactions were carried out using the light of a 200 W tungsten source that was passed through a 420 nm cut-off filter to eliminate higher energy light. The power of the light source is given based on the specifications supplied by the company when the lamps were purchased. A light detector was not used to measure the intensity during the irradiation experiments.

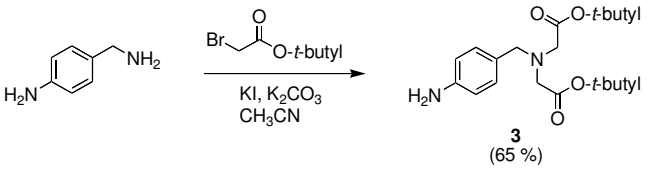

Scheme S1. Synthesis of starting material **3**.

Synthesis of [(4-amino-benzyl)-*tert*-butoxycarbonylmethylamino]acetic acid *tert*-butyl ester (3). In a 250 mL round-bottom flask, a mixture of 4-aminobenzylamine (1.9 mL, 16.4 mmol), *tert*-butylbromoacetate (4.6 mL, 31.1 mmol, 1.9 equiv), K_2CO_3 (9.0 g, 65.5 mmol, 4.0 equiv), KI (5.4 g, 32.7 mmol, 2.0 equiv) and CH_3CN (100 mL) was heated at reflux for 25 h. After cooling to room temperature, the precipitate was filtered off washed with CH_3CN and the solvent was removed *in vacuo*. Purification by column chromatography (silica, EtOAc/petroleum ether 3:2, R_f = 0.48) afforded 3.4 g (9.7 mmol, 59 %) of compound **3** as a pale yellow solid.

^{1}H-NMR (300 MHz, $CDCl_3$): δ [ppm] = 1.45 (s, 9H, CH_3), 3.38 (s, 4H, CH_2), 1.72 (br s, 2H, NH_2), 3.75 (s, 2H, CH_2), 6.62 (d, ^3J = 8.5 Hz, 2H, CH), 7.14 (d, ^3J = 8.2 Hz, 2H, CH); **^{13}C-NMR (75 MHz, $CDCl_3$):** δ [ppm] = 28.20 (+), 54.90 (–), 56.99 (–), 80.75 (C_{quat}), 114.97 (+), 128.31 (C_{quat}), 130.30 (+), 145.61 (C_{quat}), 170.72 (C_{quat}); **CI-MS (NH_3):** m/z (%) = 351.2 (100) [MH^+]; **PI-EI MS:** calcd.: 350.2206, found: 350.2207; **MP** = 83 °C; **FT-IR (ATR):** ν [cm^{-1}] = 3462 (m), 3372 (m), 2976 (w), 2828 (w), 1731 (s), 1623 (m), 1518 (m), 1457 (w), 1423 (w), 1369 (m), 1283 (m), 1252 (m), 1213 (m), 1134 (s), 987 (m), 941 (w), 831 (m), 756 (w), 592 (m), 523 (m).

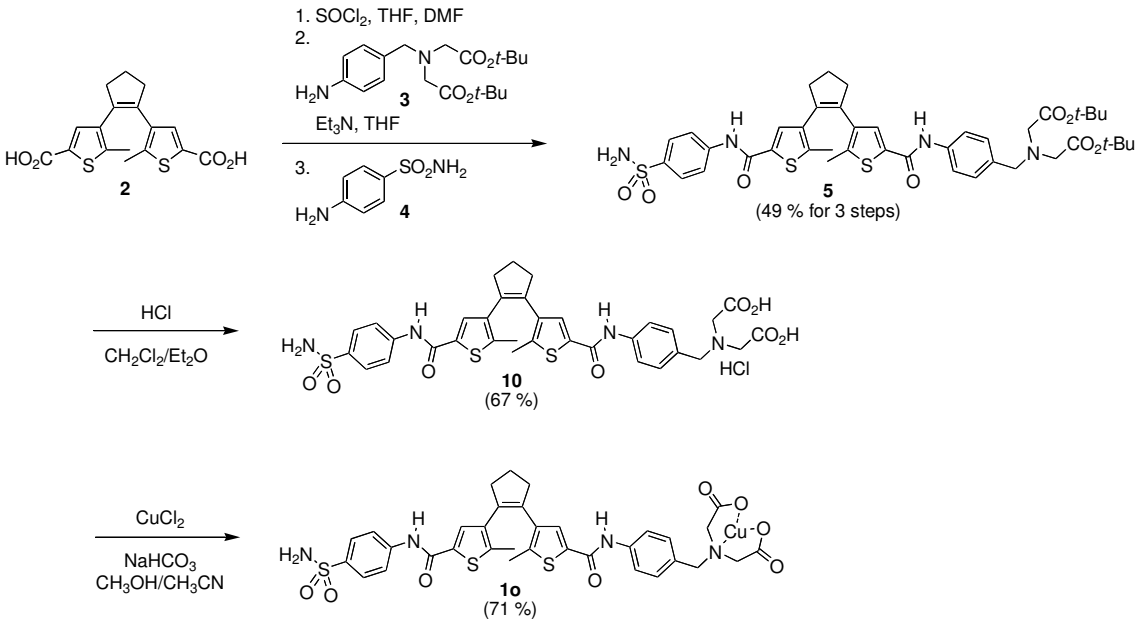

Scheme S2. Synthesis of photoresponsive DTE **1o**.

Synthesis of (*tert*-butoxycarbonylmethyl-{4-[(5-methyl-4-{2-[2-methyl-5-(4-sulfamoyl-phenylcarbamoyl)-thiophen-3-yl]-cyclopent-1-enyl}-thiophene-2-carbonyl)-amino]benzyl}-amino)acetic acid *tert*-butyl ester (5). *Diester (5).*

In a 100 mL round-bottom flask, a solution of 1,2-bis(5'-carboxy-2'-methylthien-3'-yl)cyclopentene **2** (1.5 g, 4.3 mmol) in dry THF (20 mL) was treated with 4 drops of DMF followed by $SOCl_2$ (3.7 mL, 51.6 mmol, 4 equiv) drop-wise. The resulting solution was stirred at room temperature for 15 h, at which time the solvent was evaporated *in vacuo* and the solid residue was dried under high vacuum. This residue was dissolved in dry THF (50 mL) under an N_2 atmosphere and treated with Et_3N (2 mL, 14.3 mmol) in one portion, followed by a solution of [(4-aminobenzyl)-*tert*-butoxycarbonylmethylamino]acetic acid *tert*-butyl ester **3** (0.5 g, 1.4 mmol) in dry THF (20 mL) drop-wise over 4 h. After stirring at room temperature for 1.5 h, solid sulphanilamide **4** (1.5 g, 8.58 mmol) was added in one portion. After stirring at room temperature for an additional 42 h, the insoluble materials were filtered off, washed with THF and the filtrate was evaporated to dryness. The residue purified by column chromatography (flash silica, EtOAc/petroleum ether 3:2, R_f = 0.48) yielding 0.6

g (0.7 mmol, 49 %, according to the consumption of **3**) of compound **5** as a brown solid.

^{1}H-NMR (300 MHz, CD_2Cl_2): δ [ppm] = 1.33–1.52 (m, 26H), 1.97–1.98 (m, 4H), 3.37 (s, 4H), 3.80 (s, 2H), 7.26 (d, ^3J = Hz, 2H), 7.47–7.77 (m, 10H), 8.54 (br s, 1H), 9.13 (br s, 1H); **^{13}C-NMR (75 MHz, CD_2Cl_2):** δ [ppm] = 13.06 (+), 13.77 (+), 22.98 (–), 38.00 (–), 54.28 (–), 56.41 (–), 120.79 (+), 121.31 (+), 128.13 (+), 130.49 (+), 134.05 ($C_{quat.}$), 134.37 (C_{quat}), 134.66 ($C_{quat.}$), 134.70 ($C_{quat.}$), 135.28 (C_{quat}), 136.24 ($C_{quat.}$), 136.47 (C_{quat}), 137.23 (C_{quat}), 137.50 (C_{quat}), 140.68 (C_{quat}), 141.54 (C_{quat}), 141.86 (C_{quat}), 159.61 (C_{quat}), 159.87 (C_{quat}), 166.86 (C_{quat}), 170.60 (C_{quat}); **MP** = 160–165 °C; **ES-MS (DCM/MeOH + 10 mmol/L NH_4Ac):** m/z (%) = 835.3 (100) $[M+H]^+$; **IR (KBr-pellet):** ν [cm^{-1}] = 3350 (m), 2958 (w), 2919 (m), 2849 (m), 2361 (m), 1735 (s), 1647 (s), 1594 (m), 1522 (s), 1449 (w), 1400 (w), 1315 (s), 1247 (m), 1199 (w), 1157 (s), 1098 (w), 1024 (m), 911 (w), 807 (w), 669 (s), 574 (w), 542 (m), 429 (w); **PI LSIMS (CH_2Cl_2/NBA):** calcd.: 835.2869 found: 835.2885.

Synthesis of (carboxymethyl-{4-[(5-methyl-4-{2-[2-methyl-5-(4-sulfamoylphenyl-carbamoyl)-thiophen-3-yl]-cyclopent-1-enyl}thiophene-2-carbonyl)amino]benzyl}amino)-acetic acid hydrochloride (10). ***Diacid (10).***

In a 50 mL round-bottom flask, a solution of diester **5** (150 mg, 0.18 mmol) in CH_2Cl_2 (5 mL) was cooled to 0 °C and treated with a saturated solution of HCl in Et_2O (2 mL). After stirring the mixture at room temperature for 140 min, the precipitate was collected by vacuum filtration and washed several times with CH_2Cl_2 and dried yielding 92 mg (0.12 mmol, 67 %) of diester **10** as a colorless solid, which was used without further purification.

^{1}H-NMR (300 MHz, MeOD): δ [ppm] = 1.97 (s, 3H), 1.99 (s, 3H), 2.15 (quintet, ^3J = 7.4 Hz, 2H), 2.90 (t, ^3J = 7.3 Hz, 4H), 4.16 (s, 4H), 4.53 (s, 2H), 7.49 (d, ^3J = 8.5 Hz, 2H), 7.75–7.85 (m, 8H); **ES-MS (DCM/MeOH + 10 mmol/L NH_4Ac):** m/z (%) = 721.1 (100) $[M–H]^+$; **MP** = 163–167 °C.

Synthesis of copper complex 1o. In a 10 mL round-bottom flask, a solution of compound **10** (133 mg, 0.17 mmol) in a mixture of CH_3OH (5 mL) and CH_3CN (2 mL)

was treated with $NaHCO_3$ (44 mg, 0.52 mmol, 3 equiv) and stirred at 50 °C for 10 min. A solution of $CuCl_2$ (29 mg, 0.17 mmol, 1 equiv) in CH_3OH (0.5 mL) was added at 50 °C and the resulting mixture was stirred at this temperature for 24 h. The precipitate that formed was collected by centrifugation and purified by washing the solid pellet in CH_3OH. The solid was again collected by centrifugation. This purification step was repeated 3 times yielding 92 mg (0.12 mmol, 71 %) of compound **1o** as a light blue solid. **ES-MS (H_2O/THF 1:1)**: m/z (%) = 782.2 (100) $[M–H]^+$; **UV (DMSO):** λ_{max} = 294 nm (35000); **MP** > 200 °C.

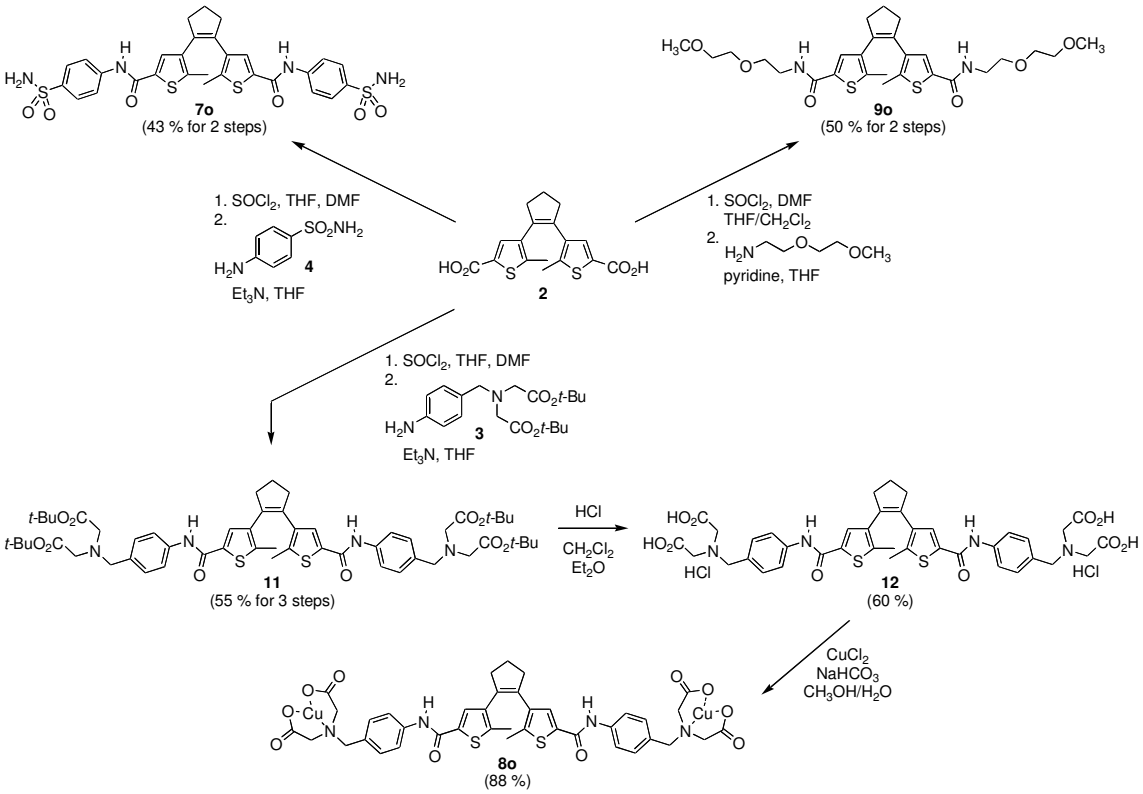

Scheme S3. Synthesis of bis(sulphonamide) **7o**, bis(IDA) **8o** and bis(glycol) **9**.

Synthesis of 4,4'-(cyclopentene-1,2-diyl)bis(5-methyl-N-(4-sulfamoylphenyl)thiophene-2-carboxamide) (7). ***Bis(sulphonamide) 7.***

In a 100 mL round-bottom flask, a solution of 1,2-bis(5'-carboxy-2'-methylthien-3'-yl)cyclopentene **2** (0.5 g, 1.4 mmol) in dry THF (10 mL) was treated with $SOCl_2$ (1.9 mL, 26.6 mmol) dropwise, followed by DMF (4 drops). The solution was stirred for

1 h at which time the solvent was evaporated and the residue dried *in vacuo*. The solid residue was dissolved in dry THF (10 mL) under an N_2 atmosphere

and treated with Et_3N (1.8 mL, 4.5 mmol) in one portion, followed by a solution of sulphanilamide **4** in dry THF (20 mL), which was added drop-wise over 10 min. After stirring the mixture for 48 h, the solvent was removed *in vacuo* and the resulting residue was suspended in a mixture of H_2O and EtOH (3:56 mL:mL). The mixture was heated at reflux for 1 h, at which time the solid was collected by vacuum filtration, washed with water and air-dried yielding 0.4 g (0.6 mmol, 43 %) compound **7** as a colorless solid. **^{1}H-NMR (300 MHz, DMSO):** δ [ppm] = 1.90 (s, 6H), 2.07–2.14 (m, 2H), 2.86 (t, ^3J = 7.5 Hz, 4H), 7.27–7.28 (m, 4H), 7.28 (br s, 4H), 7.79 (d, ^3J = 8.8 Hz, 4H), 7.88 (d, ^3J = 9.0 Hz, 4H), 7.91 (s, 2H), 10.38 (br s, 2H); **^{13}C-NMR (75 MHz, DMSO):** δ [ppm] = 14.29 (+), 30.29 (–), 46.66 (–), 119.62 (+), 126.50 (+), 130.34 (+), 134.22 (C_{quat}), 135.15 (C_{quat}), 136.33 (C_{quat}), 138.52 (C_{quat}), 140.92 (C_{quat}), 141.64 (C_{quat}), 159.78 (C_{quat}); **FT-IR (ATR):** v [cm^{-1}] = 3331 (m), 3107 (w), 1650 (m), 1591 (m), 1524 (s), 1456 (w), 1400 (w), 1315 (s), 1249 (m), 1148 (s), 1098 (w), 883 (w), 836 (w), 665 (m), 576 (m), 540 (m); **ES-MS** (DCM/MeOH + 10 mmol/L NH_4Ac): m/z (%) = 657.1 (46) $[M+H]^+$, 674.2 (100) $[M+H+NH_4]^+$, 655.2 (100) $[M–H]^+$, 691.2 (30) $[M+Cl]^+$, 715.3 (22) $[M+CH_3COO]^+$; **PI LSIMS (MeOH/ CH_2Cl_2/ NBA):** calcd.: 656.0891 found: 656.0997; **MP** > 200 °C; **UV (DMSO):** λ_{max} = 285 nm (21900).

Synthesis of {[4-({4-[2-(5-{4-[(bis-*tert*-butoxycarbonylmethylamino)methyl]phenyl-carbamoyl}-2-methylthiophen-3-yl)cyclopent-1-enyl]-5-methylthiophene-2-carbonyl}-amino)benzyl]-*tert*-butoxycarbonylmethylamino}acetic acid *tert*-butyl ester (11). *Tetraester 11*.

In a 100 mL round-bottom flask, a solution of 1,2-bis(5'-carboxy-2'-methylthien-3'-yl)cyclopentene **2** (0.5 g, 1.43 mmol) in dry THF (10 mL) was treated with $SOCl_2$ (1.9 mL, 26.6 mmol) drop-wise, followed by 4 drops DMF. The resulting solution was stirred for 1 h at room temperature, at which time the solvent was evaporated and the residue dried *in vacuo*. The residue was redissolved in dry THF (10 mL) under an N_2 atmosphere and treated with 1.8 mL of Et_3N (4.5 mmol) in one portion, followed by a solution of [(4-aminobenzyl)-*tert*-butoxycarbonylmethylamino]acetic acid *tert*-butyl ester **3** (2.8 g, 8 mmol) in THF (10 mL), which was added drop-wise over 1 h.

The resulting reaction mixture was stirred overnight and after this period, H_2O (50 mL) was added. The mixture was extracted with EtOAc (3 x 50 mL) and the combined organic phases were further extracted with a saturated $NaHCO_3$ solution (2 x 20 mL). The combined organic phases were dried (Na_2SO_4), filtered and evaporated. Purification by column chromatography (flash silica, EtOAc/petroleum ether 8:2, R_f = 0.9) yielded 0.8 g (0.8 mmol, 55 %) of compound **11** as a pale brown solid. **^{1}H-NMR (300 MHz, $CDCl_3$):** δ [ppm] = 1.44 (s, 36H), 1.85–2.02 (m, 8H), 2.65 (t, ^3J = 7.3 Hz, 4H), 3.71 (s, 8H), 3.82 (s, 4H), 7.31 (d, ^3J = 8.5 Hz, 4H), 7.35 (s, 2H), 7.53 (d, ^3J = 8.5 Hz, 4H), 8.08 (br s, 2H); **^{13}C-NMR (75 MHz, $CDCl_3$):** δ = 14.80 (+), 22.48 (–), 28.19 (+), 38.71 (–), 54.98 (–), 56.96 (–), 79.95 (C_{quat}), 120.18 (+), 129.70 (+), 130.15 (+), 133.54 (C_{quat}), 133.64 (C_{quat}), 133.72 (C_{quat}), 135.52 (C_{quat}), 139.86 (C_{quat}), 159.04 (C_{quat}), 169.59 (C_{quat}); **FT-IR (ATR):** ν [cm^{-1}] = 3298 (w), 2975 (m), 2924 (w), 1727 (s), 1626 (m), 1599 (m), 1527 (s), 1455 (m), 1410 (m), 1366 (m), 1248 (w), 1216 (w), 1139 (s), 988 (m), 880 (w), 815 (w), 742 (w), **ES-MS (DCM/MeOH + 10 mmol/l NH_4Ac):** m/z (%) = 507.4 (77) $[M+2H]^+$, 1013.6 (100) $[M+H]^+$, 1035 (10) $[M+Na]^+$; **PI LSIMS (MeOH/CH_2Cl_2/NBA):** calcd.: 1012.4689 found: 1012.4817; **MP** = 149–150 °C.

Synthesis of {[4-({4-[2-(5-{4-[(Bis-carboxymethyl-amino)-methyl]-phenylcarbamoyl}-2-methyl-thiophen-3-yl)-cyclopent-1-enyl]-5-methyl-thiophene-2-carbonyl}-amino)-benzyl]-carboxymethyl-amino}-acetic acid hydrochloride (12). ***Tetraacid 12*****.** In a 50 mL round-bottom flask a solution of tetraester **11** (0.2 g, 0.2 mmol) in CH_2Cl_2 (10 mL) was treated with a saturated solution of HCl in Et_2O (4 mL) at 0°C. After the addition of the acid, the cool bath was removed and the mixture was stirred at room temperature for 16 h at which time the solvent was evaporated to dryness to yield 0.1 g (0.12 mmol, 60 %) of compound **12** as a colorless solid.

^{1}H-NMR (DMSO, 300 MHz): δ [ppm] = 1.91 (s, 6H), 2.02–2.12 (m, 2H), 2.85 (t, ^3J = 7.3 Hz, 4H), 4.02 (s, 8H), 4.33 (s, 4H), 7.47 (d, ^3J = 8.5 Hz, 4H), 7.85 (d, ^3J = 8.8 Hz, 4H), 8.12 (s, 2H), 10.49 (br s, 2H); **FT-IR (ATR):** ν [cm^{-1}] = 2922 (w), 2854 (w), 1730 (s) 1638 (s), 1595 (m), 1518 (s), 1414 (m), 1319 (m), 1246 (m), 1069 (w), 939 (w),

881 (w), 817 (m), 741 (w), 660 (w), 597 (w); **ES-MS** (DCM/MeOH + 10 M NH_4Ac): m/z (%) = 789.3 (38) $[M+H]^+$, 393.3 (5) $[M–2H]^{2–}$, 787.4 (100) $[M–H]^–$; **MP >** 200 °C.

Synthesis of the bis(copper) complex 8o. In a 50 mL round-bottom flask, a suspension of tetraacid **12** (0.14 g, 0.2 mmol) in a mixture of CH_3OH and H_2O (1:1 v/v, 30 mL) was heated to reflux and treated, at this temperature, with solid $NaHCO_3$ (90 mg, 1 mmol, 6 equiv) in one portion, followed by $CuCl_2$ (60 mg, 0.3 mmol, 2 equiv). After the reaction was heated at reflux for 2 h, the blue precipitate was collected by centrifugation and the blue solid washed with H_2O (20 mL), CH_3CN (20 mL) and dried yielding compound **8o** (0.13 g, 0.15 mmol, 88 %) as a blue solid. **ES-MS (CH_3OH + 10 mM NH_4OAc):** m/z (%) = 911 (100) $[M–H]^+$, 971 (35) $[M+CH_3COO]^+$; **FT-IR (ATR):** ν [cm^{-1}] = 1595 (s), 1518 (s), 1441 (w), 1412 (w), 1375 (m), 1317 (m), 1249 (m), 1088 (w), 1010 (w), 855 (w), 817 (w), 740 (w), 528 (w); **MP** > 200 °C; **UV (DMSO):** λ_{max} = 290 nm (44000).

Synthesis of 4,4'-(cyclopentene-1,2-diyl)bis(*N*-(2-(2-methoxyethoxy)ethyl)-5-methylthiophene-2-carboxamide) (9o). ***Bis(glycol) 9o*.** In a 100 mL round-bottom flask, a solution of 1,2-bis(5'-carboxy-2'-methylthien-3'-yl)cyclopentene **2** (0.4 g, 1.1 mmol) in a 1:1 (v/v) mixture of CH_2Cl_2 and THF (10 mL) was treated with a catalytic amount of DMF (4 drops), followed by a drop-wise addition of $SOCl_2$ (0.3 mL, 0.5 g, 4.52 mmol, 4 equiv). The mixture was stirred at room temperature and the conversion monitored by TLC. After 3 h, the solvent was evaporated *in vacuo*, the residue was dried under high vacuum and dissolved in THF (20 mL) and treated with pyridine (0.4 mL, 0.35 g, 4.52 mmol, 4 equiv) in one portion, followed by 2-(2-methoxyethoxy)ethylamine (0.4 g, 3.4 mmol, 3 equiv). The resulting red mixture was stirred for 15 h at room temperature at which time the solvent was removed by evaporation. Purification by column chromatography (flash silica, EtOAc/5% CH_3OH, R_f = 0.16) afforded 0.3 g (0.6 mmol, 50 %) of compound **9o** as a colorless oil. **^{1}H-NMR (300 MHz, $CDCl_3$)**: δ [ppm] = 1.89 (s, 6H), 1.99–2.09 (m, 2H), 2.76 (t, ^3J = 7.5 Hz, 4H), 3.38 (s, 6H), 3.53–3.65 (m, 16H), 6.44 (br s, 1H), 7.22 (s, 2H); **^{13}C-NMR (75 MHz, $CDCl_3$):** δ [ppm] = 14.70 (+), 22.87 (–), 38.56 (–), 39.54 (–), 59.00 (+), 69.79 (–), 70.13 (–), 71.83 (–), 129.29 (+), 134.45 (C_{quat}), 134.65 (C_{quat}), 136.25 (C_{quat}), 139.86 (C_{quat}), 161.84 (C_{quat}); **ES-MS (DCM/CH_3OH + 10 mM NH_4OAc):** m/z (%) =

551.2 (100%) $[M+H]^+$, 568.2 (10 %) $[M+NH_4]^+$; **FT-IR (ATR):** *v* $[cm^{-1}]$ = 3345 (m), 2863 (m), 1646 (s), 1559 (w), 1528 (m), 1457 (w), 1427 (w), 1349 (w), 1300 (s), 1246 (m), 1197 (w), 1132 (m), 1088 (s), 1027 (w), 930 (w), 896 (w), 853 (m), 789 (m), 753 (m), 659 (m), 607 (s), 436 (w); **PI-EIMS:** calcd.: 551.2171, found: 551.2164**; UV (DMSO):** λ_{max} = 260 nm (32759).

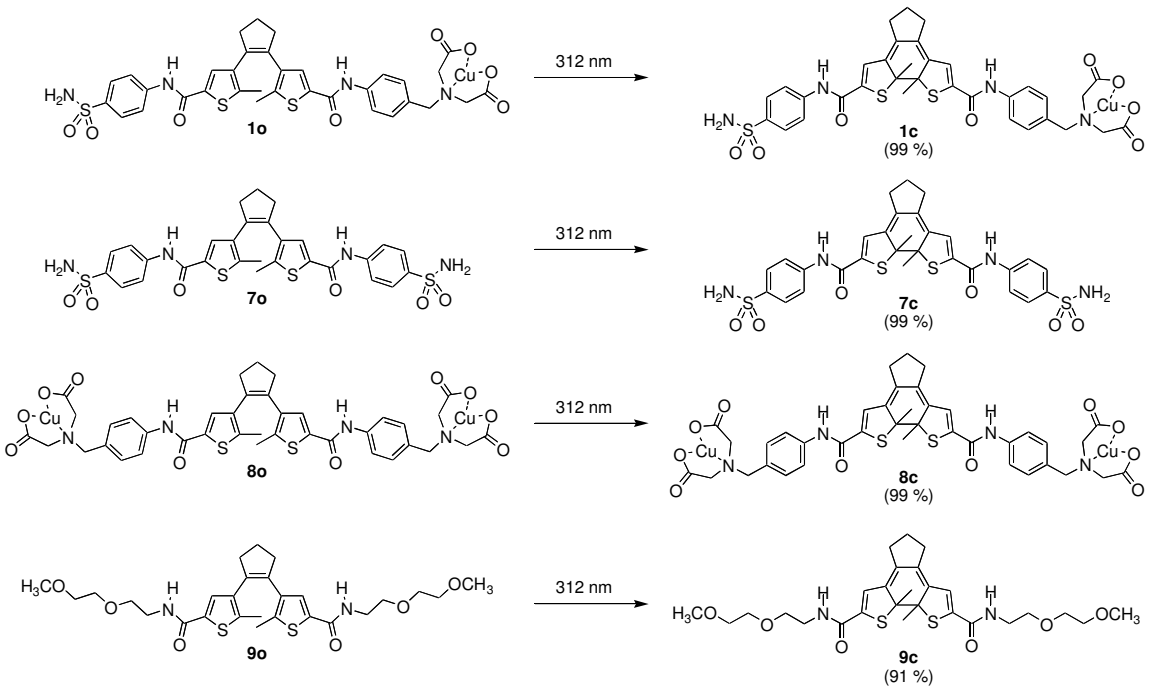

Scheme S4. Photochemical ring-closing reactions of compounds **1o**, **7o**, **8o** and **9**.

Photochemical synthesis of the ring-closed isomer 1c. A solution of compound **1o** (0.5 mg, 0.0007 mmol) in DMSO (1 mL) was irradiated for 15 min with a 312 nm lamp in an HPLC vial yielding a purple solution containing the ring-closed isomer **1c** (> 99 %) according to HPLC (NH_4OAc buffer).

Photochemical synthesis of the ring-closed isomer 7c. A solution of compound **7o** (0.5 mg, 0.0008 mmol) in DMSO (1 mL) was irradiated for 15 min with a 312 nm lamp in an HPLC vial yielding a purple solution containing the ring-closed isomer **7c** (> 99 %) according to HPLC (NH_4OAc buffer).

Photochemical synthesis of the ring-closed isomer 8c. A solution of compound **8o** (0.5 mg, 0.0005 mmol) in DMSO (1 mL) was irradiated for 15 min with a 312 nm lamp in an HPLC vial yielding a purple solution of the ring-closed isomer (> 99 %) according to HPLC (NH_4OAc buffer).

Photochemical synthesis of the ring-closed isomer 9c. A solution of compound **9o** (3 mg, 0.005 mmol) in CD_2Cl_2 (0.7 mL) was irradiated for 30 min with a 312 nm lamp in a NMR tube light yielding a red solution of a photostationary state containing 91% of the ring-closed isomer according to the ^{1}H-NMR spectroscopy. The remaining 9% were assigned to the ring-open isomer **9o**. ^{1}H-NMR (300 MHz, CD_2Cl_2): δ [ppm] = 1.87 (quintet, ^3J = 7.5 Hz, 2H), 2.00 (s, 6H), 2.78 (t, ^3J = 7.4 Hz, 4H), 3.41 (s, 6H), 3.54–3.66 (m, 16H), 6.27 (br s, 2H), 6.65 (s, 2H).

Photochromism

*Determination of the photostationary state (PPS) of DTE **1**.*

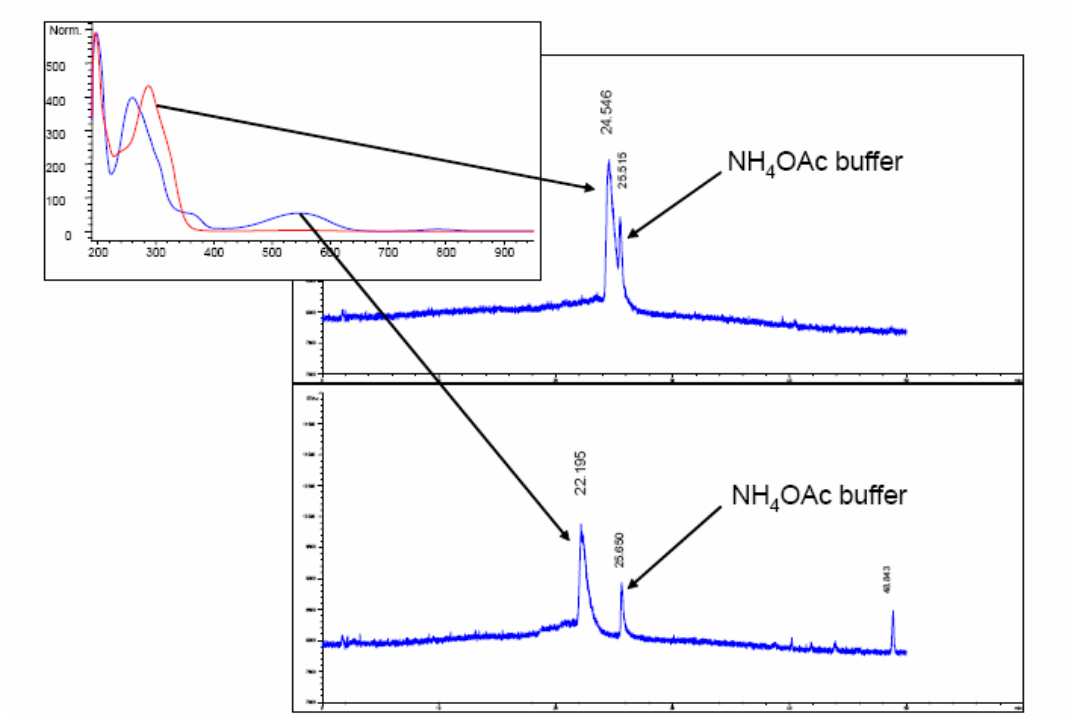

Figure S1. Representative HPLC chromatogram for the determination of the PSS of compound **1**. The chromatograms of isomer **1o** (upper) and the solution of **1c** (lower) generated with 312 nm light are shown. The entire peak for **1o** disappears and a new one appears at a lower retention time. The small peak appearing at 48 min is attributed to a photo-generated side product. The conversion from the ring-open to the ring-closed isomer is > 99 %.

Photochemical cycling studies.

a) Bivalent inhibitor **1o**.

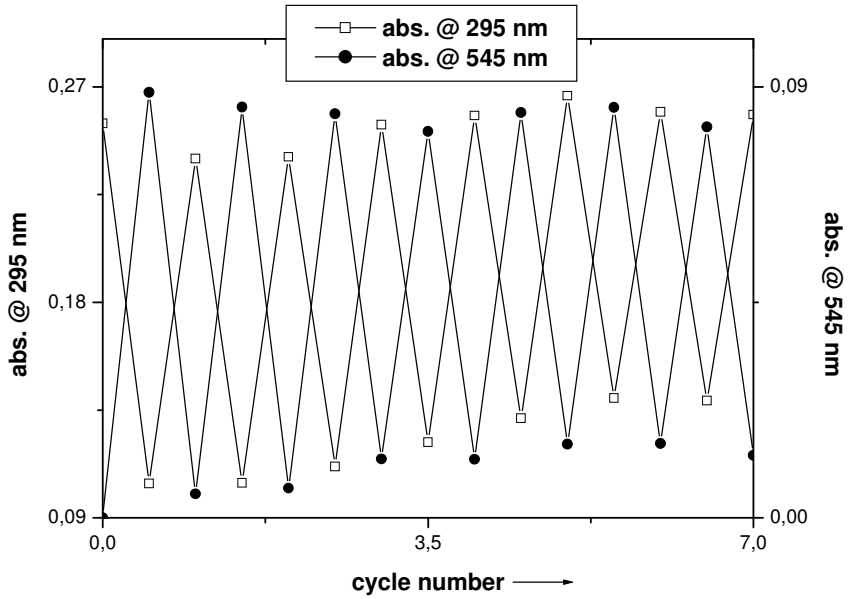

Figure S2. Modulated absorbance (abs.) at 294 nm (open squares = **1o**) and 545 nm (black circles = **1c**) during alternate irradiation of a DMSO (1.08×10^{-5} M) solution of **1o** with 312 nm light for 34 s, and greater than 420 nm light for 6 min.

b) Bis(sulphonamide) **7**.

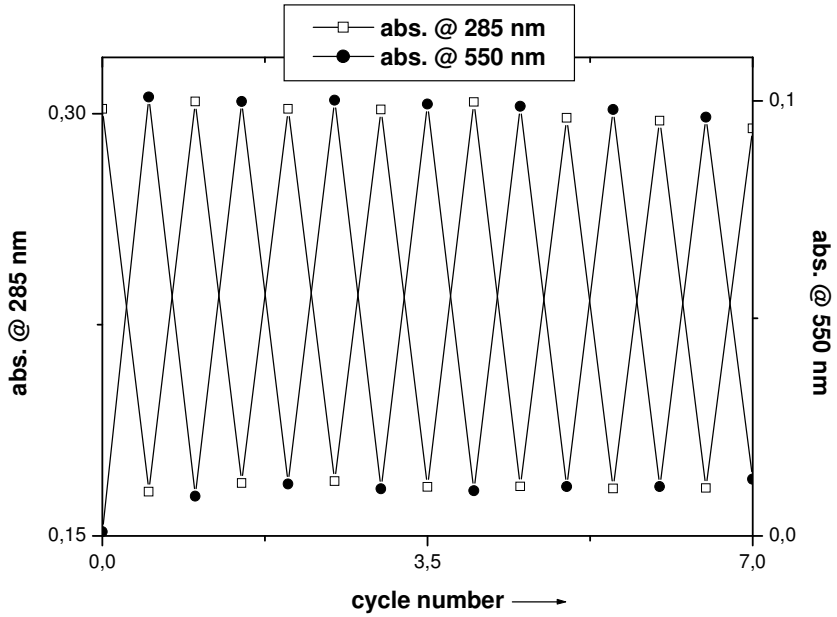

Figure S3. Modulated absorbance (abs.) at 285 nm (open squares = **7o**) and 550 nm (black circles = **7c**) during alternate irradiation of a DMSO (1.00×10^{-5} M) solution of **7o** with 312 nm light for 26 s, and greater than 420 nm light for 10 min.

c) Bis(IDA) **8**.

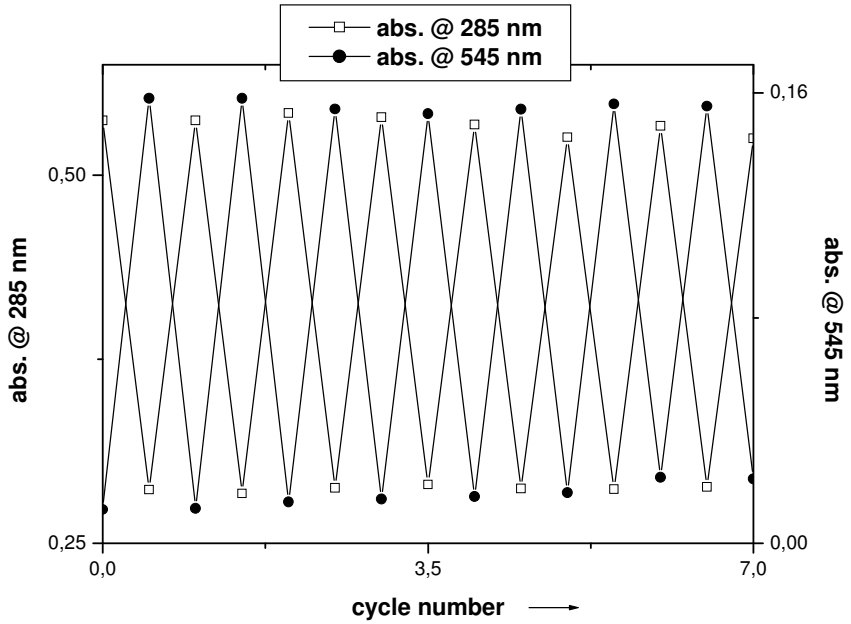

Figure S4. Modulated absorbance (abs.) at 285 nm (open squares = **8o**) and 545 nm (black circles = **8c**) during alternate irradiation of a DMSO (1.0×10^{-5} M) solution of **8o** with 312 nm light for 40 s, and greater than 420 nm light for 5 min.

d) bis(glycol) **9**.

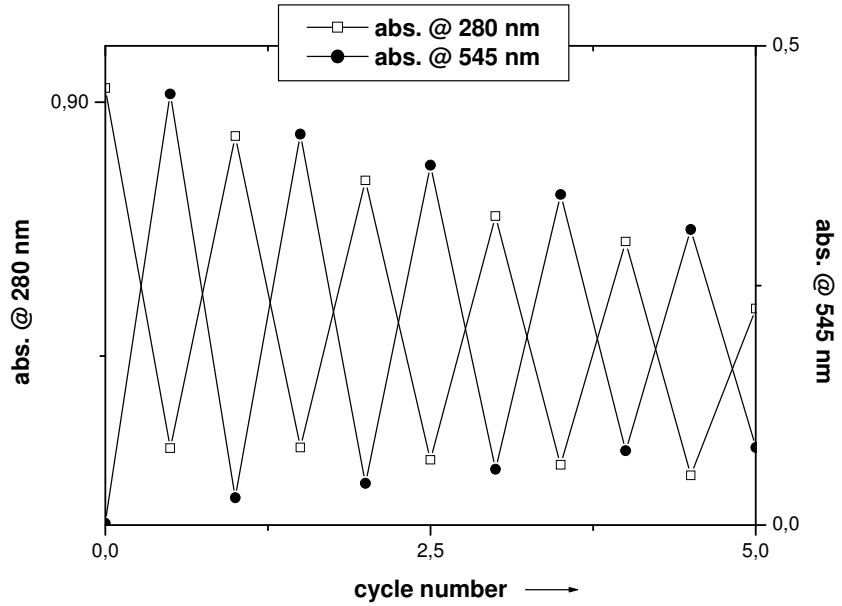

Figure S5. Modulated absorbance (abs.) at 280 nm (open squares = **9o**) and 545 nm (black circles = **9c**) during alternate irradiation of a DMSO (5.52×10^{-5} M) solution of **9o** with 312 nm light for 85 s, and greater than 420 nm light for 16 min.

Enzyme activity assay (EC 4.2.1.1)

Materials and methods

stock solutions	code
Tris sulfate buffer 20 mM, pH 8.3 at 0°C ([Phenol red] = 5.6 x 10–4 M)	**A**
distilled water	**B**
CO_2 water (2.46 x 10^{-3} M)[a]	**C**
enzyme solution (3.33 x 10^{-6} M)[b]	**D**

[a] Prepared by bubbling CO_2 from a gas bottle through 200 mL distilled water at 0°C for 10 min. The final concentration was determined by precipitation with an aqueous 0.1 M $Ba(OH)_2$ solution and back-titration with 1 N HCl solution. [b] Diluted from a 3.33 x 10^{-5} M stock solution.

blank samples[a]	
solution	vol (mL)
A	3.0
B	0.05
C	1.0

test samples[a]	
solution	vol (mL)
A	3.0
D	0.05
B	1.0

[a] Stirred at 100 rpm.

The enzyme activity was determined using the following equation:

$$\frac{t_{blank} - t_{test}}{t_{test}}$$

The binding affinity was determined using the Cheng-Prusoff equation:

$$K_i = \frac{IC_{50}}{1 = (\frac{C_{substrate}}{K_m})}$$

Results.

a) Bis(sulphonamide) **7**.

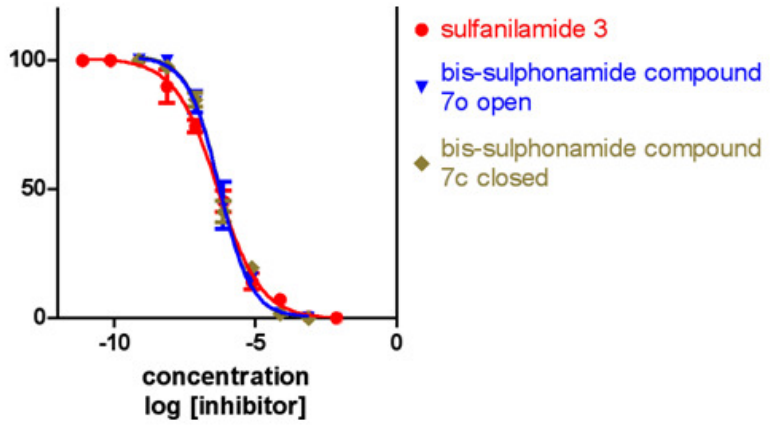

inhibitor	IC_{50} (μM)		K_i (μM)	
	ring-open	ring-closed	ring-open	ring-closed
4	0.46 ± 0.01		0.29 ± 0.007	
6	0.53 ± 0.007	0.57 ± 0.01	0.34 ± 0.005	0.35 ± 0.008

Figure S6. Inhibition measurements of bis(sulphonamide) **7** compared with sulphanilamide **4**.

b) Bis(IDA) 8.

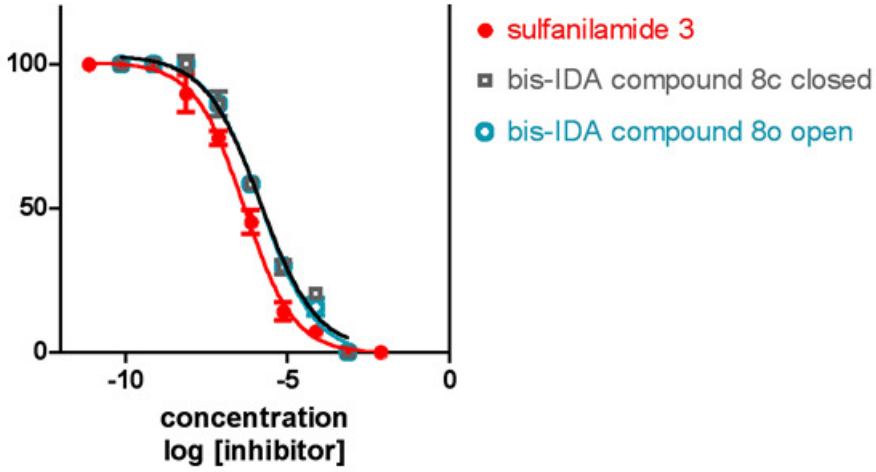

inhibitor	IC_{50} (μM)		K_i (μM)	
	ring-open	ring-closed	ring-open	ring-closed
4	0.46 ± 0.01		0.29 ± 0.007	
7	1.55 ± 0.8	1.46 ± 0.15	1.16 ± 0.05	1.00 ± 0.01

Figure S7. Inhibition measurements of bis(IDA) **8** compared with sulphanilamide **4**.

References

(1) Norsten, T.B.; Branda, N.R. *J. Am. Chem. Soc.* **2001**, *123*, 1784-1785.

(2) Egger; M.; Li; X.; Mueller; C.; Bernhardt; G.; Buschauer; A.; König, B. *Europ. J. Org. Chem* **2007**, (16), 2643-2649.

Carbonic anhydrase inhibitors: Two-prong versus mono-prong inhibitors of isoforms I, II, IX, XII and XIV exemplified by photochromic 1,2-dithienylethene derivatives[2]

This chapter deals with investigations of photoresponsive inhibitors, synthesized in chapter before, to human carbonic anhydras isoforms (hCA I, II; IV, XII) by using computer assisted stopped-flow measurements.

All the measurements on enzyme inhibtions were done by Alessio Innocenti, from the working group of Dr. Claudiu Supuran (University of Florence). The photo-isomerizations during these measurements were done by Daniel Vomasta.

[2] Daniel Vomasta, Alessio Innocenti, Burkhard König, Claudiu T. Supuran, *Bioorg. Chem. Med. Lett.* submitted.

III. Carbonic anhydrase inhibitors: Two-prong versus mono-prong inhibitors of isoforms I, II, IX, XII and XIV exemplified by photochromic 1,2-dithienylethene derivatives

Abstract

We investigated the inhibition of five physiologically relevant CA isoforms with photochromic 1,2-dithienylethene-based compounds incorporating either a benzenesulfonamide and Cu(II)-iminodiacetic acid (IDA)-, bis-benzenesulfonamide-, bis-Cu(II)-IDA- and bis-ethyleneglycol-methyl ether moieties, in both their open- and closed-ring forms. For hCA I the best inhibitors were the mono-prong bis-sulfonamide and the bis-Cu-IDA complexes (K_Is of 2-3 nM) in their open form. For hCA II, best inhibitors were the open and closed forms of the mono-prong bis-sulfonamide (K_Is of 13-18 nM). hCA IX was moderately inhibited by these compounds (K_Is of 9-376 nM) whereas hCA XII and XIV were less susceptible to inhibition (K_Is of 1.12 – 16.7 μM).

III.1 Introduction

The carbonic anhydrases (CAs, EC 4.2.1.1) are ubiquitous metalloenzymes present in prokaryotes and eukaryotes, encoded by at least five distinct, evolutionarily unrelated gene families: the α-CAs (in prokaryotes from the bacteria domain, algae, cytoplasm of green plants, and vertebrates with 15 isozymes presently known in humans), the β-CAs (predominantly in bacteria, fungi, algae, and chloroplasts of both mono- as well as dicotyledons), the γ-CAs (in archaea and some bacteria), the δ-CAs, found so far only in marine diatoms, and the recently characterized ξ-CAs, which are cadmium enzymes also present in marine diatoms.[1-8] CAs catalyze the conversion of CO_2 to the bicarbonate ion and protons. The active site of most CAs contains a zinc ion, which is essential for catalysis. The CA reaction is involved in many physiological and pathological processes, including respiration and transport of CO_2 and bicarbonate between metabolizing tissues and lungs; pH and CO_2 homeostasis; electrolyte secretion in various tissues and organs; biosynthetic reactions (such as gluconeogenesis, lipogenesis and ureagenesis); bone resorption, calcification; and tumorigenicity.[3]

Two main classes of CA inhibitors (CAIs) are known: the metal-complexing anions, and the substituted sulfonamides and their bioesters (sulfamates, sulfamides), which bind to the metal ion of the enzyme either by substituting the non-protein zinc ligand to generate a tetrahedral adduct or by addition of the metal coordination sphere, generating trigonal-bipyramidal species.[3,4] However a critical problem in the design of CAIs with pharmacological applications in the treatment and prevention of various diseases is related to the high number of isoforms (16 in mammals), their rather diffuse localization in many tissues/organs, and the lack of isozyme selectivity of the presently available inhibitors.[3-5] By attaching amino acid moieties with coordinating metal ion properties to the sulfonamide, compounds with interesting activity were obtained. Indeed, the polyamino acyl derivatized sulfonamides with tails such as IDA (iminodiacetic acid), EDTA (ethylenediamino tetraacetic acid) or DTPA (diethylenetraamino pentaacetic acid) as well as their Zn(II), Cu(II) or Al(III) complexes were shown to act as very potent CAIs against several isozymes

such as CA I, II, IV and IX.[9] The idea of this approach is to assure a high binding affinity of the inhibitor towards the enzyme through the supplementary interaction between the metal present in the CAI and amino acid residues from the active site, such as His 64, and therefore increase the inhibitory effect.[3, 9, 10] Another interesting aspect for this type of compounds is to control this effect by an external input, such as light, to have an alternative medicinal tool for influencing enzyme inhibition.[10] Molecules constructed from the photochromic diarylethene scaffold decorated with the Cu(II)-IDA (copper(II)-iminodiacetic acid) complex[11] and a sulfonamide zinc-binding group, were recently shown to act as potent inhibitors for the human isoform CA I (hCA I). In such compounds, the enzyme inhibition can be also regulated by light.[9, 10] Herein, we extend the earlier inhibition studies, and report the ability of some of these photochromic compounds to selectively inhibit physiologically relevant hCA isozymes such as hCA I, II (cytosolic, widespread isoforms) as well as hCA IX, XII and XIV (the first two are transmembrane, tumor-associated isozymes recently shown to represent promising anticancer targets).[2-5]

III.2 Results and discussion

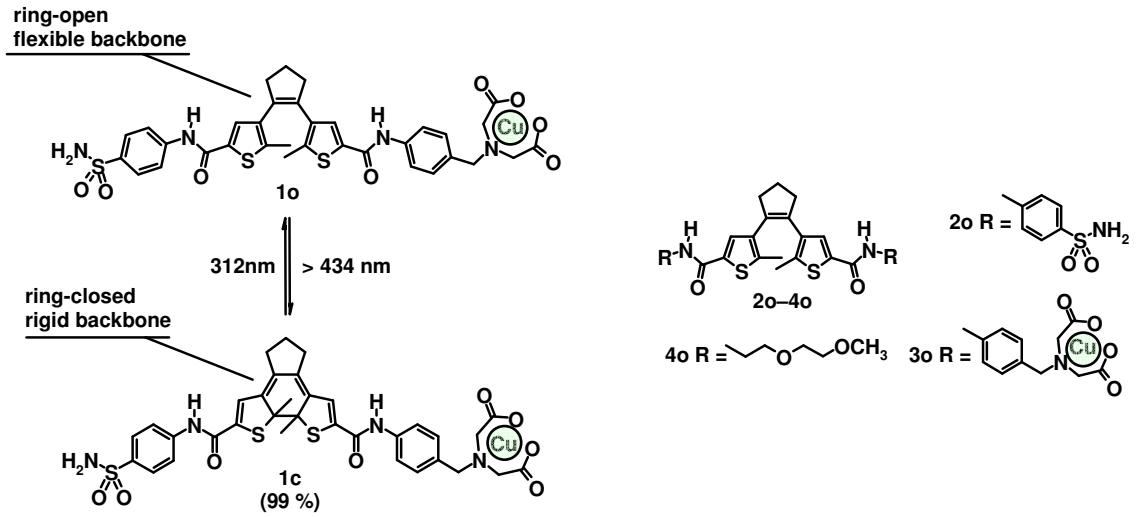

Scheme 4: *Left:* asymmetric two-prong photochromic inhibitor **1o** (open) and the photo-induced conversion of the diarylethene-scaffold with formation of the "closed" isomer **1c**. *Right:* the symmetric compounds **2** (monoprong, bis-sulfonamide), **3** (bis-Cu-IDA complex) and **4** (used as a control).

The synthesis and photochromic properties of compounds **1-4** (Scheme 1) employed in this study were recently reported [10] and will be not discussed here. Irradiation[12] of the 1,2-dithienylethene (DTE) scaffold of the "open" isomers **1o-4o** with the appropriate wavelengths (312 nm and > 420 nm) induce the ring closure due to the cycloaddition reaction, with formation of the "closed" isomers **1c-4c** (Scheme 4). In order to test the efficacy of two-prong versus mono-prong derivatives for obtaining isozyme-selective CAIs, the compound **1o**/**1c** incorporating a benzenesulfonamide head and a copper-IDA tail, together with the corresponding bis-sulfonamides **2o**/**2c** (incorporating two equivalent benzenesulfonamide heads) will be compared for their interactions with various CA isozymes. For assessing the role of the Cu-IDA moiety for the binding of the inhibitors to these enzymes, the compounds **3o**/**3c** (incorporating two equivalent Cu-IDA moieties but no sulfonamide zinc-binding group) were also used in our experiments, together with the presumably non-CA ligands **4o**/**4c**, which incorporate methoxy-ethyleneglycol moieties instead of the benzenesulfonamide/IDA moieties present in the CA ligands **1-3**, which should

have no specific affinity for the CA active site, as they lack structural elements that can coordinate to the Zn(II) ion or interact with His residues involved in the catalytic cycle.[13]

The ring-open isomers **1o** and **2o** show some structural flexibility due to the free rotation around the C-C single bonds joining the two thiophene heterocycles to the central cyclopentene ring, which allows the compounds to adopt a geometry appropriate for binding to the enzyme by means of the sulfonamide moiety (which will be anchored to the Zn(II) ion from the enzyme active site, in the case of both **1o** and **2o**) as well as by the sulfonamide moiety and the copper(II) ion (for **1o**), which may bind to His64 (or another His residue belonging to the His cluster present in the active site of several CA isozymes, such as CA I, II, IX and XII among others).[13] On the other hand, in the "closed" isomers **1c**/**2c**, the free rotation around the C-C single bond is no longer possible (due to its incorporation in the 6-membered ring), the flexibility of the compounds being drastically reduced.[10] Thus, the main difference between the open and closed isomers is the drastic change in flexibility of the molecule. Along with this conformational change, the spatial distance between the two recognition groups present in **1o**/**1c**, i.e., the sulfonamide zinc-binding moiety and the copper-IDA moiety that recognized His residues, are changed as well upon irradiation.[10]

Inhibitor	Ki (nM)*				
	hCA I	hCA II	hCA IX	hCAXII	hCA XIV
1o	4	27	54	1120	7400
1c	14	136	62	3550	2200
2o	2	13	75	4300	16700
2c	18	18	94	4700	2700
3o	3	40	9	2600	15900
3c	3	51	376	5000	2600
4o	>10000	>100000	2080	>100000	4800
4c	>10000	>100000	>100000	>25000	1600
SA	25000	240	294	37	5400
AZA	250	12	25	5.7	41

** Mean value from at least 3 different measurements.[14] Errors were in the range of ± 5 % of the obtained value (data not shown).

Table 1: CA inhibition data against isoforms I, II (cytosolic) and IX, XII and XIV (transmembrane enzymes) with the photochromic compounds **1-4** (o = opened, c = closed isomers) and standard sulfonamide sulfanilamide SA and acetazolamide AZA.

Inhibition data against five physiologically relevant CA isozymes, i.e., the cytosolic, ubiquitous hCA I and II, the transmembrane hCA IX, hCA XII (tumor-associated isoforms) and hCA XIV, with compounds **1-4** (in open (o) and closed (c) forms) as well as the clinically used sulfonamide standards sulfanilamide SA and acetazolamide AZA, are presented in Table 1.[14,15]

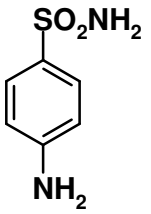

SA

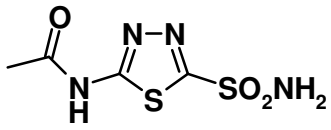

AZA

The following structure-activity relationship (SAR) can be observed for the inhibition of various CA isozymes with compounds **1-4**, SA and AZA:

(i) Against the slow cytosolic isoform hCA I, compounds **1-3** (in both open or closed form) act as very potent inhibitors, with inhibition constants in the range of 2-18 nM, in contrast to the DTE-methoxyethylenoxy-ethyl scaffold **4o**/**4c** which is devoid of any enzyme inhibitory activity. The simple sulfonamides SA and AZA are also rather weak inhibitors of hCA I, with K_Is in the range of 250 nM – 25 μM, as already reported earlier.[4,15] It may be observed that for the sulfonamide derivatives **1** and **2**, the open, more flexible isomers **1o** and **2o** are 3.5 – 9 times more potent hCA I inhibitors as compared to the corresponding closed isomer **1c** and **2c**, respectively, as already documented earlier by some of us.[10] However, two remarkable new findings emerged here. First, the symmetrical bis-sulfonamide derivative **2o** (mono-prong derivative) is two times a better hCA I inhibitor as compared to the two-prong derivative **1o**, although the Cu-IDA moiety should in principle allow a supplementary binding[16] to the His64 residue situated in the middle of the active site cavity and thus further stabilization of the enzyme-inhibitor adduct, over the corresponding bis-sulfonamide **2o**, which cannot interact with His64 or other His residues belonging to the His cluster present in this isoform.[13] Thus, this is a clear-cut example that the two-prong approach[17] is not a general one for designing tight binding CAIs, and more than ever isozyme-selective such compounds, since a bis-sulfonamide devoid of Cu-IDA moieties (**2o**) acts as a better inhibitor than the two-prong, structurally similar compound (**1o**). But what is even more interesting is the fact that the bis-Cu-IDA derivatives **3o** and **3c** showed equipotent, extremely strong hCA I inhibitory activity (K_I of 3 nM), which is intermediate between that of the two-prong inhibitor **1o** (K_I of 4 nM) and the mono-prong bis-sulfonamide **2o** (K_I of 2 nM). Furthermore, the closed ring copper(II) complex **3c** is by far the best hCA I inhibitor among the closed

derivatives **1-3** examined here, with the two-prong **1c** (K_I of 14 nM) and bis-sulfonamide **2c** (K_I of 18 nM) compounds being much less effective inhibitors. We cannot explain these data without an X-ray crystal structure for the adduct of hCA I with **3o** or **3c**, but presumably these derivatives may bind to some of the His residues present within hCA I active site (His64, His67, His200 and His243)[13] which lack in other CA isoforms among those investigated here, without interaction with the catalytically critical Zn(II) ion from the enzyme cavity.

(ii) The ubiquitous, physiologically dominant[2] isozyme hCA II is also inhibited significantly by sulfonamides **1**, **2**, AZA and the copper complexes **3** (K_Is in the range of 12-136 nM), being less susceptible to inhibition with sulfanilamide SA (K_I of 240 nM) and not at all inhibited by the scaffold of **4o**/**4c** (Table 1). Again SAR is very interesting, with the open isomers **1o-3o** being always better hCA II inhibitors than the corresponding closed ones **1c-3c**. As for hCA I, the two-prong compounds **1o**/**1c** are less effective hCA II inhibitors as compared to the mono-prong bis-sulfonamides **2o**/**2c**, but unlike hCA I, the copper complexes **3** are generally weaker inhibitors than the sulfonamides **1** and **2**. It should be also noted that simple sulfonamides such as sulfanilamide and acetazolamide are much better hCA II than hCA I inhibitors, whereas for sulfonamides **1** and **2** incorporating the DTE scaffold, just the opposite is true.

(iii) The tumor-associated isoform hCA IX is moderately inhibited by compounds **1**, **2**, **3c** and SA (K_Is in the range of 54 – 376 nM) being strongly inhibited only by the open copper complex 3o and AZA (K_Is of 9-25 nM). For this isoform, the two-prong inhibitors **1o**/**1c** showed better inhibitory activity as compared to the mono-prong ones **2o**/**2c**, but unexplainably the best inhibitor does not possess a sulfonamide moiety (**3o**). The differences of inhibitory activity between **3o** and **3c** are also quite important, with the closed isomer being 41.7 times less inhibitory than the open one.

(iv) The transmembrane isozymes hCA XII and XIV showed less susceptibility to be inhibited by the compounds investigated here, with inhibition constants in the range of 1.12 – 15.9 μM, orders of magnitude higher than for the isozymes discussed earlier. As for hCA IX, also for hCA XII and XIV the two prong inhibitors were slightly more effective than the mono-prong ones, whereas the copper complexes **3** showed also a weak inhibitory capacity. Whereas derivatives **4** showed no notable interaction with the enzymes

discussed above (except **4o** with hCA IX), these ethers seem to inhibit appreciably (in the low micromolar range) hCA XIV. Further studies are warranted to understand the inhibition mechanism of **4** against hCA XIV since this compound does not possess an obvious structural motif that should interact with the CA active site.

III.3 Conclusion

In conclusion we investigated the inhibition of five physiologically relevant CA isoforms with DTE-based compounds incorporating both a sulfonamide and Cu-IDA, bis-sulfonamide, bis-Cu-IDA and bis-ethyleneglycol-methyl ether moieties, in both their open- and closed-ring forms. For hCA I the bst inhibitors were the mono-prong bis-sulfonamide and the bis-Cu-IDA complexes (K_Is of 2-3 nM) in their open form. For hCA II, best inhibitors were the open and closed forms of the mono-prong bis-sulfonamide (K_Is of 13-18 nM). HCA IX was moderately inhibited by these compounds (K_Is of 9-376 nM) whereas hCA XII and XIV were less susceptible to inhibition (K_Is of 1.12 – 16.7 μM).

III.4 References and notes

(1) a) Krishnamurthy, V. M.; Kaufman, G. K.; Urbach, A. R.; Gitlin, I.; Gudiksen, K. L.; Weibel, D. B.; Whitesides, G. M. *Chem. Rev.* 2008, *108*, 946; b) Xu, Y.; Feng, L.; Jeffrey, ; Shi, Y.; F. M. Morel, F. M. *Nature* 2008, *452*, 56.

(2) Supuran, C. T. *Nat. Rev. Drug. Discov.* 2008, *7*, 168.

(3) Chiche, J.; Ilc, K.; Laferrière, J.; Trottier, E.; Dayan, F.; Mazure, N.M.; Brahimi-Horn, M.C.; Pouysségur, J. *Cancer. Res*. 2009, *69*, 358-68.

(4) *Carbonic anhydrase - Its inhibitors and activators;* Supuran, C. T., Scozzafava, A., Conway, J., Eds.; CRC Press: Boca Raton (FL), USA, 2004; pp. 1–376. and references therein.

(5) a) Supuran, C. T.; Scozzafava, A.; Casini, A. *Med. Res. Rev.* 2003, *23*, 146; b) Supuran, C. T.; Scozzafava, A. *Bioorg. Med. Chem.* 2007, *15*, 4336; c) Innocenti, A.; Scozzafava, A. ; Parkkila, S.; Puccetti, L.; De Simone, G.; Supuran, C. T. *Bioorg. Med. Chem. Lett.* 2008, *18*, 2267.

(6) Tripp, B. C.; Smith, K. S.; Ferry, J. G. *J. Biol. Chem.* 2001, *276*, 48615.

(7) Klengel, T.; Liang, W. J.; Chaloupka, J.; Ruoff, C.; Schropel, K.; Naglik, J. R.; Eckert, S. E.; Morgensen, E. G.; Haynes, K.; Tuite, M. F.; Levin, L. R.; Buck, J.; Mühlschlegel, F. A. *Curr. Biol.* 2005, *15*, 2021.

(8) Cox, E. H.; McLendon, G. L.; Morel, F. M.; Lane, T. W.; Prince, R. C.; Pickering, I. J.; George, G. N. *Biochemistry* 2000, *39*, 12128.

(9) a) Scozzafava, A.; Menabuoni, L.; Mincione, F.; Supuran, C. T. *J. Med. Chem.* 2002, *45*, 1466; b) Scozzafava, A.; Menabuoni, L.; Mincione, F.; Mincione, G.; Supuran, C.T. *Bioorg. Med. Chem. Lett*. 2001, *11*, 575

(10) Vomasta, D.; Högner, C.; Branda, N. R.; König, B. *Angew. Chem. Int. Ed.* 2008, *47*, 7644.

(11) Kruppa, M.; König, B. *Chem. Rev.* 2006, *106*, 3520.

(12) Standard hand-held lamps used for visualizing TLC plates (Herolab, 6 W) were used to carry out the ring-closing reactions at 312 nm. The ring-opening reactions were carried out using the light of a 200 W tungsten source that was passed through a 420 nm cut-off filter to eliminate higher energy light. The power of the light source is given based on the

specifications supplied by the company when the lamps were purchased. A light detector was not used to measure the intensity during the irradiation experiments.

(13) a) Briganti, F.; Mangani, S.; Orioli, P.; Scozzafava, A.; Vernaglione, G.; Supuran, C.T. *Biochemistry* 1997, *36*, 10384; b) Di Fiore, A.; Monti, S.M.; Hilvo, M.; Parkkila, S.; Romano, V.; Scaloni, A.; Pedone, C.; Scozzafava, A.; Supuran, C.T.; De Simone, G. *Proteins*, 2008, *74*, 164.

(14) Khalifah, R.G.; *J. Biol. Chem.* 1971, *246*, 2561. An Applied Photophysics stopped-flow instrument has been used for assaying the CA catalyzed CO_2 hydration activity. Phenol red (at a concentration of 0.2 mM) has been used as indicator, working at the absorbance maximum of 557 nm, with 20 mM Hepes (pH 7.5) as buffer, and 20 mM Na_2SO_4 (for maintaining constant the ionic strength), following the initial rates of the CA-catalyzed CO_2 hydration reaction for a period of 10-100 s. For each inhibitor at least six traces of the initial 5-10% of the reaction have been used for determining the initial velocity. The uncatalyzed rates were determined in the same manner and subtracted from the total observed rates. Stock solutions of inhibitor (10 mM) were prepared in distilled-deionized water and dilutions up to 0.01 nM were done thereafter with distilled-deionized water. Inhibitor and enzyme solutions were preincubated together for 15 min at room temperature prior to assay, in order to allow for the formation of the E-I complex. The inhibition constants were obtained by non-linear least-squares methods using PRISM 3, as reported earlier,[9] and represent the mean from at least three different determinations. Mammalian CA isozymes were prepared in recombinant form as reported earlier by our group. [15]

(15) a) Nishimori, I.; Vullo, D.; Innocenti, A.; Scozzafava, A.; Matrolorenzo, A.; Supuran, C.T. *Bioorg. Med. Chem. Lett.* 2005, *15*, 3828; b) Ozensoy, O.; Nishimori, I.; Vullo, D.; Puccetti, L.; Scozzafava, A.; Supuran, C.T. *Bioorg. Med. Chem.* 2005, *13*, 6089; c) Vullo, D.; Innocenti, A.; Nishimori, I.; Pastorek, J.; Scozzafava, A.; Pastorekova, S.; Supuran, C.T. C *Bioorg. Med. Chem. Lett*. 2005, *15*, 963.

(16) Roy, B.C.; Banerjee, A.L.; Swanson, M.; Jia, X.G.; Haldar, M.K.; Mallik, S.; Srivastava, DK. *J. Am. Chem. Soc*. 2004, *126*, 13206

(17) Banerjee, A.L.; Eiler, D.; Roy, B.C.; Jia, X.,.;Haldar, M.K.; Mallik, S.; Srivastava, D.K. *Biochemistry* 2005, *44*, 3211.

Binding of Phosphates using a Photochromic bis-Zn(II)-cyclen Derivative

This chapter deals with the use of photoresponsive dithienylethenes (DTE), decorated with Zn(II)-cyclen moieties, in order to create photoswitchable recognition of phosphate dianions.

Synthesis of the compounds as well as all the measurements were done by Daniel Vomasta.

IV. Binding of Phosphates using a Photochromic bis-Zn(II)-cyclen Derivative

IV.1 Introduction

Recently, considerable attention has been paid to the design of receptors and sensors that have the ability to bind biologically important anions selectively by electrochemical or optical response. Anions such as pyrophosphate (PP_i) and adenosine triphosphate (ATP) play an important role in the energy metabolism of organisms and the control of metabolic enzymatic processes.[1,2] ATP hydrolysis with the concomitant release of PP_i is central to many biochemical reactions, such as DNA polymerization and the synthesis of cyclic adenosine monophosphate (cAMP) catalyzed by DNA polymerase and adenylyl cyclase, respectively.[1,2] Therefore, synthetic receptors with photoregulated affinity to important phosphate anions can be envisaged as a powerful tool in biomolecular and medicinal chemistry. Existing examples of photo-regulated coordinative binding processes use azobenzenes[3-6], spirobenzopyrans[7,8] or pyrene[9] in combination with crown ethers to sense cations, like for example caesium and ammonium ions. However, these photoresponsive units lack thermal stability and interconvert without irradiation. Therefore diarylethenes have been combined with crown ethers to create photoresponsive tweezers for various cations.[10,11] Molecules that are known to bind phosphate anions in water at physiological pH are either Lewis acidic bis-pyridylmethylamine (Zn(II)-BPA) zinc complexes [12,13] or cyclen (1,4,7,10-tetraazacyclodecane) zinc complexes.[14,15]

We report the synthesis of photoresponsive bis-Zn(II)-cyclen derivatives using dithienylethenes as photochromic unit.[16]

IV.2 Results and discussion

Synthesis

The synthesis of photoresponsive cyclen derivatives started with the symmetric coupling of the acid chloride of compound **3**[17] with protected cyclen **4** or **5** (Figure 5, see experimental part for their synthesis). After removal of the protecting groups under acidic conditions, neutralization on an ion exchange column and treatment with $ZnCl_2$ afforded photoresponsive compounds **1o** and **2o** in very good yields.

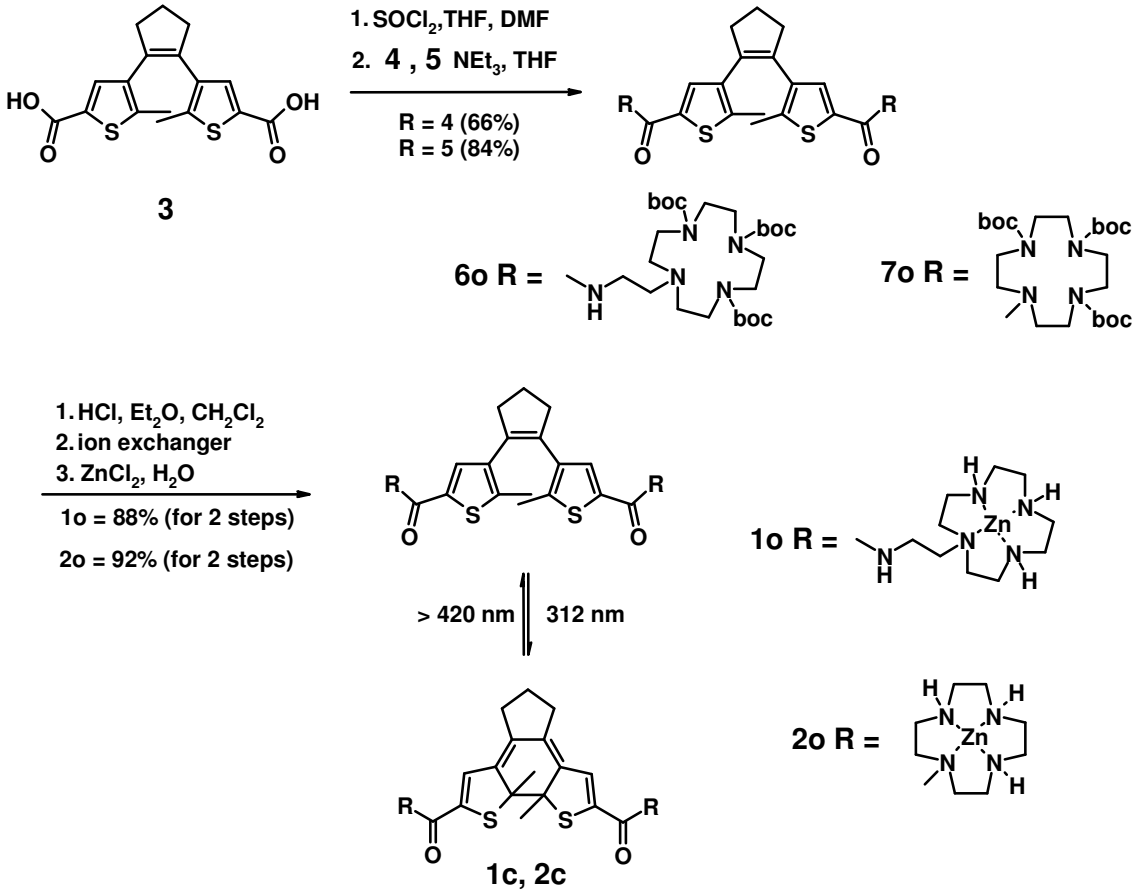

Figure 5. Synthesis of photochromic cyclen-derivatives **1o** and **2o** and the photochemical ring-closing reaction

Photochromism

Irradiating an aqueous solution of **1o** (HEPES = 2-(4-(2-Hydroxyethyl) - 1-piperazinyl)-ethansulfonic acid, 50 mM, pH = 7.4, I = 154 mM NaCl, 25 °C) with 312 nm light resulted in immediate changes of the UV/VIS absorption spectra that are typical for photoresponsive dithienylethene (DTE) derivatives. The high energy band (λ_{max}= 265 nm) decreases in intensity and an absorption band at λ_{max}= 350 nm as well as in the visible spectral region (λ_{max}= 529 nm) appears as the solution changes from colourless to red upon formation of the ring-closed isomer **1c** (Figure 6 left part). These spectral changes are completed after irradiation for 60 s (at a concentration of 50 µM), and a photostationary state containing at least 95% of the ring-closed isomer is generated according to ^{1}H-NMR analysis of the reaction mixture. For compound **2** the high energy band (λ_{max}= 280 nm) decreases in intensity and an absorption band in the visible spectral region (λ_{max}= 490 nm) evolves (Figure 6 right part). These spectral changes are completed after irradiation for 140 s (at a concentration of 10 µM), and a photostationary state containing at least 92% of the ring-closed isomer is generated according to ^{1}H-NMR analysis of the reaction mixture.

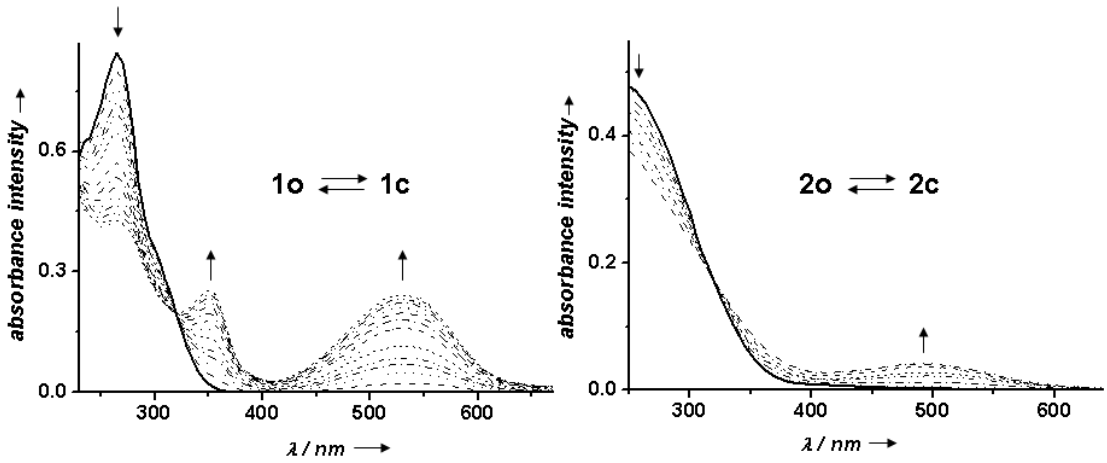

Figure 6. *Left*: Changes in the UV/VIS absorption spectra of an aqueous solution of **1o** (50 µM) in HEPES buffer (50 mM, pH 7.4, 154 mM NaCl), when irradiated with 312 nm light. Irradiation periods were 0, 2, 4, 6, 8, 11, 14, 18, 22, 26, 30, 35, 40, 50, 60 s. *Right*: Changes in the UV/VIS absorption spectra of an aqueous solution of **2o** (50 µM) in HEPES buffer (50 mM, pH 7.4, 154 mM

NaCl), when irradiated with 312 nm light. Irradiation periods were 0, 3, 10, 20, 30, 50, 70,100,140 s.

This effective photoconversion shows the versatility of the dithienylethene backbone as photoresponsive unit.

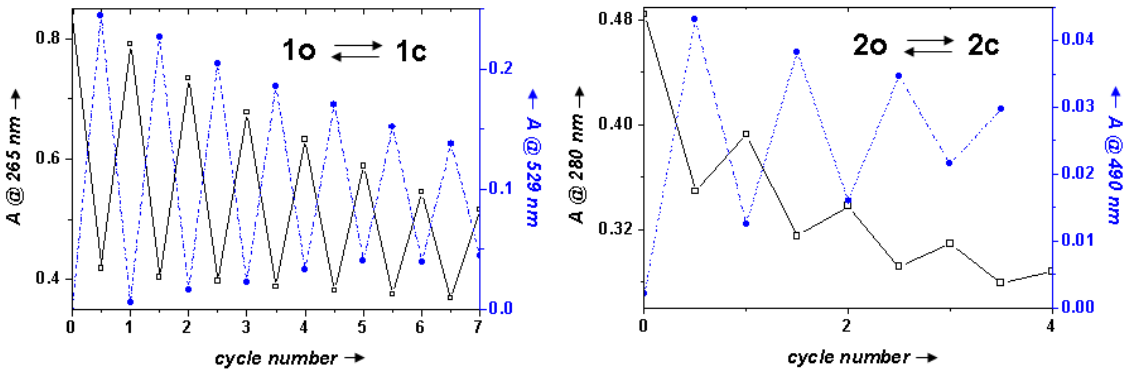

Figure 7. *Left*: Cycle performance of photochromic cyclen-derivative **1**. The changes in absorbance upon alternate irradiation, with UV- and visible light (312 nm and > 420 nm), of the ultraviolet band (λ_{max}= 265 nm, black solid line) as well as of the visible band (λ_{max}= 529 nm, blue dotted line) were plotted against the cycle number. *Right*: Cycle performance of photochromic cyclen-derivative **2**. The changes in absorbance upon alternate irradiation, with UV- and visible light (λ = 312 nm and > 420 nm), of the ultraviolet band (λ_{max}= 280 nm, black solid line) as well as of the visible band (λ_{max}= 490 nm, blue dotted line) were plotted against the cycle number.

The durability of the photochromic Zn(II)-cyclen derivatives **1** and **2**, was studied by alternate irradiation with UV-light (λ = 312 nm) and visible light (λ > 420 nm), respectively. The absorption band in the UV-region as well as in the visible region were followed and plotted against the cycle number (Figure 7). Compound **1** shows a fast loss of performance and therefore a high tendency of photodegradation. This process is even faster for compound **2**. The compound is almost completely degraded after only four cycles. This is due to the labile amide bond between the dithienylethene scaffold and the zinc(II)-cyclen moiety, which is cleaved by UV-light and leads to decomposition of the photochromic scaffold.

Binding studies

Indicator displacement assay

Photoresponsive Zn(II)-cyclen derivatives **1** and **2** do not emit light upon irradiation at their absorbance maximum, neither as the ring-open isomer nor as in the ring-closed isomer. Therefore, an indicator displacement assay[18,19] was used to study the binding of various phosphate anions.

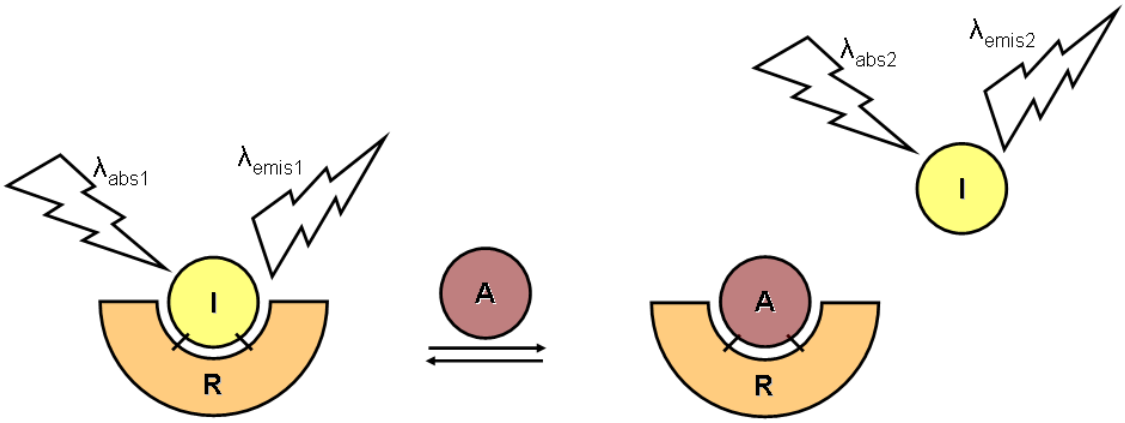

Figure 8. Cartoon of the indicator displacement method (I = indicator, R = receptor, A = analyte). Excitation arrows indicate excitation and emission of the indicator (I).

In an indicator displacement assay, a receptor (R) with an affinity for a given analyte (A) forms a reversible non-covalent complex with an indicator (I), usually a fluorescent or UV/Vis indicator dye. Upon complexation with the receptor (R), the spectral properties of the indicator change (shift of the absorption maximum, enhancement, wavelength shift or quenching of the emission signal). Treatment of the receptor-indicator complex with the analyte displaces the indicator from the receptor, thereby restoring the indicator's original spectral properties and signalling the presence of the analyte (Figure 8). Coumarine methyl sulfonate (CMS) was used as indicator for the photoresponsive Zn(II)-cyclen derivatives **1** and **2**,. The maximal excitation wavelength of λ_{ex} = 397 nm of the indicator matches the wavelength range

where compounds **1** and **2** have no absorption (ring open isomers **1o** and **2o**) or a minimum in their absorption intensity (ring-closed isomers **1c** and **2c**).

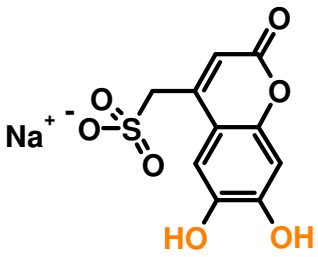

CMS

Figure 9. Indicator coumarine methyl sulfonate (CMS), which is used in the indicator displacement assay. The orange colour indicates the groups which are presumably interacting with the metal complex.

Phosphate analytes

Five different phosphates including mono-phosphates and di-phosphates were investigated as the analytes for binding to compounds **1** and **2**.

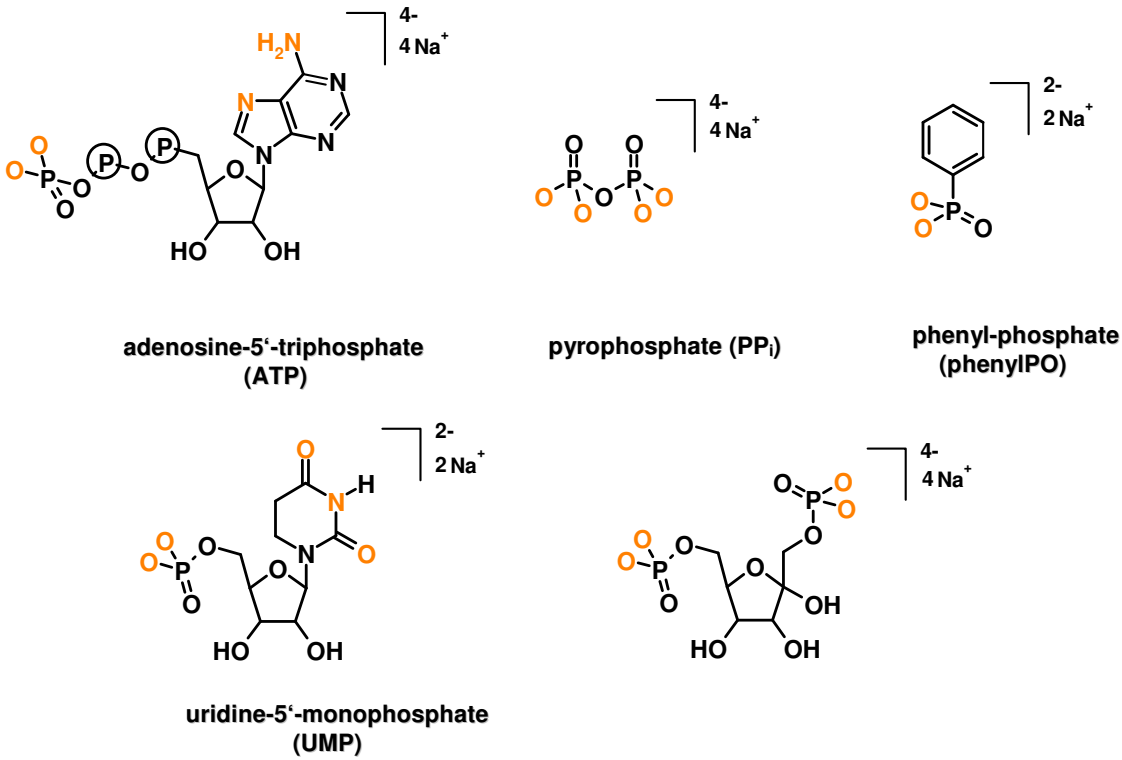

Figure 10. Representative phosphate anions (ATP, PP_i, phenylPO, UMP, 1, 6-FruPO, all sodium salts) for binding studies with Zn(II)-cyclen derivatives **1** and **2**. Orange atoms indicate potentially interacting atoms.

*Binding studies for compound **1***

Zn(II)-cyclen derivative **1** exhibits high flexibility in the ring-open isomer **1o**, due to the free rotation around the bond connecting the central cyclopentene ring and the thiophene heterocycles as well as in the side-chain connecting the Zn(II)-cyclen moiety and the DTE scaffold. In the ring-closed isomer **1c** the flexibility is reduced, however this isomer is still very flexible due to the flexibility of the side-chain. The

affinity of lg K = 4 for the interaction of compound **1o** and of compound **1c** with the indicator (CMS) is comparable (Table 2). The flexibility of both isomers may account for this observation and leads to two coordinative aggregates which are detected in solution (see experimental part, Figure 23, for an illustration).

*Fluorescence titration of CMS with Zinc(II)-cyclen derivative **1***:

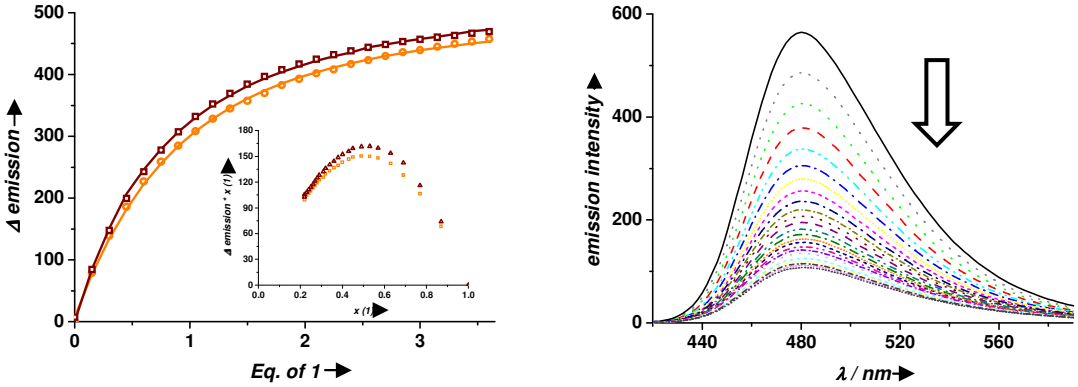

Figure 11. *Left*: Fluorescence titration of CMS (50 µM) in HEPES buffer (50 mM, physiological pH (7.4), 25°C, I = 154 mM NaCl) with compound **1o** and **1c** (300 µM). Changes in emission intensity are plotted against equivalents (eq) of compound **1o** and **1c**. The inset shows the Job's plot analysis. Yellow circles represent **1o** and the solid line represents the best fit of the data. Brown squares represent **1c** and the solid brown line represents the best fit of the data. *Right*: Changes in fluorescence upon addition of increasing amounts of zinc(II)-cyclen derivatives. The solid black line indicates the initial spectrum of coumarine methyl sulfonate (CMS).

Results:

	1o vs CMS (1o:CMS)	1c vs CMS (1c:CMS)
fluorescence[a]	$\log K_1$ (1:1) = 4.3	$\log K_1$ (1:1) = 4.3
	$\log K_2$ (1:2) = 3.0	$\log K_2$ (1:2) = 2.1
ITC[b]	$\log K_1$ (1:1) = 4.3 ± 0.6	$\log K_1$ (1:1) = 4.1 ± 0.2
	$\log K_2$ (1:2) = 3.2 ± 0.1	$\log K_2$ (1:2) = 2.5 ± 0.2

[a]Errors were in the range of ± 10 % of the obtained value (data not shown).

[b]ITC measurements shown in the experimental section.

Table 2. Results of the fluorescence titration of compound **1** with coumarine methyl sulfonate and the comparison with data obtained from isothermal titration calorimetry (ITC).

The interaction with the analytes showed similar behaviour like for the indicator (Table 3). For PP_i, also ITC measurements were performed in order to confirm the data obtained by fluorescence.

	open logK (1 : A)	closed logK (1 : A)	ITC open logK (1 : A)	ITC closed logK (1 : A)
ATP	4.0 (1:2)	5.0 (1:1)	-	-
	3.52 (1:1)	-		
	3.0 (2:2)			
PP_i	4.9 (2:2)	5.8 (1:1)	5.2±0.4 (2:2)	6.1±0.6 (1:1)
	3.0 (1:2)	4.4 (2:2)	3.4±0.3 (1:2)	3.9±0.3 (2:2)
UMP	< 4.3	< 4.3	-	-
1, 6-FruPO	< 4.3	< 4.3	-	-
PhenylPO	< 4.3	< 4.3	-	-

A = analyte; errors were in the range of ± 10 % of the obtained value (data not shown)

Table 3. Results of the fluorescence measurements of **1** (50 µM) against different analytes (300 µM) in HEPES buffer (50 mM, physiological pH (7.4), 25 °C, I = 154 mM NaCl) as well as the results from ITC measurements for PP_i.

Analytes UMP, 1,6-FruPO and PhenylPO do not interact with photo-isomers **1o** and **1c** with a significant larger affinity than CMS as the indicator is not displaced. Analytes ATP and PP_i are able to displace the indicator and therefore an increase in the fluorescence intensity is observed. The difference in affinity between the ring-open **1o** and the ring-closed isomer **1c** are about one order of magnitude for PP_i. In the case of ATP the binding ability of **1o** and **1c** is different as three aggregates could be detected in the ring-open form and only one aggregate for the ring-closed isomer. The formed aggregate changes and the binding affinities show a drastic change. However, currently no detailed

explanation of the different binding situations is available. (For illustrations of possible binding motifs see experimental part).

*Binding studies for compound **2***

Compared to compound **1** Zn(II)-cyclen derivative **2** shows larger changes in its conformational rigidity upon irradiation with UV-light. Upon irradiation the more flexible open isomer of the DTE is converted into the planar-rigid isomer and therefore the flexibility of the whole structure is decreased. Although the change in conformational constrain is presumably more pronounced in this compound compared to **1** the affinity towards CMS is still within the same range (lg K = 4) for the ring-open **2o** and the ring-closed isomer **2c**. Also in this case two coordinative aggregates were observed which are present in the solution. (For illustrations of possible binding motifs see experimental part, Figure 23).

*Emission titration of CMS with Zinc(II)-cyclen derivative **2***:

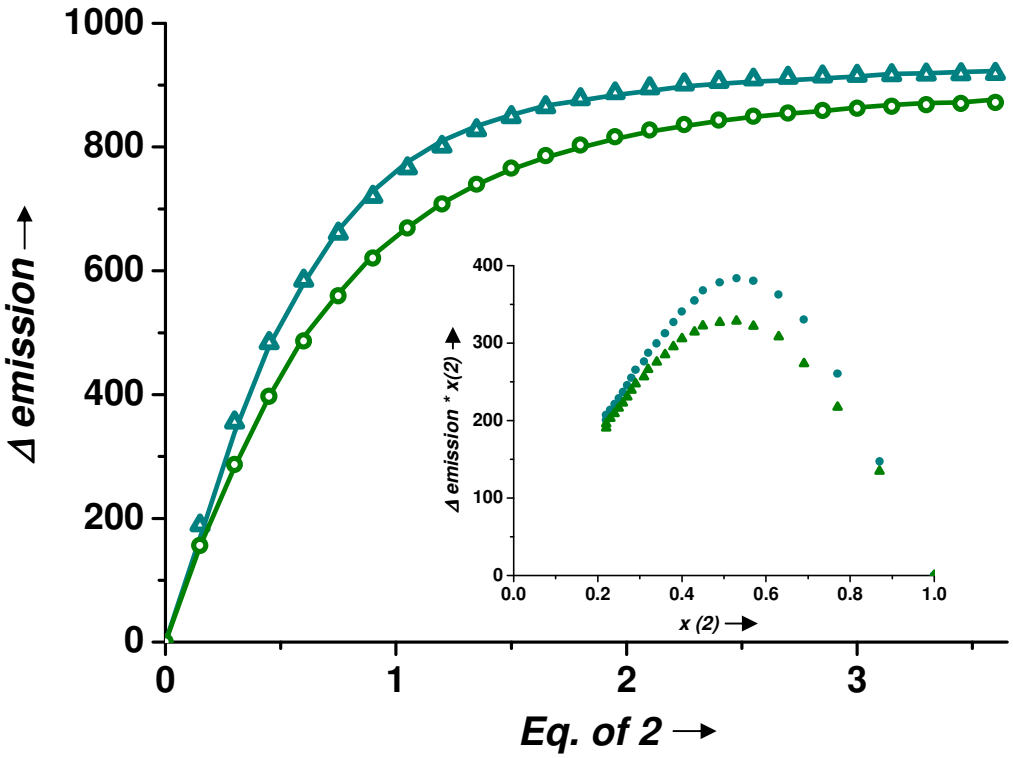

Figure 12. Fluorescence titration of CMS (50 µM) in HEPES buffer (50 mM, physiological pH (7.4), 25°C, I = 154 mM NaCl) with compounds **2o** and **2c** (300 µM).

Changes in emission intensity are plotted against equivalents (eq) of compound **2o** or **2c**. The inset shows the Job's plot analysis. Blue triangles represent **2o** and the solid line represents the best fit of the data. Green circles represent **2c** and the solid green line represents the best fit of the data.

Results:

	2o vs CMS (2o:CMS)	**2c vs CMS (2c:CMS)**
fluorescence[a]	$\log K_1$ (1:1) = 4.4	$\log K_1$ (1:1) = 4.8
	$\log K_2$ (1:2) = 2.5	$\log K_2$ (1:2) = 2.2
ITC[b]	$\log K_1$ (1:1) = 4.5 ± 0.1	$\log K_1$ (1:1) = 4.7 ± 0.4
	$\log K_2$ (1:2) = 2.0	$\log K_2$ (1:2) = 2.7 ± 2.1

[a]Errors were in the range of ± 10 % of the obtained value (data not shown)

[b]ITC measurements shown in the experimental section.

Table 4. Results of fluorescence titration of CMS with compound **1**. Data obtained from emission measurements are compared with data obtained from isothermal titration calorimetry (ITC).

	open logK (2 : A)	closed logK (2 : A)	ITC open logK (2 : A)	ITC closed logK (2 : A)
ATP	< 4.4	4.5 (1:1)	-	-
		3.7 (1:2)		
PP_i	5.0 (1:1)	4.7 (1:1)	4.5±0.4 (1:1)	5.3±0.3 (1:1)
	3.0 (2:2)	3. 6 (2:2)	3.4±0.3 (2:2)	3.6±0.1 (2:2)
UMP	< 4.4	< 4.8	-	-
FruPO	< 4.4	< 4.8	-	-
PhenylPO	< 4.4	< 4.8	-	-

A = analyte; Errors were in the range of ± 10 % of the obtained value (data not shown)

Table 5. Results of the fluorescence measurements of **2** (50 µM) against different analytes (300 µM) in HEPES buffer (50 mM, physiological pH (7.4), 25°C, I = 154 mM NaCl) as well as the results from ITC measurements for PP_i.

Table 4 summarizes the response from the displacement assay of the **2**-CMS complex to several analytes. ITC measurements of the binding of compound **2** and PP_i were performed in order to confirm the data obtained by fluorescence. Analytes UMP, 1, 6-FruPO and PhenylPO do not displace CMS from **2o** and **2c** indicating a smaller affinity. Added PP_i replaces the indicator (lg K = 5), but there are no differences in the affinity of **2o** and **2c**. However, added ATP does not displace CMS in the ring-open isomer **2o**, whereas in the ring-closed isomer **2c** ATP is able to remove CMS from the complex (lg K = 4.5). Although CMS could not be displaced in the ring-open isomer, this is only indicating an affinity lower than the indicator (lg K < 4.8). The exact value for the binding is not known, therefore no mechanism explaining the difference in binding affinity between ring-open and –closed isomer can be given on the basis of the present results.

IV.3 Conclusion

Photoresponsive Zn(II)-cyclen derivatives **1** and **2** were synthesized and tested for phosphate ion recognition using an indicator displacement assay. Compound **1** is conformationally very flexible in the ring-open **1o** as well as in the ring-closed isomeric form **1c**, whereas in complex **2** the conformational mobility is controlled by the DTE scaffold presumably leading to more pronounced differences in conformational constrains. From the investigated analytes only PP_i and ATP are able to displace the indicator CMS and therefore have a higher affinity towards the complexes **1** and **2** compared to the indicator. With both derivatives no distinct coordinative aggregate is observed: In the case of derivative **1** affinity changes were in the range of one order of magnitude for the analyte PP_i. Three coordinative aggregates of ATP with complex **1o** were detected, whereas in the ring-closed isomer **1c** only one single coordinative aggregate structure is present as derived from the analysis of the fluorescence measurement data.

In the case of compound **2** affinities for PP_i within the same order were observed. ATP interacts with the ring-closed isomer **2c** with a larger affinity than CMS, whereas in the ring-open form **2o** the affinity to ATP is lower than for CMS. However, due to the fact that the indicator displacement assay is an indirect method, the exact binding constant of **2o** to ATP remains unknown and no conclusive interpretation about the difference in binding affinity between ring-open –closed isomer can be made.

The synthesis of a more rigid system (Figure 13) is suggested to overcome problems arising from different aggregates in solution. A larger difference in binding affinity to ATP of the ring-open and the ring-closed form is likely.

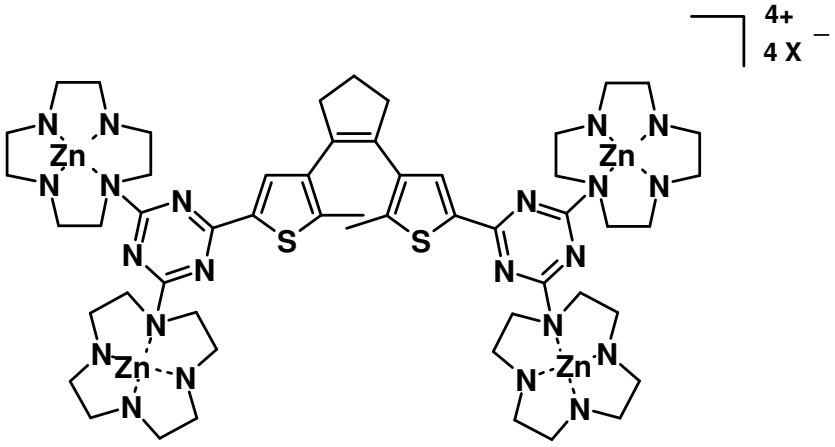

Figure 13. Suggested structure of a more ridgid photoresponsive tetra-Zn(II)-cyclen-DTE[20]

IV.4 Experimental Part

1. Synthesis and characterization of new compounds

General. Thin layer chromatography (TLC) was performed on alumina plates coated with silica gel (Merck silica gel 60 F 254, layer thickness 0.2 mm). Column chromatography was performed on silica gel (70–230 mesh) from Merck. Starting materials were purchased from either Acros or Sigma-Aldrich and used without any further purification. Solvents were purchased from Aldrich and used without further purification except for dry THF, which was prepared by distillation from potassium.

Analytical methods. Melting points (MP) were determined with a Büchi SMP 20. IR-spectra were recorded with a Bio-Rad FTS 2000 MX FT-IR spectrometer. NMR spectra were recorded on a Bruker Avance 400 (1H: 400.1 MHz, 13C: 100.6 MHz, T = 300 K) or a Bruker Avance 300 (1H: 300.1 MHz, 13C: 75.5 MHz, T = 300 K). The spectra are referenced against the NMR-solvent and chemical shifts are reported in ppm. MS-Spectra were determined on a Varian CH-5 (EI), a Finnigan MAT 95 (CI; FAB and FD) or a Finnigan MAT TSQ 7000 (ESI). UV–Vis absorption spectroscopy was performed using a Cary 50 Bio spectrophotometer, fluorescence spectroscopy was performed using a Varian Cary Eclipse fluorescence spectrophotometer.

Photochemistry. Standard hand-held lamps used for visualizing TLC plates (Herolab, 6 W) were used to carry out the ring-closing reactions at 312 nm. The ring-opening reactions were carried out using the light of a 200 W tungsten source that was passed through a 420 nm cut-off filter to eliminate higher energy light. The power of the light source is given based on the specifications supplied by the company where the lamps were purchased. A light detector was not used to measure the intensity during the irradiation experiments.

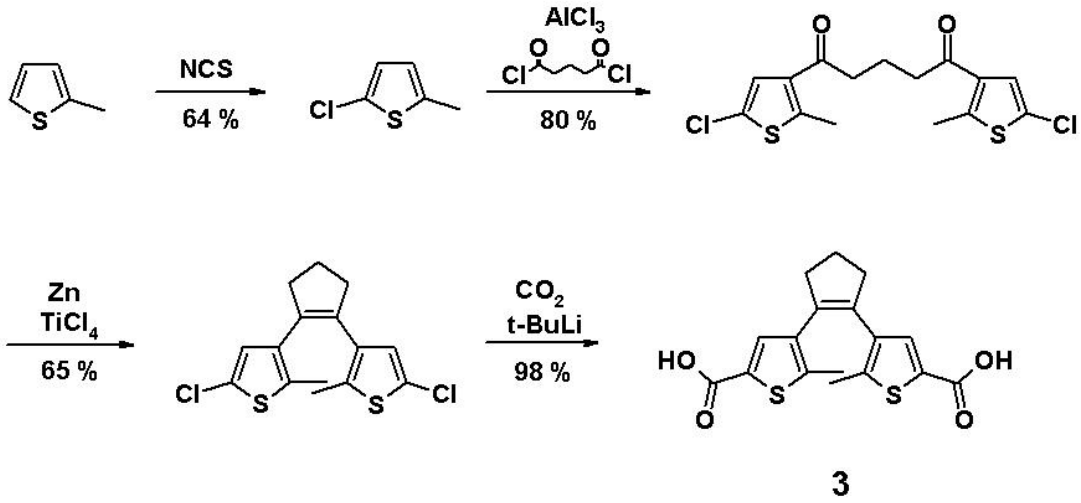

Figure 14. Synthesis of compound **3**[21]

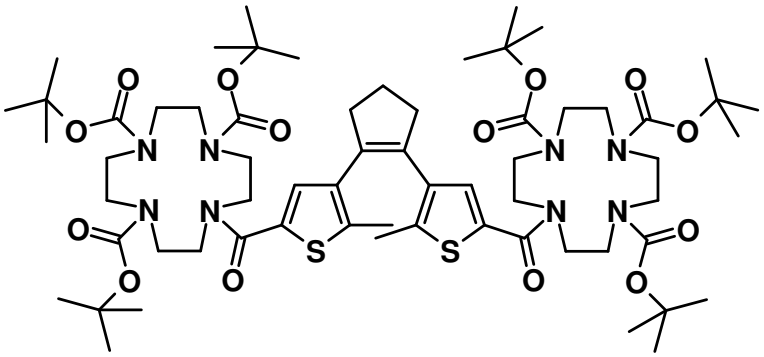

tri-tert-Butyl-10-(5-methyl-4-(2-(5-(4,7,10-tris(tert-butoxycarbonyl)-1,4,7,10-tetraazacyclododecane-1-carbonyl)thiophen-3-yl)cyclopent-1-enyl)thiophene-2-carbonyl)-1,4,7,10-tetraazacyclododecane-1,4,7-tricarboxylate (7o).

3,3'-(Cyclopentene-1,2-diyl)bis(4-methylcyclopenta-1,3-dienecarboxylic acid) **3** (0.2 g, 0.56 mmol), was dissolved in 10 mL of dry THF and 4 drops of DMF were added followed by $SOCl_2$ (0.2 mL, 0.3 g, 2.2 mmol, 4 eq) and stirred at room temperature for 1 h. After this period the solvent was evaporated in *vacuo*, the residue dried in high-vacuum for 2 h and was taken up with dry THF under a N_2-atmosphere. Triethylamine (0.2 mL, 0.2 g, 1.7 mmol, 3 eq) was added in one portion followed by solid tri-tert-butyl 1,4,7,10-tetraazacyclododecane-1,4,7-tricarboxylate (0.5 g, 1.1 mmol, 2 eq) in one portion and the resulting mixture was stirred at room temperature for 20 h. The solvent was evaporated in *vacuo* and the residue purified by column chromatography (flash silica, ethyl acetate/ petroleum ether 2:1 (v/v), $R_f = 0.53$) affording 0.6 g (0.5 mmol, 84 %) of the product as pale orange solid.

^{1}H-NMR (600 MHz, $CDCl_3$): δ [ppm] = 1.38 (s, 36 H), 1.40 (s, 18 H); 1.95-2.03 (m, 8 H), 2.75 (t, ^3J = 7.5 Hz, 4 H), 3.30-3.77 (m, 32 H), 7.28 (s, 2 H);

^{13}C-NMR (150 MHz, $CDCl_3$): δ [ppm] = 14.12, 22.49, 27.70, 28.02, 28.40, 28.45, 28.77, 38.70, 49.73, 68.39, 80.17, 131.08, 133.41, 134.53, 139.04, 156.76, 164.77;

MP: 120-121°C; **FT-IR (ATR):** 2973 (m), 2927 (m), 1687 (s), 1609 (w), 1466 (m), 1407 (m), 1364 (s), 1245 (s), 1158 (s), 1102 (s), 969 (w), 858 (w), 776 (s), 621 (w), 559 (w) ; **ES-MS (dichloromethane/CH_3OH + 10 mM NH_4OAc):** m/z (%) = 1274.9 (100) [MNH_4^+], 1257.8 (60) [MH^+]; **PI-EIMS:** calcd.: 1256.6800, found: 1256.6756**.**

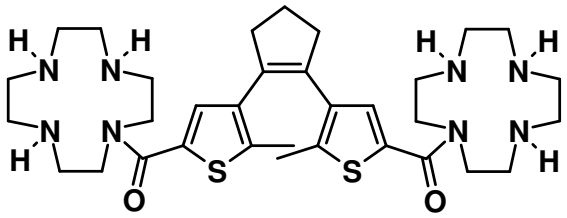

(5-Methyl-4-{2-[2-methyl-5-(1,4,7,10tetraaza-cyclododecane-1-carbonyl)-thiophen-3-yl]-cyclopent-1-enyl}-thiophen-2-yl)-(1,4,7,10tetraaza-cyclododec-1-yl)-methanone.

Compound **7o** (0.4 g, 0.32 mmol) was dissolved in 10 mL of dry dichloromethane under a N_2-atmosphere and then 11 mL of HCl sat. diethyl ether was added. This mixture was stirred in the dark at room temperature for 20 h. After this period the solvent was removed in *vacuo* and the residue dried in high-vacuum. The resulting colourless solid was then dissolved in H_2O (4 mL) and passed through a short weak basic ion-exchanger resin (3 g). The H_2O was removed by lyophilization yielding the product as a brown solid (0.2 g, 0.32 mmol, quant.).

^{1}H-NMR (600 MHz, $CDCl_3$): δ [ppm] = 1.98-2.08 (m, 8 H), 2.75 (t, ^{3}J = 7.4 Hz, 4 H); 3.08-3.15 (m, 8 H), 3.16-3.22 (m, 8 H), 3.30-3.37 (m, 8 H), 3.78 (t, ^{3}J = 4.8 Hz, 8 H), 7.12 (s, 2 H);

MP: 183-185°C; **FT-IR (ATR):** 3293(w), 3237(w), 2962 (w), 1609 (s), 1489 (m), 1446 (m), 1411 (m), 1361 (s), 1262 (m), 1169 (w), 1115 (w), 1061 (w), 884 (s), 770 (m), 722 (s), 549 (m), 523 (m); **ES-MS (dichloromethane/CH_3OH + 10 mM NH_4OAc):** m/z (%) = 329.1 (100) [M+2H$^+$], 657.3 (2) [MH$^+$]; **PI-EIMS:** calcd.: 656.3654, found: 656.3528.

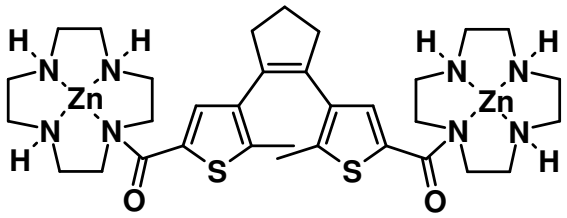

Compound 2o.

The bis-cyclen ligand (0.1 g, 0.15 mmol) was dissolved in 5 mL of H_2O, solid $ZnCl_2$ (0.05 g, 0.33 mmol, 2.2 eq) was added in one portion and the mixture

was heated to 80 °C for 16 h. The solvent was removed by lyophilization, washed two times with ethanol (2 x 14 mL) and with CH_3CN (2 x 14 mL) yielding 0.1 g (83 %) of a light brown solid.

^{1}H-NMR (300 MHz, D_2O): δ [ppm] = 1.90-1.98 (m, 8 H), 2.69 (t, ^3J = 7.3 Hz, 4 H), 2.95-3.14 (m, 25 H), 3.26-3.28 (m, 13 H), 3.71-3.73 (m,10 H), 7.05 (s, 2 H); **MP**: 155-159 °C, **ES-MS (H_2O/CH_3OH + 10mM NH_4OAc):** m/z (%) = 452.0 (100) [M^{4+} + 2 CH_3COO^-]; **FT-IR (ATR):** 3752 (w), 3030 (m), 2830 (m), 1703 (w), 1669 (w), 1591 (s), 1448 (s), 1363 (s), 1272 (m), 1229 (w), 1102 (w), 1047 (m), 975 (m), 867 (m), 684 (w), 633 (m), 580 (m), 534 (m); **UV (HEPES buffer):** λ_{max} (ε) = 280 nm (21900).

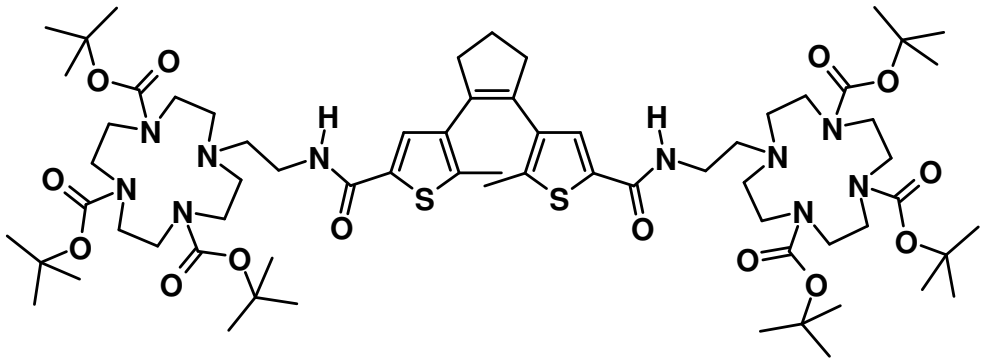

tri-tert-Butyl 10-(2-(5-methyl-4-(2-(5-(2-(4,7,10-tris(tert-butoxycarbonyl)-1,4,7,10-tetraazacyclododecan-1-yl)ethylcarbamoyl)thiophen-3-yl)cyclopent-1-enyl)thiophene-2-carboxamido)ethyl)-1,4,7,10-tetraazacyclododecane-1,4,7-tricarboxylate (6o).

3,3'-(Cyclopentene-1,2-diyl)bis(4-methylcyclopenta-1,3-dienecarboxylic acid) **3** (0.4 g, 1.0 mmol) was dissolved in dry THF (10 mL), 4 drops of DMF were added followed by $SOCl_2$ (0.3 mL, 0.5 g, 4 mmol, 4 eq) in one portion. This solution was stirred at room temperature for 1.5 h and the solvent removed in *vacuo*. The residue was dried in high vacuum for 2 h and redissolved in dry THF (10 mL) in an N_2-atmosphere. Triethylamine (0.4 mL, 0.3 g, 3 mmol, 3 eq) was added in one portion followed by solid 10-(2-amino-ethyl)-1,4,7,10tetraaza-cyclododecane-1,4,7-tricarboxylic acid tri-tert-butyl ester (1 g, 2 mmol, 2 eq) and the resulting mixture was stirred at room temperature for 20 h. The solvent was evaporated in *vacuo* and the residue purified by column chromatography (flash silica, dichloromethane/10% CH_3OH, R_f = 0.58). The product was obtained as a colourless solid (0.8 g, 0.6 mmol, 66%).

^{1}H-NMR (600 MHz, $CDCl_3$): δ [ppm] = 1.37 (s, 36 H), 1.39 (s, 18 H), 1.84 (s, 6 H), 1.88-2.02 (m, 2 H), 2.59-2.75 (m, 16 H), 3.21-3.41 (m, 16 H), 3.42-3.60 m (12 H), 6.54 (bs, 2 H), 7.22 (s, 2 H); **^{13}C-NMR (150 MHz, $CDCl_3$):** δ [ppm] = 14.60, 22.76, 28.42, 28.59, 36.46, 38.44, 47.92, 49.89, 51.79, 54.48, 55.19, 79.31, 79.60, 129.32, 134.32, 134.63, 136.25, 139.82, 161.99; **FT-IR (ATR):** v [cm^{-1}] = 2974 (m), 2932 (m), 1686 (s), 1531 (w), 1460 (m), 1460 (s), 1413 (s), 1364 (s), 1246 (s), 1153 (s), 1045 (w), 975 (w), 859 (w), 772 (m), 543 (w), 462 (w); **MP:** 155-158 °C; **ES-MS (dichloromethane/CH_3OH + 10 mM NH_4OAc):** m/z (%) = 672.5 (100) [M+2H$^+$], 1344 (16) [MH$^+$]; **PI-EIMS:** calcd.: 1342.7644, found:1342.7576.

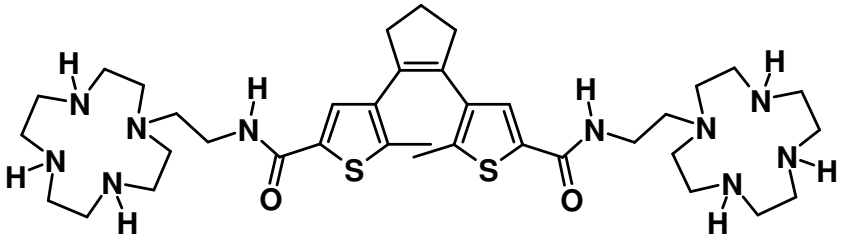

tri-tert-Butyl 10-(2-(5-methyl-4-(2-(5-(2-(4,7,10-tris(tert-butoxycarbonyl)-1,4,7,10-tetraazacyclododecan-1-yl)ethylcarbamoyl)thiophen-3-yl)cyclopent-1-enyl)thiophene-2-carboxamido)ethyl)-1,4,7,10-tetraazacyclododecane-1,4,7-tricarboxylate.

Compound **6o** (0.4 g, 0.3 mmol) was dissolved in dry DCM (10 mL) and 6 mL of an HCl saturated diethylether solution was added in one portion. The resulting mixture was stirred at room temperature for 20 h, the solvent was removed in *vacuo* and the solid residue dried under high-vacuum. The solid HCl-salt was taken up with H_2O (4 mL) and passed through a short weak basic ion exchange resin column. Lyophilization of the eluate afforded the product (0.3 g, 0.3 mmol) as a pale brown solid.

^{1}H-NMR (600 MHz, $CDCl_3$):1.83 (s, 6 H), 1.89-2.00 (m, 2 H), 2.57-2.86, 2.95-3.09 (m, 28 H), 3.30-3.11 (m, 20 H), 3.29-3.38 (m, 4 H), 7.35 (s, 2 H); **FT-IR (ATR):** 1647(w), 1525 (s), 1429 (m), 1384 (m), 1113 (w), 1088 (w), 1014(w), 937 (w), 869 (w), 723 (w), 560 (m); v [cm^{-1}] =; **MP:** 160-161°C; **ES-MS (H_2O/CH_3OH + 0.1% FAc):** m/z (%) = 372.2 (100) [$M+2H^+$], 743.5 (2) [MH^+]; **PI-EIMS:** calcd.: 742.4499, found: 742.4493.

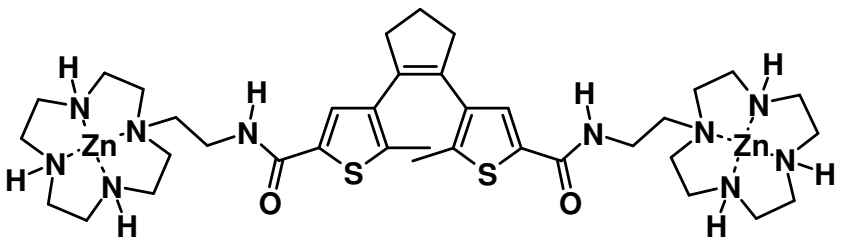

Compound 1o.

The bis-cyclen ligand (0.23 g, 0.3 mmol) was dissolved in 5 mL of H_2O and solid $ZnCl_2$ (0.01 g, 0.7 mmol) was added in one portion. This mixture was stirred at

80 °C for 18 h and after this period the solvent was removed by lyophilization. The resulting solid was washed with EtOH (2 x 14 mL), yielding complex **1o** (0.2 g, 0.23 mmol, 75%) as a light brown solid.

^{1}H-NMR (300 MHz, D_2O): δ [ppm] = 1.83-1.99 (m, 8 H), 2.64-2.90 (m, 32 H), 2.96-3.21 (m, 16 H), 3.35-3.39 (m, 4 H), 7.39 (s, 2H); **MP:** 183-185 °C; **ES-MS (H_2O/CH_3OH + 10 mM NH_4OAc):** m/z (%) = 435.1 (100) [M^{4+}-2H^+], 979.2 (1.3) [M^{4+} + 3 Cl^-]; **FT-IR (ATR):** 1620 (w), 1557 (s), 1449 (m), 1302 (m), 1133 (w), 1084 (w), 1044(w), 967 (w), 871 (w), 753 (w), 530 (m); **UV (HEPES buffer):** λ_{max} (ε) = 265 nm (32759).

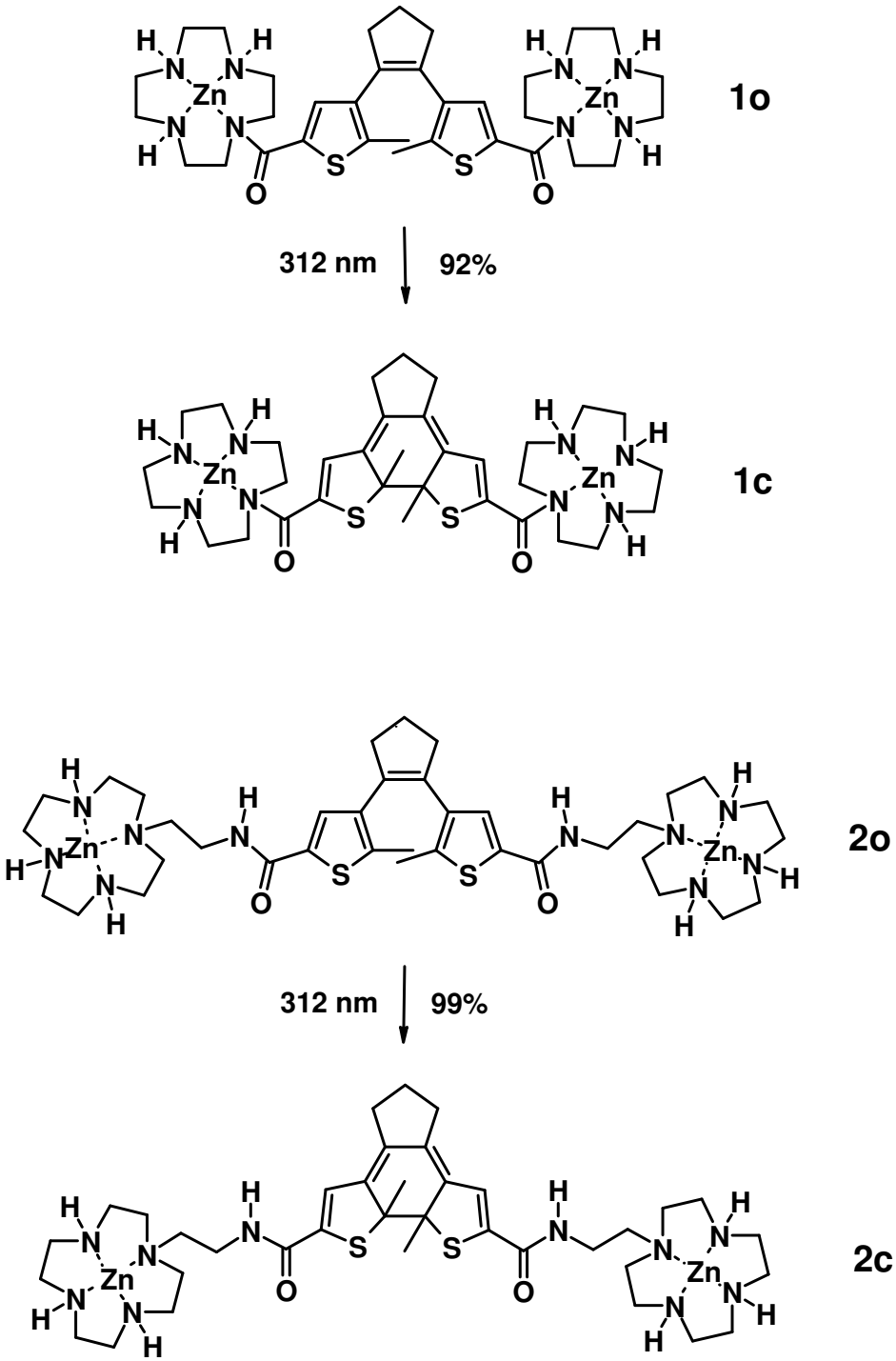

Figure 15. Photostationary states (PSS) of cyclen-derivatives **1** and **2**

Photochemical synthesis of the ring-closed isomer 2c. A solution of compound **2o** (2 mg, 0.002 mmol) in D_2O (0.7 mL) was irradiated for 30 min with a 312 nm lamp in an NMR tube light yielding a red solution containing 92% of the ring-closed isomer according to the ^{1}H-NMR spectroscopy in the photostationary state. The remaining 8% were assigned to the ring-open isomer **2o**.

^{1}H-NMR (300 MHz, D_2O): δ [ppm] = 1.62-1.77 (m, 2H), 1.89 (s, 6H), 2.33-2.41 (m, 4H), 3.06-3.20 (m, 18 H), 3.22–3.36 (m, 10 H), 3.60-3.77 (m, 8 H), 6.32 (s, 2H);

Photochemical synthesis of the ring-closed isomer 1c. A solution of compound **1o** (2 mg, 0.002 mmol) in D_2O (0.7 mL) was irradiated for 30 min with a 312 nm lamp in a NMR tube light yielding a red solution containing 95% of the ring-closed isomer according to the ^{1}H-NMR spectroscopy in the photostationary state.

^{1}H-NMR (300 MHz, D_2O): δ [ppm] = 1.73-1.78 (m, 2 H), 1.87 (s, 6 H), 2.38 (t, ^{3}J = 7.3 Hz, 4 H), 2.62-2.64 (m, 4 H), 2.72–2.89 (m, 15 H), 3.00-3.16 (m, 15 H), 3.33-3.43(m, 6 H);

Spectra

Compound 6o:

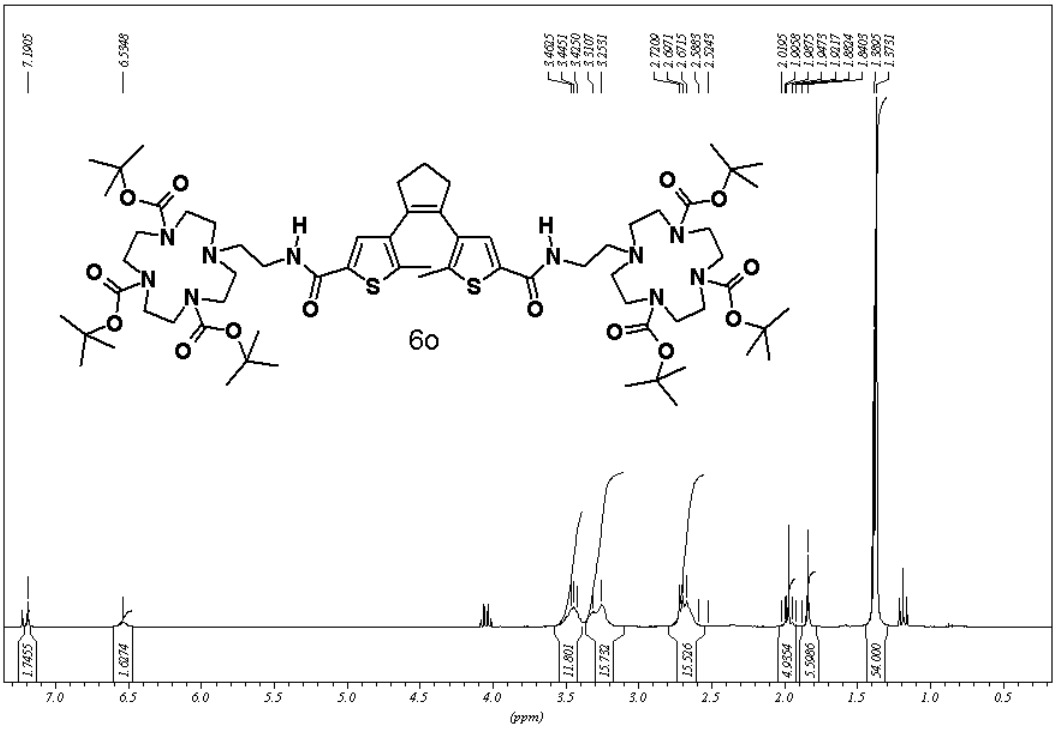

Precursor of 1o:

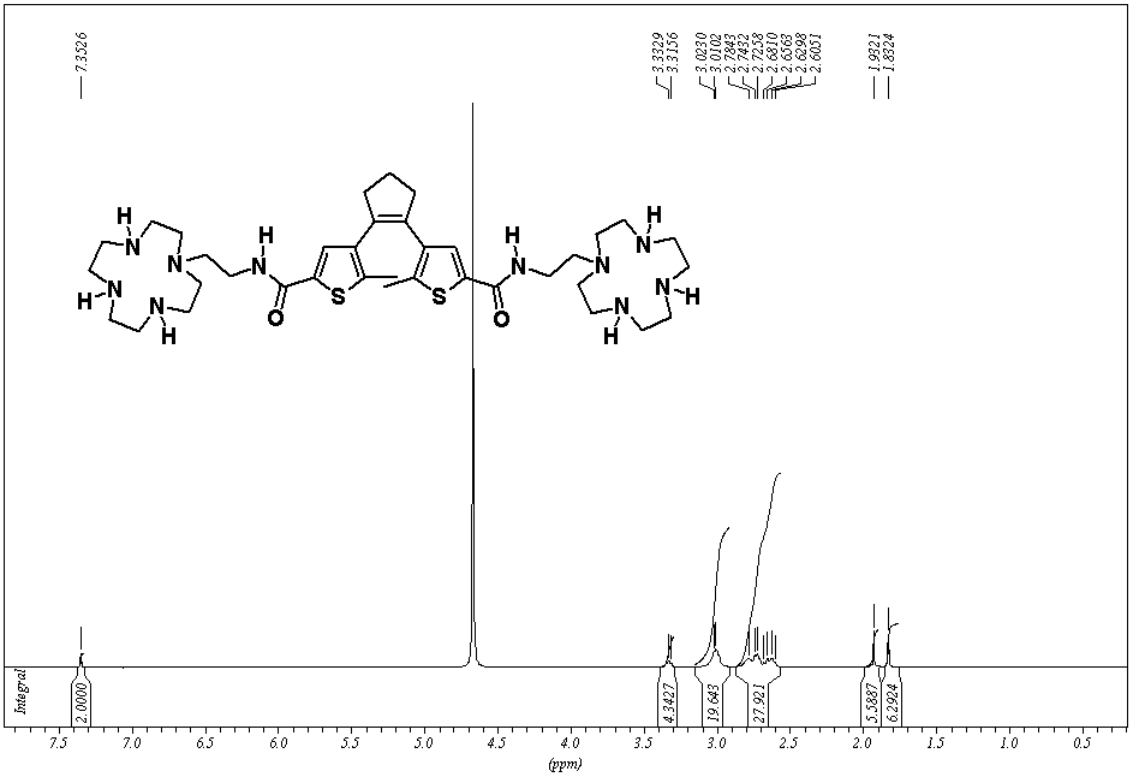

Zn-complex 1o:

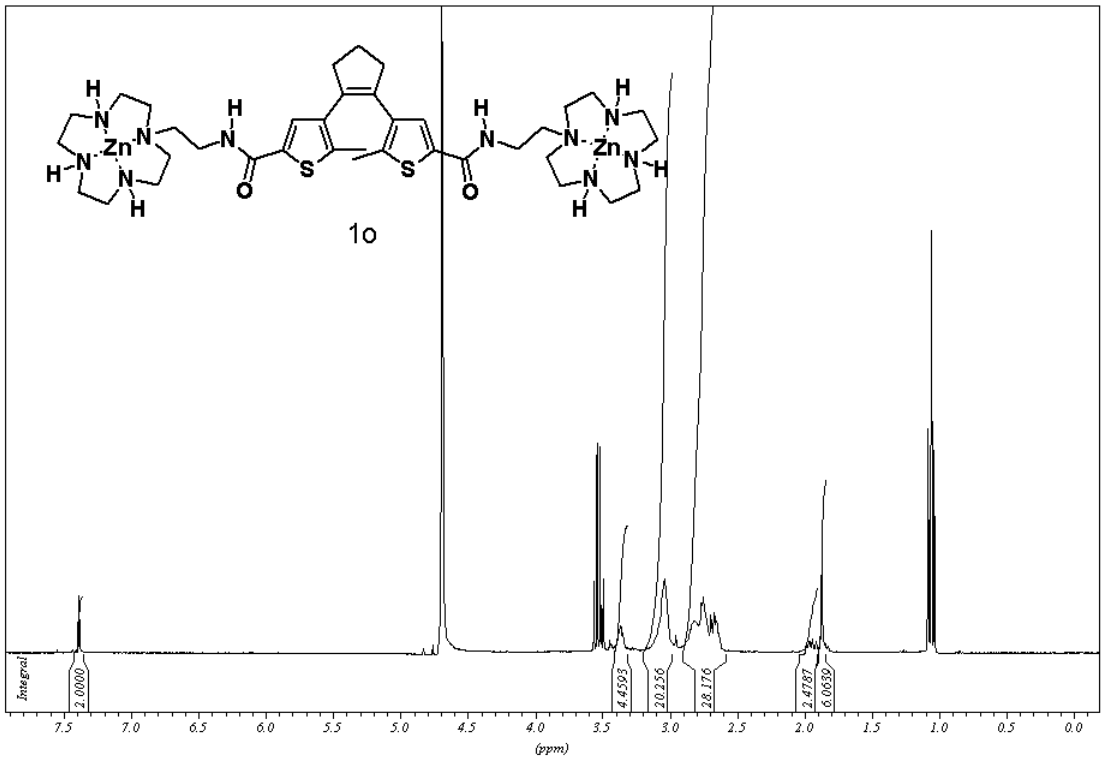

Zn-complex 1c:

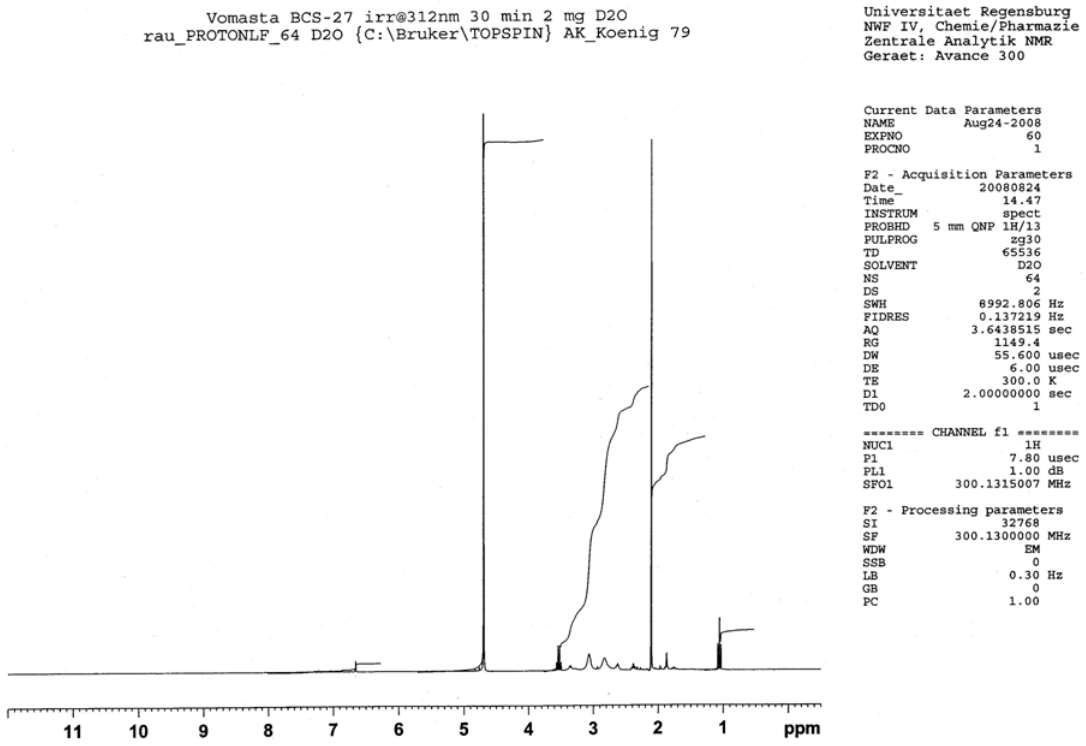

Compound 7o:

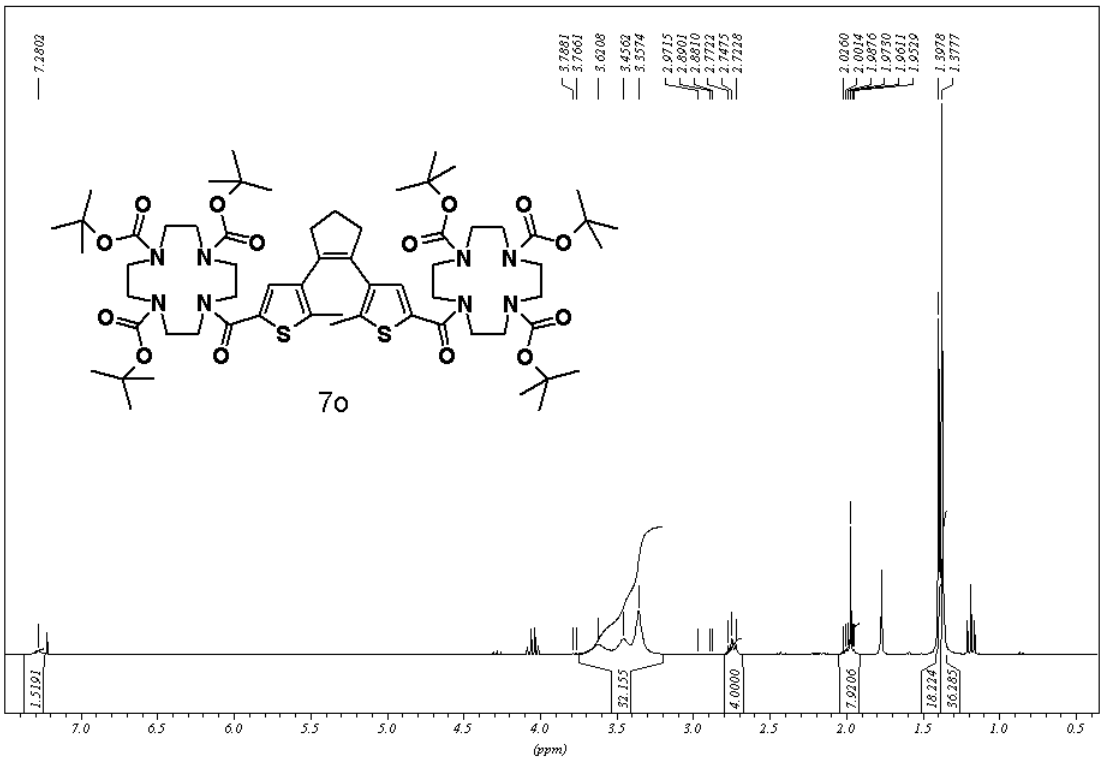

Precursor of compound 2o:

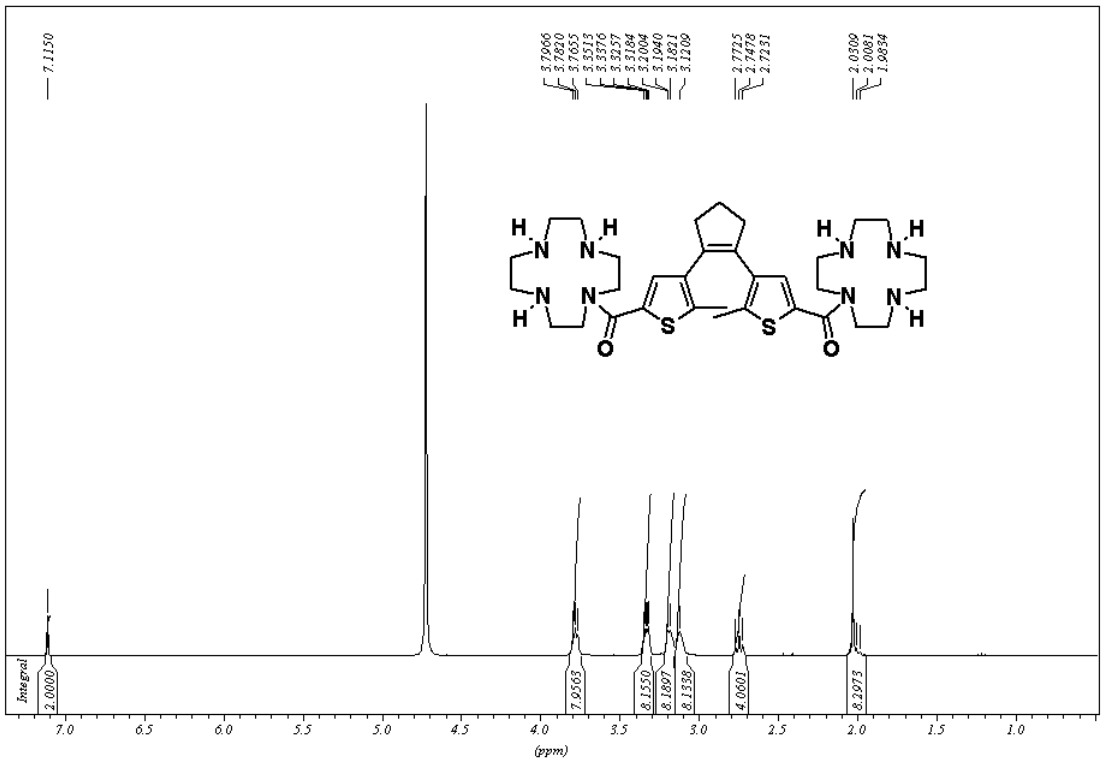

Zn-complex 2o:

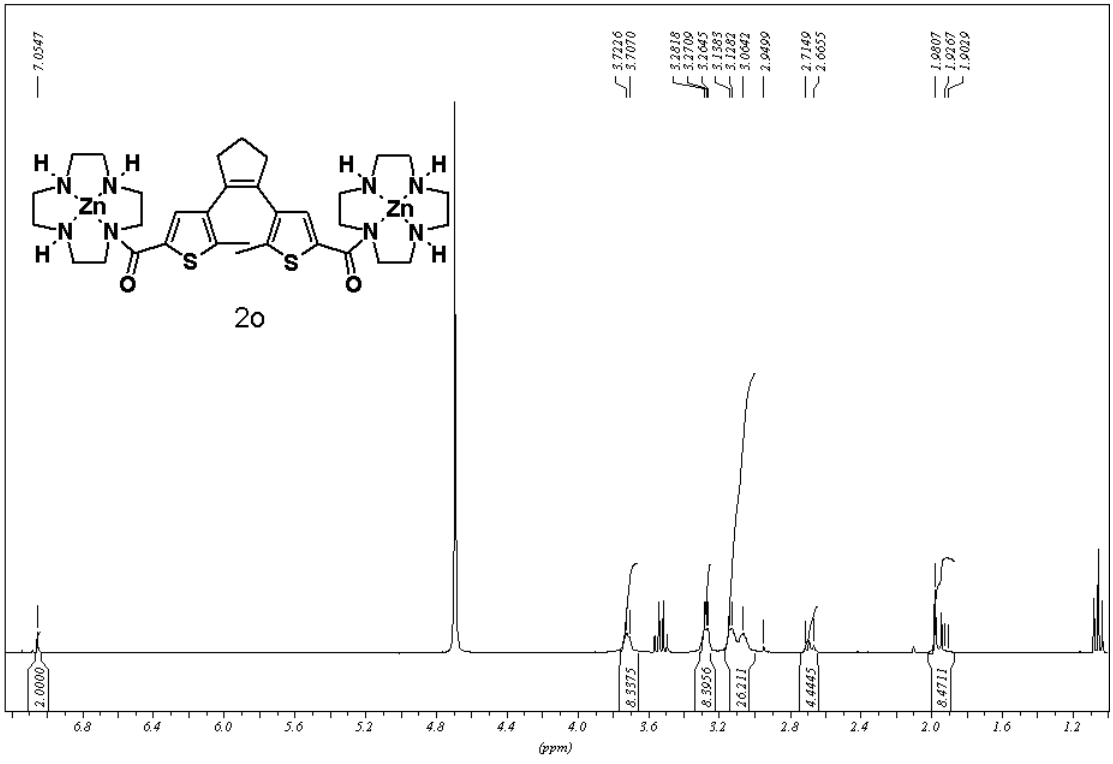

2o

Zn-complex 2c:

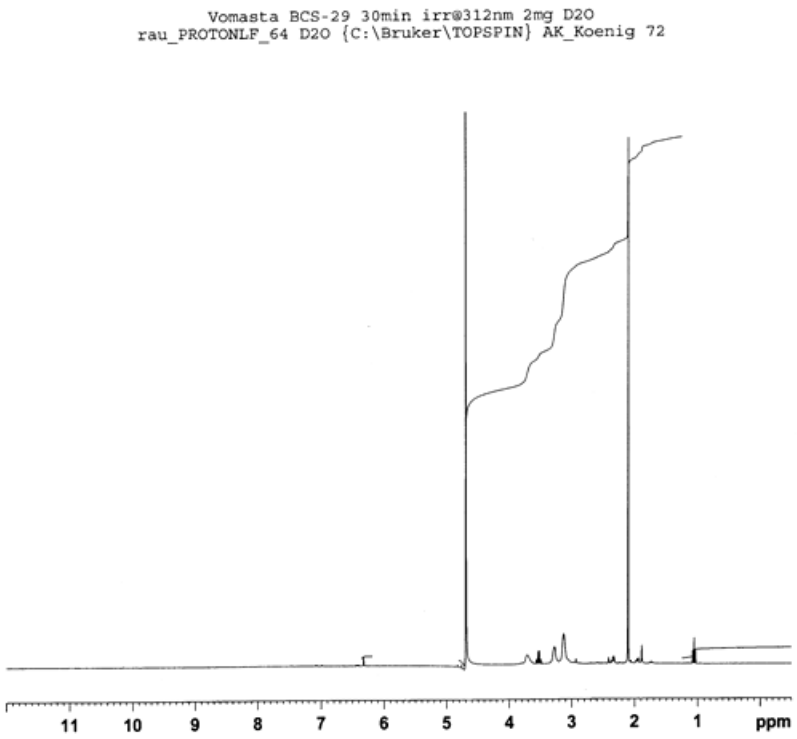

Universitaet Regensburg
NWF IV, Chemie/Pharmazie
Zentrale Analytik NMR
Geraet: Avance 300

Current Data Parameters

NAME	Aug24-2008
EXPNO	40
PROCNO	1

F2 - Acquisition Parameters

Date_	20080824
Time	13.47
INSTRUM	spect
PROBHD	5 mm QNP 1H/13
PULPROG	zg30
TD	65536
SOLVENT	D2O
NS	64
DS	2
SWH	8992.806 Hz
FIDRES	0.137219 Hz
AQ	3.6438515 sec
RG	1149.4
DW	55.600 usec
DE	6.00 usec
TE	300.0 K
D1	2.00000000 sec
TD0	1

======== CHANNEL f1 ========

NUC1	1H
P1	7.80 usec
PL1	1.00 dB
SFO1	300.1315007 MHz

F2 - Processing parameters

SI	32768
SF	300.1300000 MHz
WDW	EM
SSB	0
LB	0.30 Hz
GB	0
PC	1.00

ITC measurements

*Compound **1** vs. CMS*

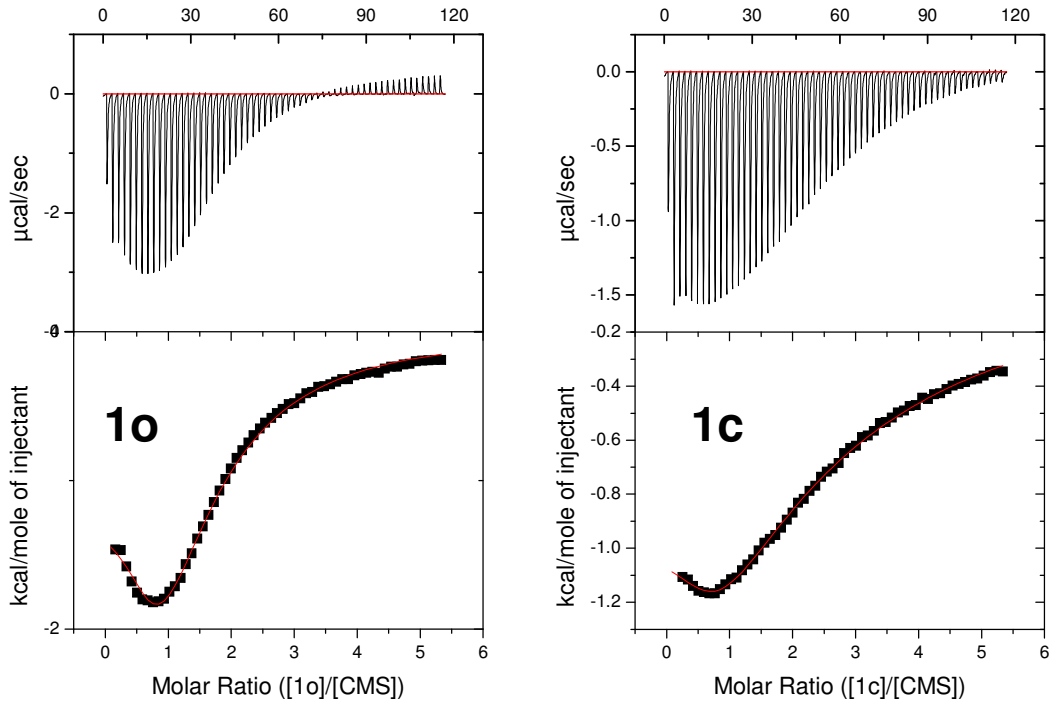

Figure 16. *Left:* Isothermal titration calorimetry (ITC) studies for the binding of the Zn(II)-cyclen derivative **1o** to CMS. The top panel on the right shows the raw data, generated by titration of 1.43 mL of 0.5 *m*M **1o** by 60 injections (5 *µ*L each) of 12 *m*M CMS. The area under each peak was integrated and plotted against the molar ratio **1o** to CMS in the right bottom panel. The solid smooth line (left) is the best fit of the data according to the *two-binding site* model for the following stoichiometries (N_1 and N_2), association constants (K_{a1} and K_{a2}), and enthalpic changes (ΔH°_1 and ΔH°_2). The values of N_1, N_2, K_{a1}, K_{a2}, ΔH°_1, ΔH°_2 were determined to be 0.75 ± 0.04, 0.6 ± 0.08, (3.2 ± 0.6) x 10^4 M^{-1}, (2.2 ± 0.9) x 10^3 M^{-1}, -1.2 ± 0.07 kcal/mol, and -6.3 ± 0.05 kcal/mol, respectively. *Right*: isothermal titration calorimetry (ITC) studies for the binding of the Zn(II)-cyclen derivative **1c** to CMS. The top panel on the right shows the raw data, generated by titration of 1.43 mL of 0.5 *m*M **1c** by 60 injections (5 *µ*L each) of 12 *m*M CMS. **1o** was irradiated for 25 min with λ = 312 nm before the

measurement to generate **1c**. The area under each peak was integrated and plotted against the molar ratio **1c** to CMS in the right bottom panel.

The solid smooth line (left) is the best fit of the data according to the *two-binding site* model for the following stoichiometries (N_1 and N_2), association constants (K_{a1} and K_{a2}), and enthalpic changes (ΔH°_1 and ΔH°_2). The values of N_1, N_2, K_{a1}, K_{a2}, ΔH°_1, ΔH°_2 were determined to be 1 ± 0.002, 0.6 ± 0.02, (1.3 ± 0.2) x 10^4 M^{-1}, (5.4 ± 0.2) x 10^2 M^{-1}, -0.9 ± 0.003 kcal/mol, and -6.8 ± 0.06 kcal/mol, respectively.

*Compound **2** vs. CMS*

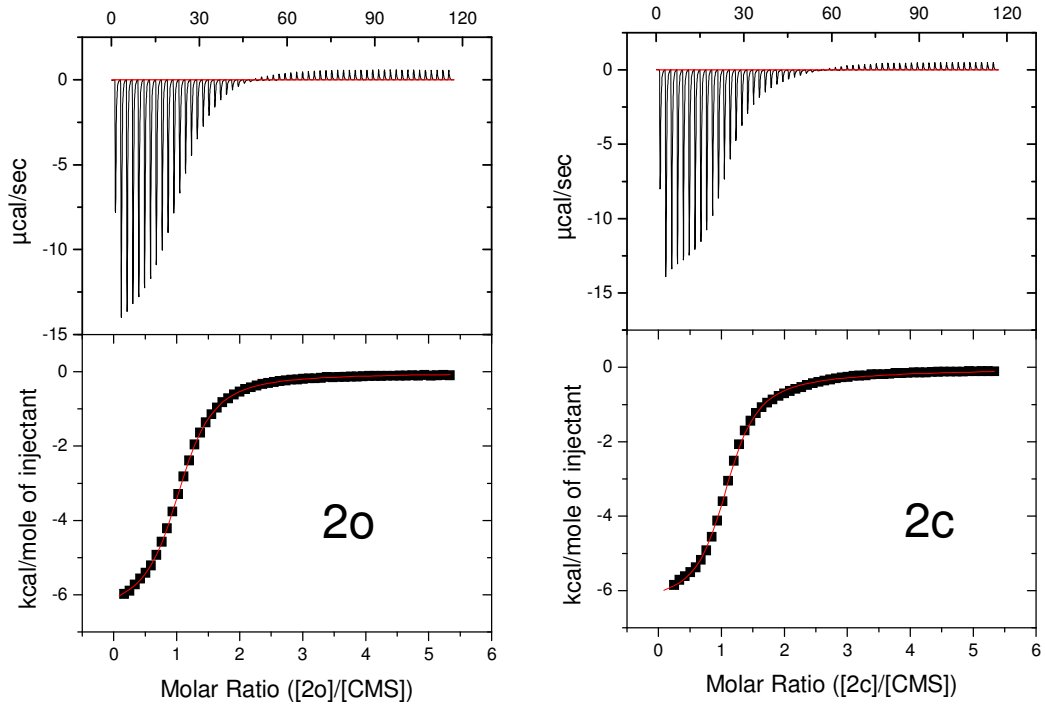

Figure 17. *Left:* Isothermal titration calorimetry (ITC) studies for the binding of the Zn(II)-cyclen derivative **2o** to CMS. The top panel on the right shows the raw data, generated by titration of 1.43 mL of 0.5 *m*M **2o** by 60 injections (5 *µ*L each) of 12 *m*M CMS. The area under each peak was integrated and plotted against the molar ratio **2o** to CMS in the right bottom panel. The solid smooth line (left) is the best fit of the data according to the *two-binding site* model for the following stoichiometries (N_1 and N_2), association constants (K_{a1} and K_{a2}), and enthalpic changes (ΔH°_1 and ΔH°_2). The values of N_1, N_2, K_{a1}, K_{a2}, ΔH°_1, ΔH°_2 were determined to be 1 ± 0.004, 0.6 ± 0.1, (2.9 ± 0.03) x 10^4 M^{-1}, (1.0 ± 0)

x 10^2 M^{-1}, -6.5 ± 0.01 kcal/mol, and -1.0 ± 0.4 kcal/mol, respectively. *Right*: isothermal titration calorimetry (ITC) studies for the binding of the Zn(II)-cyclen derivative **2c** to CMS.

The top panel on the right shows the raw data, generated by titration of 1.43 mL of 0.5 *m*M **2c** by 60 injections (5 *μ*L each) of 12 *m*M CMS. **2o** was irradiated for 25 min with λ = 312 nm before the measurement to generate **2c**. The area under each peak was integrated and plotted against the molar ratio **2c** to CMS in the right bottom panel. The solid smooth line (left) is the best fit of the data according to the *two-binding site* model for the following stoichiometries (N_1 and N_2), association constants (K_{a1} and K_{a2}), and enthalpic changes (ΔH°_1 and ΔH°_2). The values of N_1, N_2, K_{a1}, K_{a2}, ΔH°_1, ΔH°_2 were determined to be 1 ± 0.008, 0.65 ± 0.02, (5.0 ± 0.8) x 10^4 M^{-1}, (6.0 ± 2.0) x 10^2 M^{-1}, -6.3 ± 0.02 kcal/mol, and -1 ± 0.2 kcal/mol, respectively.

*Compound **1** vs. PP_i*

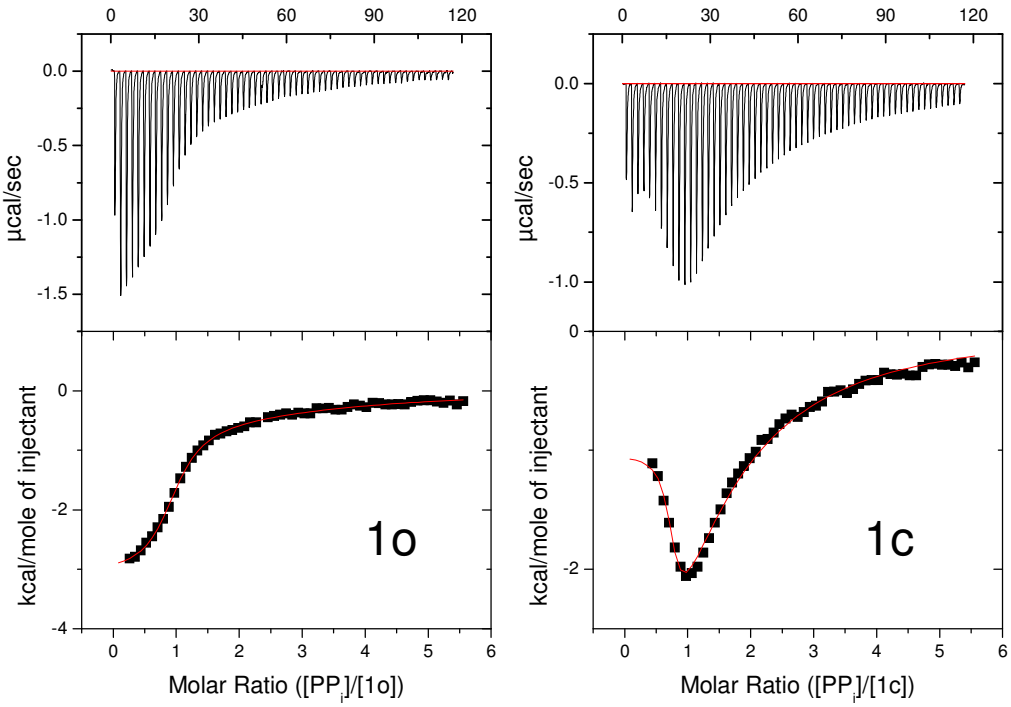

Figure 18. *Left:* Isothermal titration calorimetry (ITC) studies for the binding of the Zn(II)-cyclen derivative **1o** to PP_i. The top panel on the right shows the raw

data, generated by titration of 1.43 mL of 0.1 *m*M **1o** by 60 injections (5 *μ*L each) of 5 *m*M PP_i. The area under each peak was integrated and plotted against the molar ratio PP_i to **1o** in the right bottom panel. The solid smooth line (left) is the best fit of the data according to the *two-binding site* model for the following stoichiometries (N_1 and N_2), association constants (K_{a1} and K_{a2}), and enthalpic changes (ΔH°_1 and ΔH°_2). The values of N_1, N_2, K_{a1}, K_{a2}, ΔH°_1, ΔH°_2 were determined to be 0.9 ± 0.01, 1.7 ± 0, (1.7 ± 0.3) x 10^5 M^{-1}, (2.8 ± 0.6) x 10^3 M^{-1}, -3.2 ± 0.05 kcal/mol, and -1.8 ± 0.1 kcal/mol, respectively. *Right*: isothermal titration calorimetry (ITC) studies for the binding of the Zn(II)-cyclen derivative **1c** to PP_i. The top panel on the right shows the raw data, generated by titration of 1.43 mL of 0.1 *m*M **1c** by 60 injections (5 *μ*L each) of 5 *m*M PP_i. **1o** was irradiated for 25 min with λ = 312 nm before the measurement to generate **1c**. The area under each peak was integrated and plotted against the molar ratio **1c** to PP_i in the right bottom panel. The solid smooth line (left) is the best fit of the data according to the *two-binding site* model for the following stoichiometries (N_1 and N_2), association constants (K_{a1} and K_{a2}), and enthalpic changes (ΔH°_1 and ΔH°_2). The values of N_1, N_2, K_{a1}, K_{a2}, ΔH°_1, ΔH°_2 were determined to be 0.7 ± 0.02, 0.8 ± 0.01, (1.3 ± 0.3) x 10^6 M^{-1}, (8.2 ± 0.3) x 10^3 M^{-1}, -1.0 ± 0.05 kcal/mol, and -6.8 ± 0.08 kcal/mol, respectively.

*Compound **2** vs. PP_i*

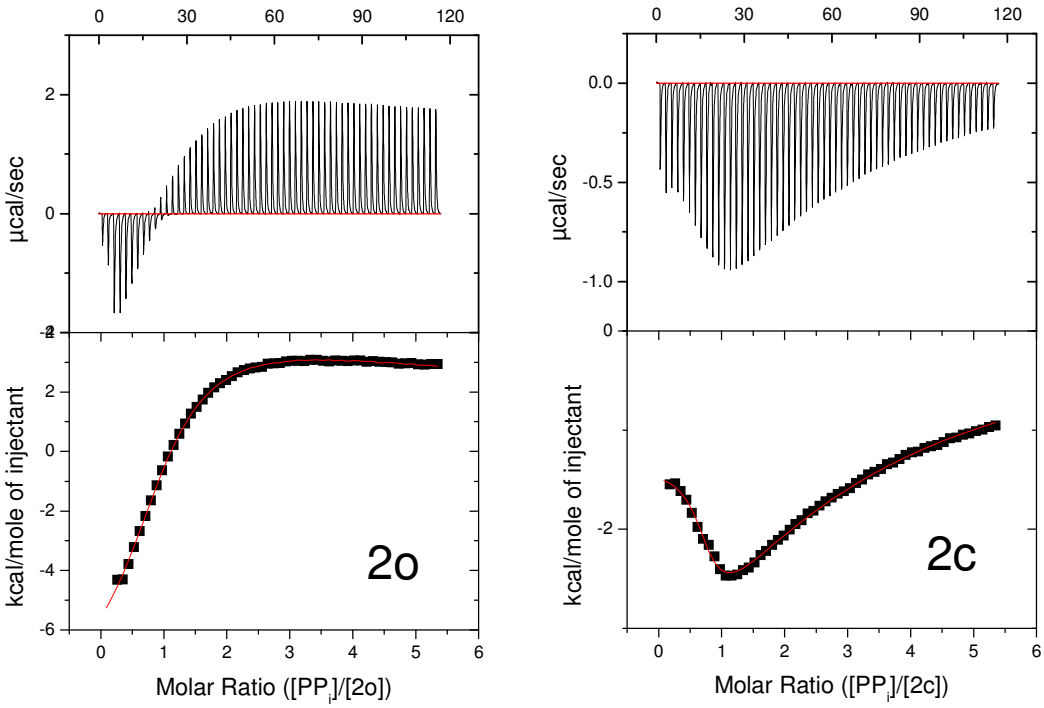

Figure 19. *Left:* Isothermal titration calorimetry (ITC) studies for the binding of the Zn(II)-cyclen derivative **2o** to PP_i. The top panel on the right shows the raw data, generated by titration of 1.43 mL of 0.1 *m*M **2o** by 60 injections (5 *µ*L each) of 5 *m*M PP_i. The area under each peak was integrated and plotted against the molar ratio PP_i to **2o** in the right bottom panel. The solid smooth line (left) is the best fit of the data according to the *two-binding site* model for the following stoichiometries (N_1 and N_2), association constants (K_{a1} and K_{a2}), and enthalpic changes (ΔH°_1 and ΔH°_2). The values of N_1, N_2, K_{a1}, K_{a2}, ΔH°_1, ΔH°_2 were determined to be 1.0 ± 0.01, 1.2 ± 0, (2.8 ± 0.2) x 10^4 M^{-1}, (1.6 ± 0.6) x 10^2 M^{-1}, -8.7 ± 0.5 kcal/mol, and 303 ± 96 kcal/mol, respectively. *Right*: isothermal titration calorimetry (ITC) studies for the binding of the Zn(II)-cyclen derivative **2c** to PP_i. The top panel on the right shows the raw data, generated by titration of 1.43 mL of 0.1 *m*M **2c** by 60 injections (5 *µ*L each) of 5 *m*M PP_i. **2o** was irradiated for 25 min with λ = 312 nm before the measurement to generate **2c**. The area under each peak was integrated and plotted against the molar ratio **2c** to PP_i in the right bottom panel. The solid smooth line (left) is the best fit of the data according to the *two-binding site* model for the following stoichiometries (N_1 and N_2), association constants (K_{a1} and K_{a2}), and enthalpic changes (ΔH°_1

and ΔH°_2). The values of N_1, N_2, K_{a1}, K_{a2}, ΔH°_1, ΔH°_2 were determined to be 0.8 ± 0.02, 0.9 ± 0.4, (1.5 ± 0.4) x 10^5 M^{-1}, (3.3 ± 0.4) x 10^3 M^{-1}, -0.5 ± 0.07 kcal/mol, and -12 ± 6 kcal/mol, respectively.

Indicator displacement assay (IDA)

*Compound **1** vs. analytes*

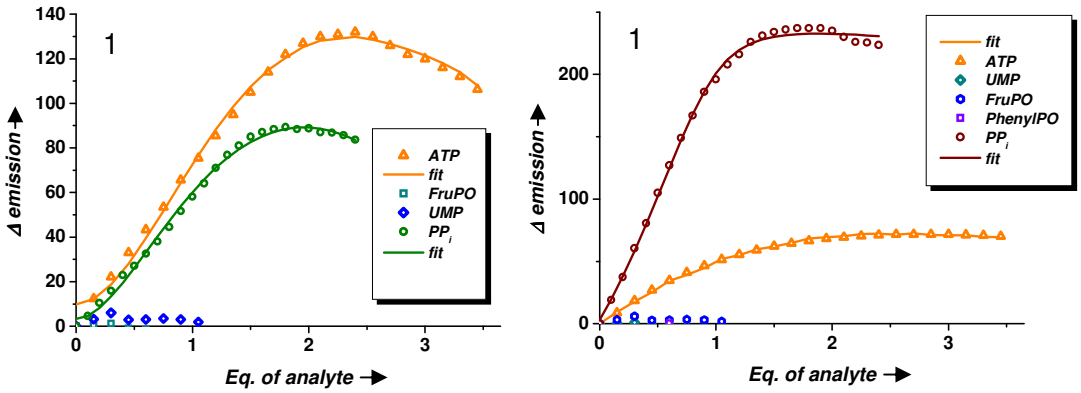

Figure 20. *Left*: indicator displacement assay (IDA) of the ring-open isomer **1o** (50 µM) against analytes (300 µM) in HEPES buffer (50 mM, I = 154 mM NaCl) at physiological pH (7.4). *Right*: indicator displacement assay (IDA) of the ring-open isomer **1c** (50 µM) against analytes (300 µM) in HEPES buffer (50 mM, I = 154 mM NaCl) at physiological pH (7.4).

*Compound **1** vs. ATP*

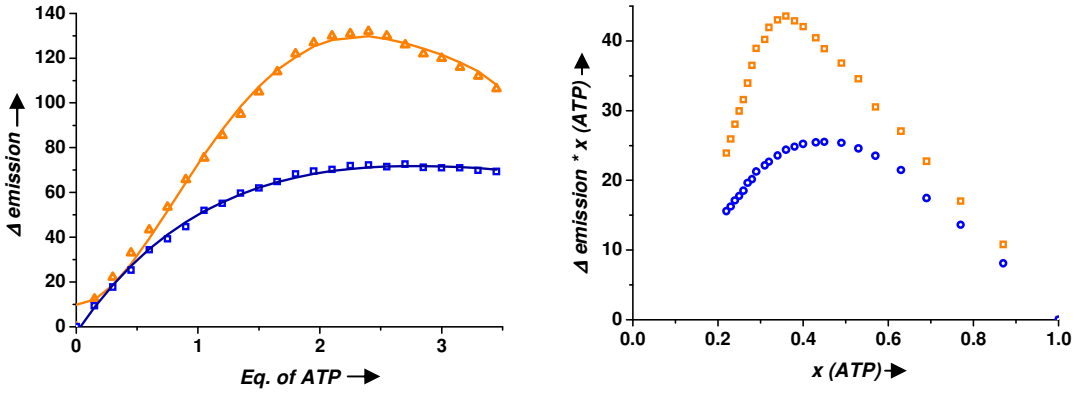

Figure 21. *Left*: fluorescence titration of the ring-open isomer **1o** (orange triangles and fit) and the ring-closed isomer **1c** (blue squares and fit) (50 µM) against ATP (300 µM) in HEPES buffer (50 mM, I = 154 mM NaCl) at physiological pH (7.4). *Right*: Job's plot analysis of **1o** (orange, maximum at about 0.33) and **1c** (blue, maximum at about 0.42) vs. ATP.

*Compound **2** vs. analytes*

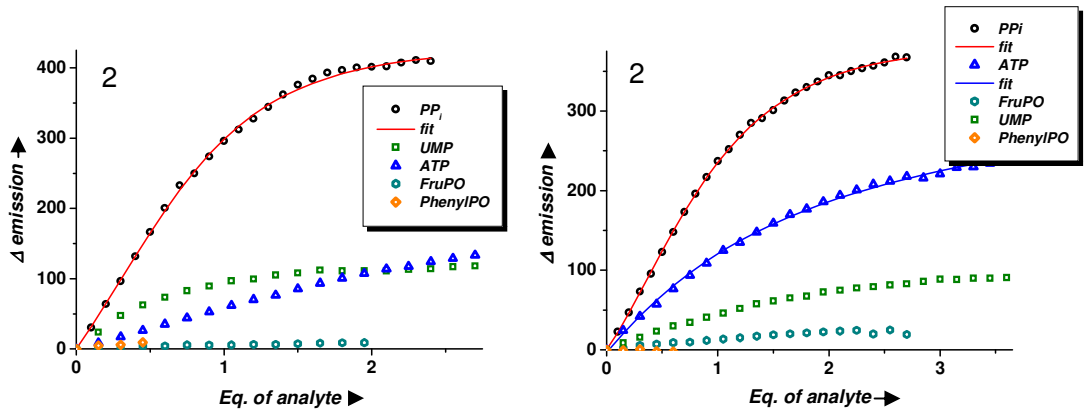

Figure 22. *Left*: IDA of the ring-open isomer **2o** (50 µM) against analytes (300 µM) in HEPES buffer (50 mM, I = 154 mM NaCl) at physiological pH (7.4). *Right*: IDA of the ring-open isomer **2c** (50 µM) against analytes (300 µM) in HEPES buffer (50 mM, I = 154 mM NaCl) at physiological pH (7.4).

Possible binding motifs:

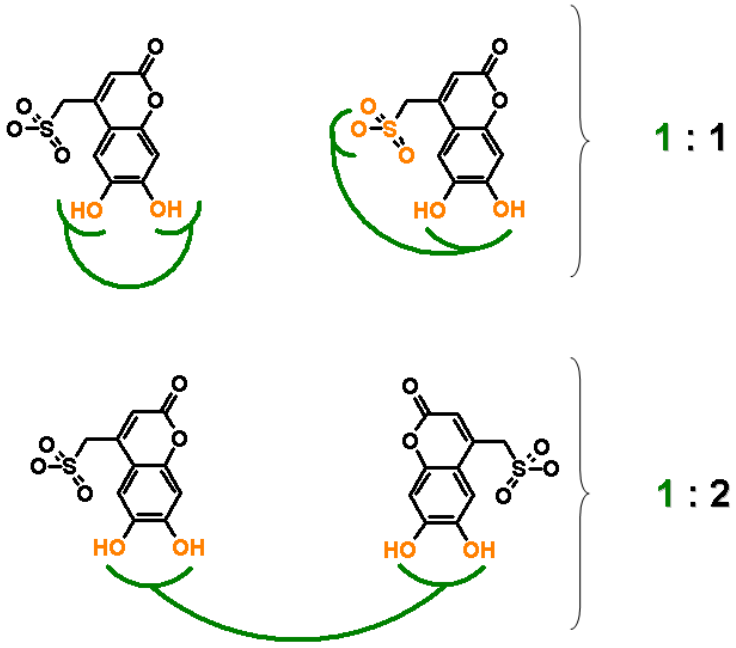

Figure 23. Possible binding motif compound 1 or 2 vs. CMS. Lines in green represent compounds 1 and 2 in their ring-open as well as in their ring-closed form.

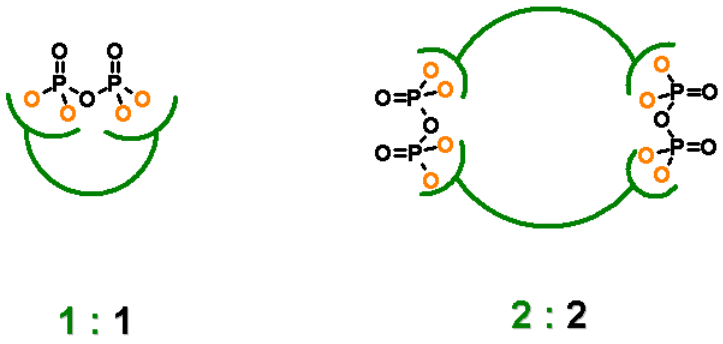

Figure 24. Possible binding motif compound 1 or 2 vs. PPi. Lines in green represent compounds 1 and 2 in their ring-open as well as in their ring-closed form.

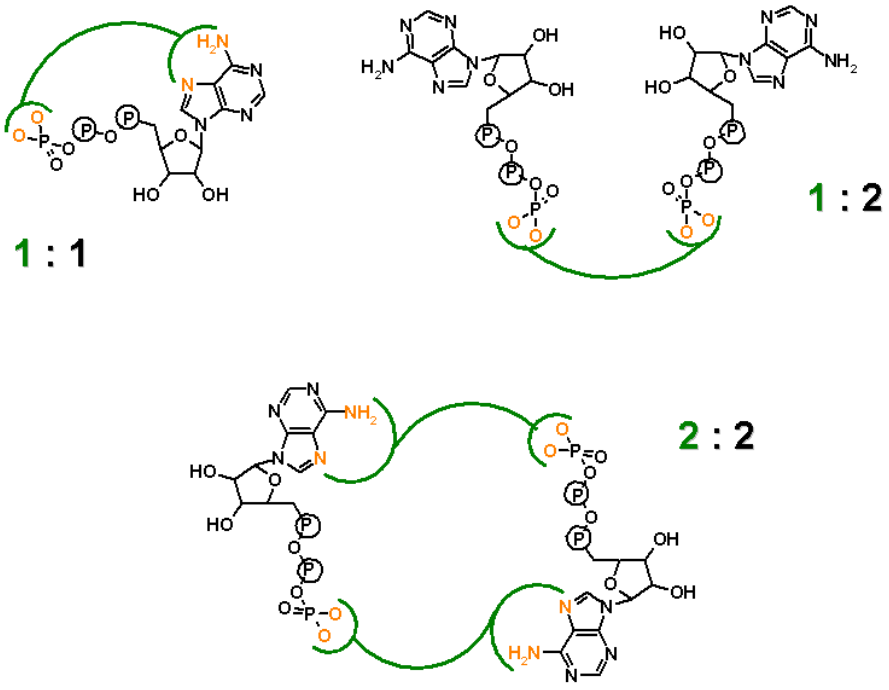

Figure 25. Possible binding motifs compound 1 or 2 vs. ATP. Lines in green represent compounds 1 and 2 in their ring-open as well as in their ring-closed form.

IV.5 References

(1) Lipscomb, W. N.; Straeter, N. *Chem. Rev.* **1996**, *96*, 2375-2433.

(2) Lee Dong, H.; Kim Soon, Y.; Hong, J.-I. *Angew. Chem. Int. Ed.* **2004**, *43*, 4777-4780.

(3) Shinkai, S.; Ishihara, M.; Ueda, K.; Manabe, O. *J. Chem. Soc., Perk. Trans 2:* **1985**, 511-518.

(4) Shinkai, S.; Nakamura, S.; Nakashima, M.; Manabe, O.; Iwamoto, M. *Bull. Chem. Soc. Jpn.* **1985**, *58*, 2340-2347.

(5) Akabori, S.; Miura, Y.; Yotsumoto, N.; Uchida, K.; Kitano, M.; Habata, Y. *J. Chem. Soc., Perk. Trans 1* **1995**, 2589-2594.

(6) Yagai, S.; Karatsu, T.; Kitamura, A. *Chem. Eur. J.* **2005**, *11*, 4054-4063.

(7) Kimura, K.; Kado, S.; Sakamoto, H.; Sakai, A.; Yokoyama, M.; Tanaka, M. *J. Chem. Soc., Perk. Trans 2* **1999**, 2539-2544.

(8) Kimura, K.; Teranishi, T.; Yokoyama, M.; Yajima, S.; Miyake, S.; Sakamoto, H.; Tanaka, M. *J. Chem. Soc., Perk. Trans 2* **1999**, 199-204.

(9) Itagaki, H.; Masuda, W.; Hirayanagi, Y.; Sugimoto, K. *J. Phys. Chem. B* **2002**, *106*, 3316-3322.

(10) Takeshita, M.; Irie, M. *Tetrahedron Lett.* **1998**, *39*, 613-616.

(11) Takeshita, M.; Irie, M. *J. Org. Chem.***1998**, *63*, 6643-6649.

(12) Ojida, A.; Takashima, I.; Kohira, T.; Nonaka, H.; Hamachi, I. *J. Am. Chem. Soc.* **2008**, *130*, 12095-12101.

(13) Dirscherl, G.; Schwab, M.; Seufert, W.; König, B. *Inorg. Chim. Acta* **2009**, *362*, 537-542.

(14) Grauer, A.; Riechers, A.; Ritter, S.; Koenig, B. *Chem. Eur. J.* **2008**, *14*, 8922-8927.

(15) Kruppa, M.; König, B. *Chem. Rev.* **2006**, *106*, 3520-3560.

(16) Irie, M. *Chem. Rev.* **2000**, *100*, 1685-1716.

(17) Norsten, T. B.; Branda, N. R. *J. Am. Chem. Soc.* **2001**, *123*, 1784-1785.

(18) Hanshaw, R. G.; Hilkert, S. M.; Jiang, H.; Smith, B. D. *Tetrahedron Lett.* **2004**, *45*, 8721-8724.

(19) Nguyen, B. T.; Anslyn, E. V. *Coord. Chem. Rev.* **2006**, *250*, 3118-3127.

(20) This compound will be synthesized by Susanna Schmidbauer (Diploma thesis).

(21) Myles, A. J.; Branda, N. R. *J. Am. Chem. Soc.* **2001**, *123*, 177-178.

Bis-indolylethene revisited

This chapter deals with di-indolylethene as a group of photoresponsive diarylethenes, which are known in literature that their ring-closed isomer are thermally reversible. This molecule was tested for special features such as switching on and off basicitiy, fluorescence and solvent dependency.

The syntheses of the compounds as well as the measurements were done by Daniel Vomasta. Calculations about the cyclization energy barrier are in progress in the group of Prof. Dr. M. Schütz (University of Regensburg).

V. Bis-indolylethene - revisited

V.1. Introduction

Photochromic compounds have received considerable interest because of their potential use in optical data storage.[1-6] Among such compounds, 1,2-diarylethenes containing heterocyclic rings are particular promising for practical use.[1-11] The compounds undergo conrotatory electrocyclic reactions yielding the ring-closed isomer which absorb light in the visible region.[1] Alteration of the π-conjugated chain length of diarylethene derivatives by photoirradiation can be used to control reactivity, donor-acceptor interactions, magnetic properties and physiological response.[12-19] Such triggered changes, induced by light, are essential for creation of new materials and devices as well as for molecules of biological relevance.[20] A phenolic diarylethene that changes its pK_a upon isomerization was reported by Lehn. The phenolic group acts as the proton source and a pyridinium group as the acidifying electron acceptor positioned at each end of the diarylethene π-conjugated chain.[21] The acidity increases in the closed-ring isomer by the enhanced acceptor effect of the pyridinium ion and the connection of the two units was controlled by toggling the switch by light. In another example, Irie and co-workers reported the same principle but placed the two interacting units in the same aryl unit. Changing the orbital hybridization of the reactive carbon from sp^2 to sp^3 allowed control of the π-conjugated chain length.[22] In both examples a modulation of the pK_a by about one unit was observed.

Di-indolylethenes (DIE) molecules can have interesting features, but the big drawback of these photoresponsive compounds is that diarylethenes with indole moieties as the aryl group tend to be thermally reversible. This is due to the aromatic stabilization energy of the indole groups, which is larger than that of thiophene for example. This effect plays an important role in terms of thermal stability.[1] However, thermal stability is one very important feature a photoresponsive molecule must have to be applicable for various materials. Fan and co-workers therefore synthesized various symmetric DIEs with modifications in the central ring and at the indole-nitrogen.[23] They found that the central ring size and the substituent at the indole-nitrogen play a very important

role for the thermal stability of these compounds. In terms of this property, a six-membered central ring (which connects the two indole moieties) and a C-16 alkyl chain as well as an ethyl-residue at the indole-nitrogen seems to give the ring-closed isomers a useful stability for at least 4 to 48 hours at room temperature.[23] The authors focussed mainly on increasing the thermal stability, whereas other properties such as solvent dependency of the thermal stability, photostationary states (PSS) and fluorescence were not discussed in their publication. The synthetic experimental part provides the general procedure for the McMurray reduction for the synthesized compounds, but a detailed description of all the other steps is missing. Therefore, we re-synthesized the compound described as most thermal stable and tested its properties in order to get more information of this class of 1, 2-diarylethenes.

V.2 Results and discussion

Synthesis

Starting from commercially available 2-methylindole **2** and subsequent reaction with ethylmagnesium bromide followed by quenching with adipoyldichloride gives diketone **3**. Alkylation under basic conditions and McMurry coupling completes the synthesis and affords the desired product **1**.

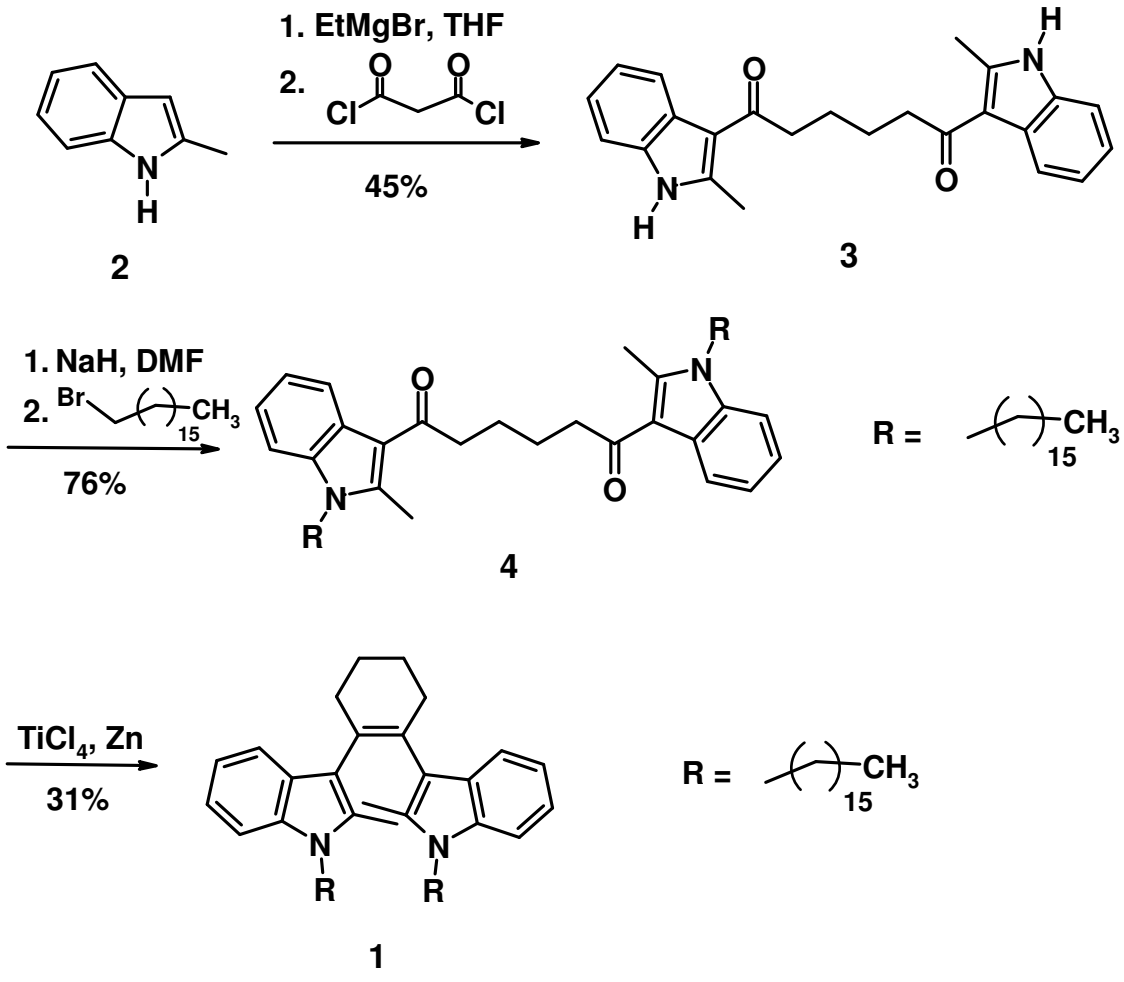

Figure 26. Synthesis of photoresponsive bis-indole-cyclohexene **1**.[23]

Spectroscopy and photochromism

Di-indolylethene (DIE) **1o** emits upon excitation at λ_{ex} = 297 nm at a wavelength of λ_{em} = 375 nm (Figure 27, stokes shift ~ 80 nm).

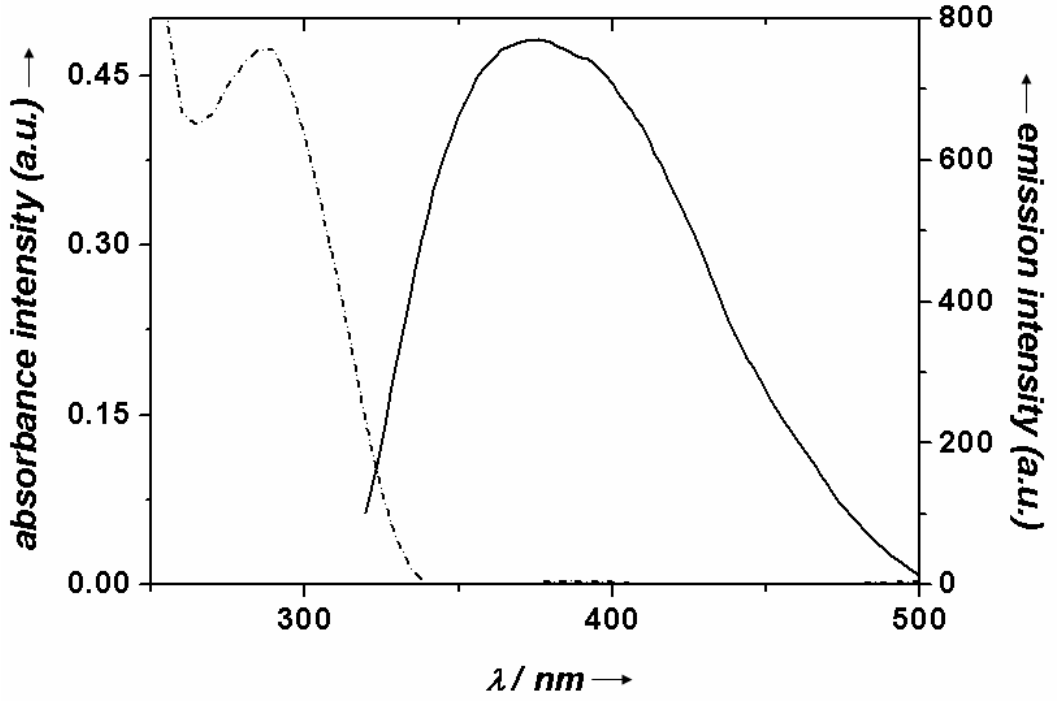

Figure 27. Absorbance (dotted black line) and emission spectrum (black line) of compound **1** (10 µM) in 1, 4-dioxane.

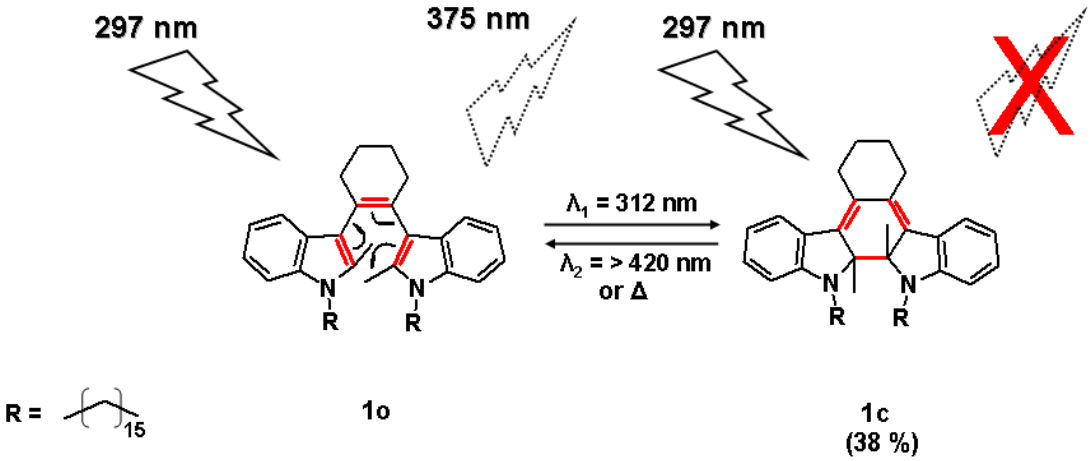

Figure 28. Photochromic reaction of DIE **1**. Upon irradiation with UV-light ($\lambda = 312$ nm) an electrocyclic ring-closing reaction takes place (indicated by black arrows). This reaction can be reversed to the initial state by addressing only the ring-closed isomer through irradiation with visible light ($\lambda > 420$ nm). Excitation arrows indicate that compound **1o** (open) is emitting ($\lambda_{em} = 375$ nm) upon excitation with $\lambda_{ex} = 297$ nm whereas the closed form **1c** is non-fluorescent. Therefore, the closing-reaction can also be monitored by a decrease of the fluorescence emission intensity.

Irradiation of the indole-switch **1** with UV-light of 312 nm results in immediate changes of the UV/VIS absorption spectra at a concentration of 13 µM in 1, 4-dioxane. The band at $\lambda_{max} = 297$ nm decreases in intensity whereas two bands, one at $\lambda_{max} = 370$ nm and one at $\lambda_{max} = 490$ nm, are increasing (Figure 29). This affects the colour of the solution as it turns from colourless to red. These spectral changes are complete after irradiation for 30 s (13 µM) and a photostationary state containing 38% of the ring-closed isomer is generated according to the decrease of the fluorescence intensity.

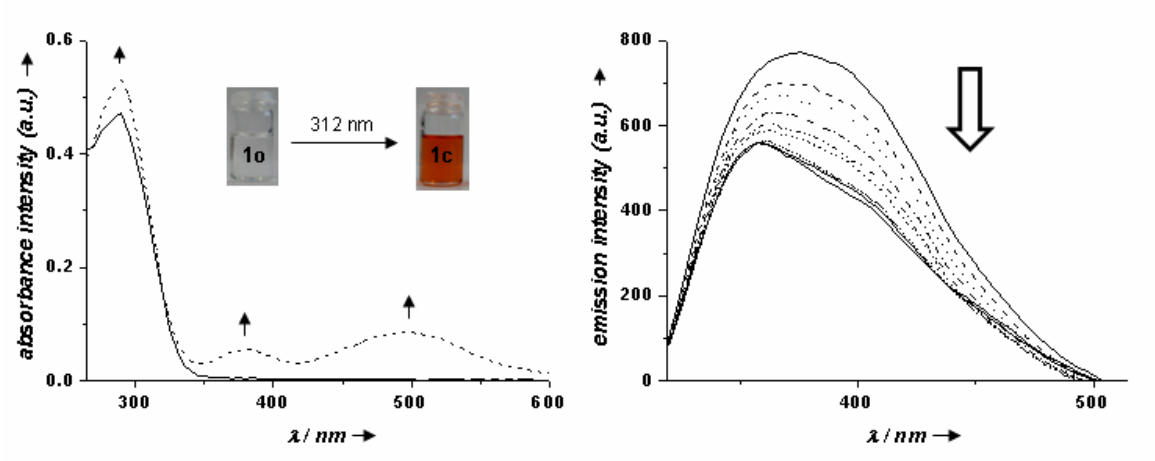

Figure 29. *Left*: UV-profile of compound **1** (13 µM) in 1, 4-dioxane. Upon irradiation with λ = 312 nm for 30 s, the photostationary state of the compound was reached. The colour changed from colourless to red. The band at 297 nm is increasing and new bands (370 nm and 490 nm) are coming up upon irradiation. *Right*: fluorescence emission change upon irradiation with 312 nm wavelength in 1, 4-dioxane (13 µM). The fluorescence of the initial state is decreasing in intensity and the maximum of the emission shifts from 375 nm to 357 nm (shift ~ 20 nm).

Also, the fluorescence is influenced by the photo-induced conversion to the ring-closed isomer. Upon irradiation with 312 nm for 30 s, the emission band decreases and its maximum shifts from 375 nm to 357 nm. Figure 30 shows the cycle study of DIE **1** in 1, 4-dioxane (50 µM), the visible band (black line/ squares) shows only a slow decrease even after 10 cycles, whereas the ultraviolet band (blue line/ circles) the loss of performance starts from the second cycle on. Up to date this effect cannot be explained.

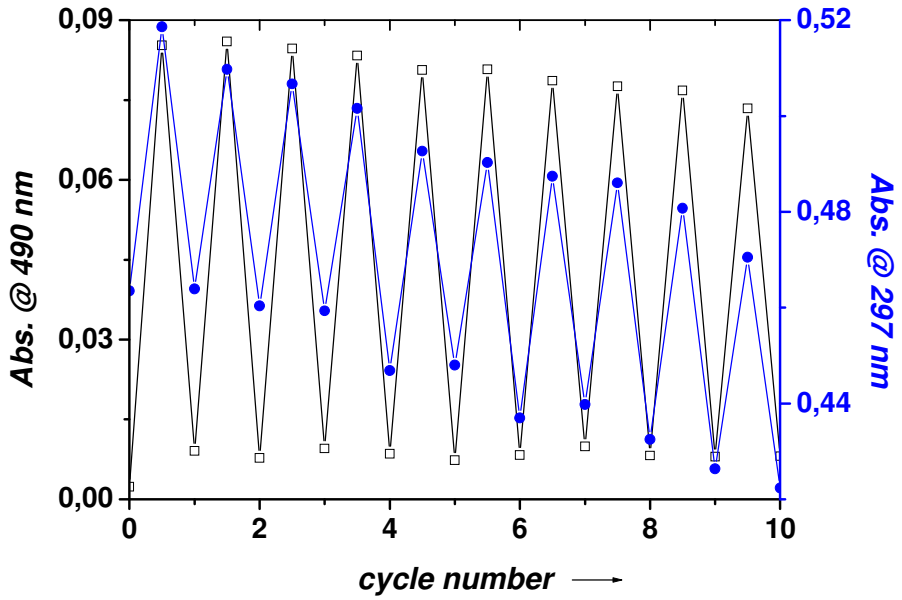

Figure 30. Performance of compound **1** (50 µM, 1, 4-dioxane) upon alternate irradiation with UV-light (λ = 312 nm) and visible light (λ > 420 nm), respectively. Changes in the visible band at λ = 490 nm (black line/ squares) and in the ultraviolet (UV) band at λ = 297 nm (blue line/ circles) were followed.

Solvent dependency of **1c**

Hypsochromic shift of the visible band

The photo-generated low-energy band of compound **1** is strongly dependant on solvent polarity. In THF, benzene, cyclohexane and 1, 4-dioxane a band in the visible region at λ = 490 nm evolves. In polar solvents such as acetonitrile (Figure 31, left) or tetrahydrofuran/water mixtures, there is a very strong hypsochromic shift (~ 150 nm) of the low-energy absorption band of the closed-isomer (λ = 350 nm).

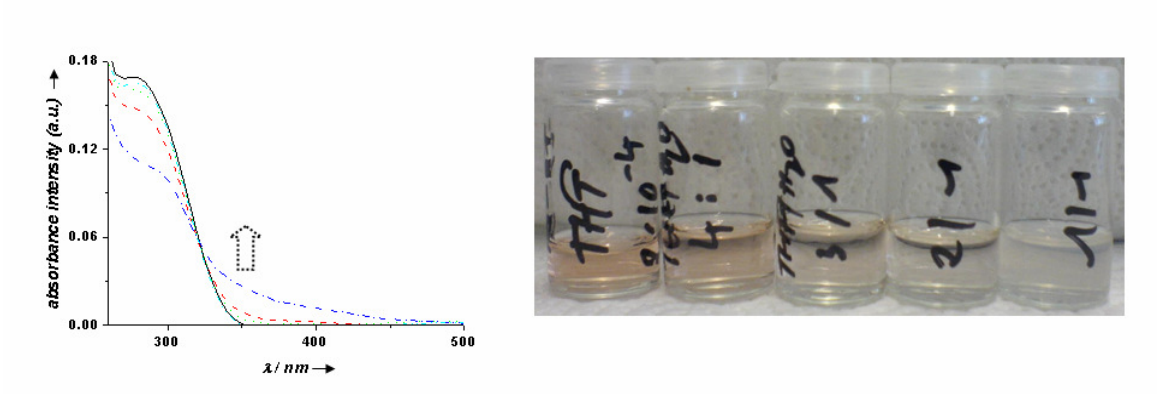

Figure 31. *Left*: UV-profile of compound **1** in acetonitrile (CH_3CN, 50 µM). The solid black line indicates the initial absorbance of **1o**. The arrow indicates the band increasing upon irradiation with UV-light (λ = 312 nm). *Right*: Solutions of indole-switch **1** (200 µM) in tetrahydrofurane / water mixtures with increasing amount of water (left to right: 0, 20, 25, 33 and 50%).

This hypsochromic shift can be followed by the naked eye (Figure 31, right). With increasing amount of water the colour is fading until at 50% water the solution is completely colourless.

Thermal stability

The thermal stability of indole switches such as compound **1** is controlled by the substituent at the indole-nitrogen and by the central ring-size.[23] However, as a third parameter the thermal stability of DIE depends on the solvent (Figure 32).

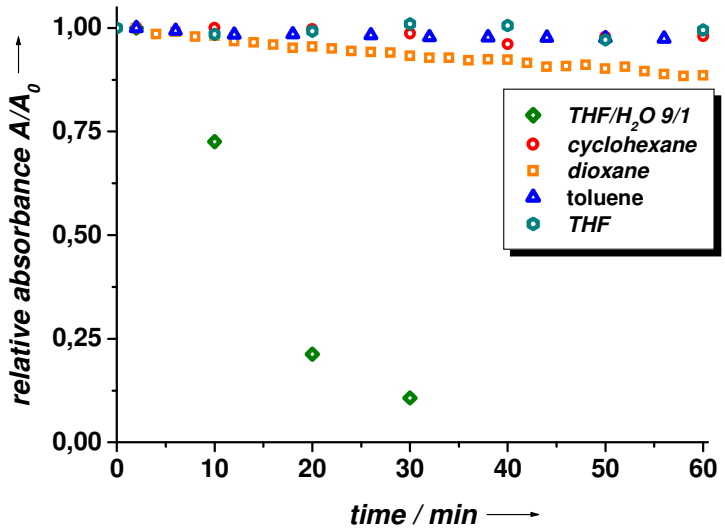

Figure 32. Thermal stability of **1c** in various solvents at room temperature. The relative absorbance A/A_0 is plotted against time.

For the thermal stability of compound **1c** changes of the visible band (λ = 490 nm) were followed at room temperature, starting from the absorbance intensity at the photostationary state (PSS). UV-spectra were recorded after defined time periods.

For solvents like THF, cyclohexane, toluene etc. the compound shows thermal stability for at least 1 h. However, increasing the polarity by the addition of even small amounts of an polar protic solvent (THF/H_2O, 9/1) results in a drastic decrease in thermal stability of the closed-ring isomer of compound **1**.

Light-induced changes in reactivity by dearomatization of indole

In order to investigate light-induced changes in reactivity due to de-aromatization of the indole moiety (Figure 33) the reactivity of the open- and closed-form isomer against Brönstedt acids were tested.

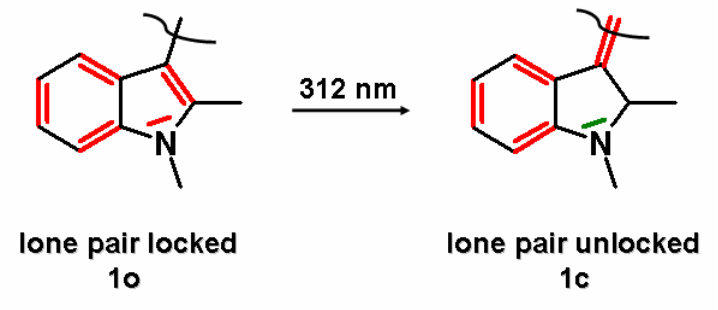

Figure 33. De-aromatization of indole upon irradiation with UV-light (λ = 312 nm). The nitrogen lone pair is involved in the aromatic π-system in the open-form isomer **1o**, whereas in the closed-form isomer **1c** the aromaticity of the indole heterocycle is interrupted and the nitrogen atom lone-pair becomes more basic.

Due to the light-induced change in the π-system, the aromaticity of the heterocyclic five-membered ring is interrupted. In the case of an indole-heterocycle the nitrogen lone pair is no longer part of the aromatic system and therefore can react as a tertiary amine. In the open-form the lone pair is part of the indole heteroarene.

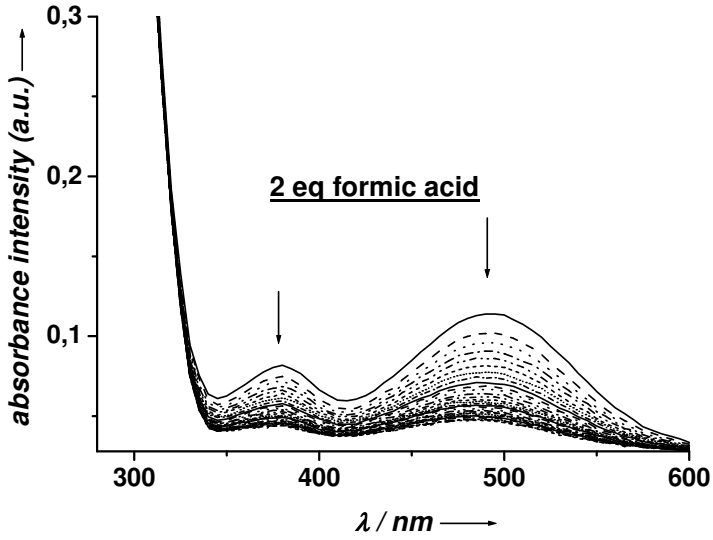

Figure 34. Proton-mediated changes in the UV/VIS spectrum of **1** (50 µM, 1, 4-dioxane) upon addition of two equivalents (eq) of an acid (as an example formic acid was chosen). Spectra were recorded every 2 min for a 1 h-period.

Protonation of the nitrogen atom lone pair by a Brönstedt acid induces a rapid ring opening of the closed-form **1c** yielding isomer **1o**. The proton-mediated ring-opening reaction can be followed by UV/VIS spectroscopy (Figure 34). Upon addition of two equivalents of a Brönstedt acid, for example formic acid, the visible band at λ = 490 nm decreases over an hour.

Catalyzed rearrangements by electron-withdrawing groups, such as cations generated by protonation or Lewis acids, are well known in literature.[24-31] Especially, those using cope rearrangement routes.[24-26] Also, 6π electro-cyclizations can be catalyzed by electron-withdrawing groups, lowering the cyclization energy barrier.[29-31]

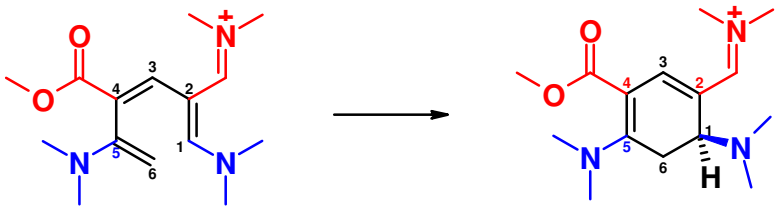

Figure 35. Computational example for a 6π electro-cyclization catalyzed by electron-withdrawing groups (marked in red) and – donating groups (marked in blue).[30]

Is a 6π system decorated with electron-withdrawing groups in C_2 and C_4 position and – donating groups in C_1 and C_5 position, the cyclization barrier can be decreased remarkably by 17-25 kcal/mol (Figure 35).[30, 31]
Therefore, we assume that the protonation of the indole-nitrogen atoms, generates an electron withdrawing nitrogen cation in the ring-closed (basic) isomer and this is induces a rapid reaction to the ring-open (not basic) isomer.

It was observed that the strength of the Brönstedt acid is related to the rate of the generation of the ring-open isomer **1o** indicated by the decreasing visible absorption band (Figure 36).

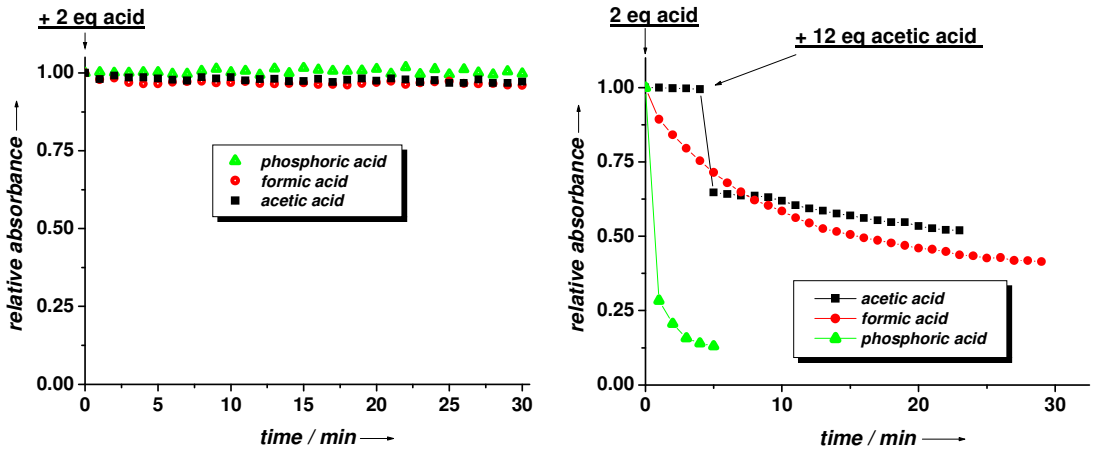

Figure 36. *Left*: Reactivity profile of the reaction of the open-isomer **1o** (50 µM, 1, 4-dioxane) against Brönstedt acids (phosphoric acid = green triangles, formic acid = red squares and acetic acid = black squares). *Right*: Reactivity profile of the reaction of the closed-isomer **1c** (50 µM, 1, 4-dioxane) against Brönstedt acids (phosphoric acid = green triangles, formic acid = red squares and acetic acid = black squares).

When adding two equivalents (one equivalent for each nitrogen) of acetic acid (pKa = 4.75 in water) to compound **1c** no decrease of the visible band can be observed. After addition of another twelve equivalents a decrease is visible, the conversion is however rather slow. This indicates that the acidity of acetic acid is not high enough to protonate the compound which induces the ring opening and decreases the visible absorption band of **1c**. In the case of formic acid (pKa = 3.75 in water) however, after the addition of two equivalents the visible absorption band decreases almost completely within 60 min. After the addition of two equivalents of phosphoric acid (pKa = 2.2 in water) to compound **1c** the absorption band vanished almost immediately (Figure 36 right part), showing that instant protonation and therefore decrease of the visible absorption band occurs.

The open-isomer **1o** showed no reaction with Brönstedt acids, after the addition of two equivalents of acid (Figure 36 left part).

Due to this observation it can be concluded that the lone-pair of the indole-nitrogen atom can be activated for protonation by light and reacts as tertiary amine.

The pK_b value of the nitrogen atoms of **1c** is expected to be between the pK_b values of formate and acetate in 1, 4-dioxane, which are ~ 11 and ~10 respectively. The photo-generated base has a high structural similarity to dimethylaniline, which has a pK_b value in the range of about 10.[32] Therefore, it is concluded that the pK_b value of the generated base is in that range. Acetic acid is just acidic enough if used in large excess to protonate the nitrogen of **1c** and induces a decreasing of the visible absorption band. Formic acid is more acidic and induces a decrease of the absorption band slowly within 60 min. The acidity of phosphoric acid is high (pKa = 2.2). The nitrogens are almost instantly protonated and an immediate decrease of the visible absorption band as a consequence of a rapid ring opening reaction is observed.

V.3 Conclusion

A bis-indole diarylethene **1** was synthesized. The compound shows typical characteristics of diarylethene compounds and cyclizes upon alternate irradiation with light of an appropriate wavelength. The ring-open isomer shows emission, whereas the ring-closed isomer is non-fluorescent. The basicity of the compound can be changed by irradiation with UV-light (λ = 312 nm): In the open-form isomer the nitrogen atom lone pair is involved in the aromatic system of the indole-moiety, whereas in the closed-form isomer it is not. The ring-closed isomer is readily protonated by acids, such as formic or phosphoric acid, but protonation induces the rapid conversion of the closed-form isomer into the open-form isomer. The detailed mechanism of this proton-induced reaction is unknown, but we assume that it occurs via a concerted reaction, catalyzed by protonation of the generated tertiary amines. Computational chemistry invesitigations are in progress to unravel the mechanism of the acid catalyzed ring-opening reaction.

V.4 Experimental Part

1. Synthesis and characterization of new compounds

General. Thin layer chromatography (TLC) was performed on alumina plates coated with silica gel (Merck silica gel 60 F 254, layer thickness 0.2 mm). Column chromatography was performed on silica gel (70–230 mesh) from Merck. Starting materials were purchased from either Acros or Sigma-Aldrich and used without any further purification. Solvents were purchased from Aldrich and used without further purification except for dry THF, which was prepared by distillation from potassium. 1,2-bis(1-hexadecyl-2-methyl-1H-indol-3-yl)cyclohex-1-ene **1**[23] is literature known but the synthetic procedure was improved.

Techniques. Melting points (MP) were determined with a Büchi SMP 20. IR-spectra were recorded with a Bio-Rad FTS 2000 MX FT-IR spectrometer. NMR spectra were recorded on a Bruker Avance 400 (1H: 400.1 MHz, 13C: 100.6 MHz, T = 300 K) or a Bruker Avance 300 (1H: 300.1 MHz, 13C: 75.5 MHz, T = 300 K). The spectra are referenced against the NMR-solvent and chemical shifts are reported in ppm. MS-Spectra were determined on a Varian CH-5 (EI), a Finnigan MAT 95 (CI; FAB and FD) or a Finnigan MAT TSQ 7000 (ESI). UV–Vis absorption spectroscopy was performed using a Cary 50 Bio spectrophotometer.

Photochemistry. Standard hand-held lamps used for visualizing TLC plates (Herolab, 6 W) were used to carry out the ring-closing reactions at 312 nm. The ring-opening reactions were carried out using the light of a 200 W tungsten source that was passed through a 420 nm cut-off filter to eliminate higher energy light. The power of the light source is given based on the specifications supplied by the company when the lamps were purchased. A light detector was not used to measure the intensity during the irradiation experiments.

1-(1H-Indol-3-yl)-6-(2-methyl-1H-indol-3-yl)hexane-1,6-dione 3. [23]

Under a N_2-atmosphere 2-methylindole 4.52 g (34.28 mmol, 5 eq) was dissolved in 50 mL dry THF and cooled to 0°C by an ice/water bath. EtMgBr 11.43 mL (34.28 mmol, 5 eq) was added dropwise and after the addition the mixture was

refluxed for 60 min. After this period adipoyldichloride (1 ml, 6.86 mmol, 1 eq) was added to the refluxing mixture and after the addition refluxing was continued for 17 h. The reaction mixture was then quenched by the addition of 40 mL 1 M HCl und 80 mL H_2O. The resulting precipitate was collected by vacuum filtration and the solid lyophilized, yielding 1.14 g (3.06 mmol, 45 %) of a red solid. **^{1}HNMR (300 MHz, $CDCl_3$):** δ [ppm] = 1.72-1.80 (m, 4H), 2.68 (s, 6 H), 2.88-2.98 (m, 4 H), 7.05-7.19 (m, 4 H), 7.30-7.42 (m, 2 H), 7.94-8.09 (m, 2 H), 11.62 (bs, 2 H).

1,6-Bis(1-hexadecyl-2-methyl-1H-indol-3-yl)hexane-1,6-dione 4.[23]

Under a N_2-atmosphere compound **3** (0.5 g, 1.3 mmol) was suspended in 10 mL of dry DMF. NaH (214 mg, 5.36 mmol) was then added in portions and the compound dissolved, after the addition the mixture was heated to 40° C for 60 min. 1-Bromohexadecane (1.64 mL, 5.36 mmol) was added with the help of a syringe and stirring was continued at 40°C for further 16 h. The reaction was quenched by the addition of 20 mL 1 M HCl und 20 mL H_2O and the precipitate was collected by vacuum filtration and the resulting solid was dried by lyophilization, yielding 0.5 g (0.6 mmol, 76%) of a colourless solid.

^{1}HNMR (300 MHz, $CDCl_3$): δ [ppm] = 0.88 (t, ^{3}J = 7.0 Hz, 6 H), 1.33-1.25 (m, 56 H), 1.75 (quintet, ^{3}J = 7.0 Hz, 4 H), 1.92-2.00 (m, 4 H), 2.78 (s, 6 H), 3.06-3.16 (m, 4 H), 4.11 (t, ^{3}J = 7.5 Hz, 4 H), 7.21-7.26 (m, 4 H), 7.30-7.37 (m, 2 H), 7.92-8.00 (m, 2 H).

1,2-Bis(1-hexadecyl-2-methyl-1H-indol-3-yl)cyclohex-1-ene 1o. [25]

Under a N_2-atmosphere zinc dust (0.3 g, 4.9 mmol, 4 eq) was suspended in 30 mL dry THF. The suspension was then cooled to -20°C by an acetone/liquid nitrogen bath and $TiCl_4$ (0.4 mL, 0.5 g, 2.4 mmol, 2 eq) was added dropwise with the help of a syringe. The resulting mixture was then refluxed for 60 min. After this period compound **4** was added in four portions and the mixture was

refluxed for another 26 h. The black suspension was then poured into a 10% aq. K_2CO_3 solution and stirred at room temperature for 20 min. The resulting dark blue slurry was passed through Celite, which was purged several times with diethyl ether (20 mL). The two phase system was separated and the aqueous phase further extracted with diethyl ether (3 times 50 mL). The combined org. phases were dried (Na_2SO_4), filtered and the solvent removed in *vacuo*. The resulting orange oil was purified by flash column chromatography (flash silica, petroleum ether/ethyl acetate v/v 40/1 to petroleum ether/ethyl acetate v/v 15/1, R_f (petroleum ether/ethyl acetate v/v 15/1) = 0.73) affording 0.3 g (0.4 mmol, 31 %) as a yellow oil.

^{1}H-NMR (300 MHz, $CDCl_3$): δ [ppm] = 0.88 (t, ^{3}J = 7.0 Hz, 6 H), 1.02-1.27 (m, 52 H), 1.30-1.43 (m, 4 H), 1.52 (s, 6 H), 1.83-1.94 (m, 4 H), 2.19-2.40 (m, 4 H), 3.39-3.87 (m, 8 H), 6.79-7.13 (m, 6 H), 7.47-7.57 (m, 2 H).

Photochemical synthesis of the ring-closed isomer 1c

A solution of compound **1o** (2 mg, 2.5 µmol) in C_6D_6 (0.7 mL) was irradiated for 30 min with light of a wavelength of 312 nm in an NMR tube yielding a red solution of. In this photostationary state the reaction mixture contains 38% of the ring-closed isomer **1c** according to ^{1}H-NMR spectroscopy. The remaining 62% were assigned to the ring-open isomer **1o**.

^{1}H-NMR (300 MHz, $CDCl_3$): δ [ppm] = 0.88 (t, ^{3}J = 7.0 Hz, 6 H), 1.02-1.27 (m, 52 H), 1.30-1.43 (m, 4 H), 1.62 (s, 6 H), 1.83-1.94 (m, 4 H), 1.97-2.07 (m, 4 H), 3.69-3.97 (m, 8 H), 6.79-7.13 (m, 6 H), 7.47-7.57 (m, 2 H).

Apendix: Spectra

Compound 3

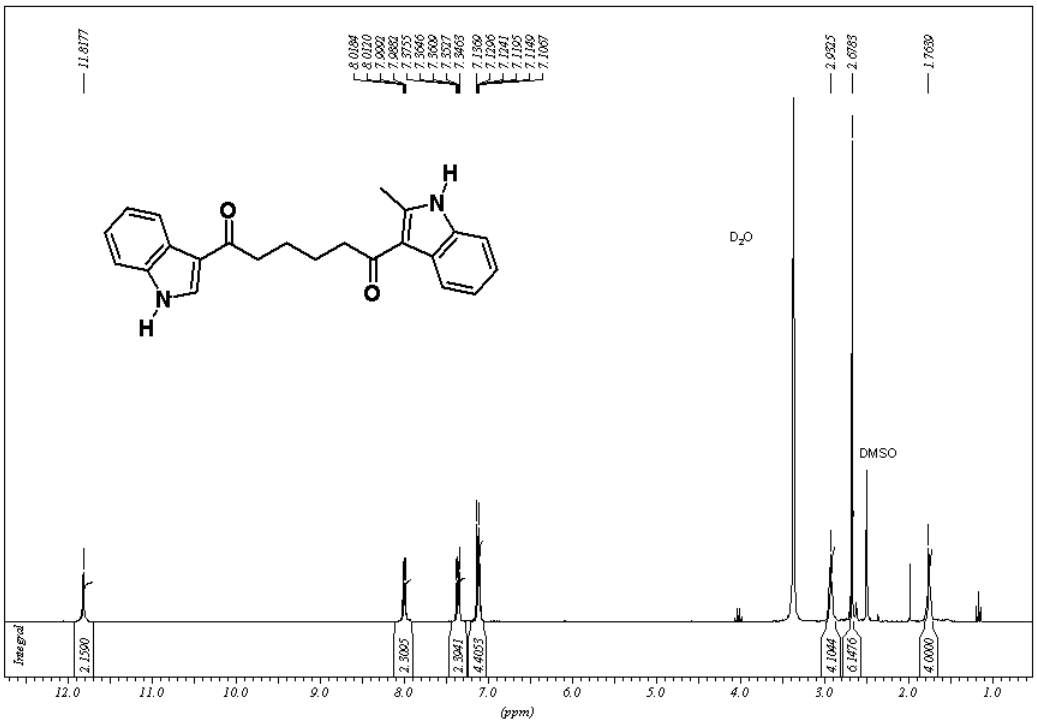

Compound 4

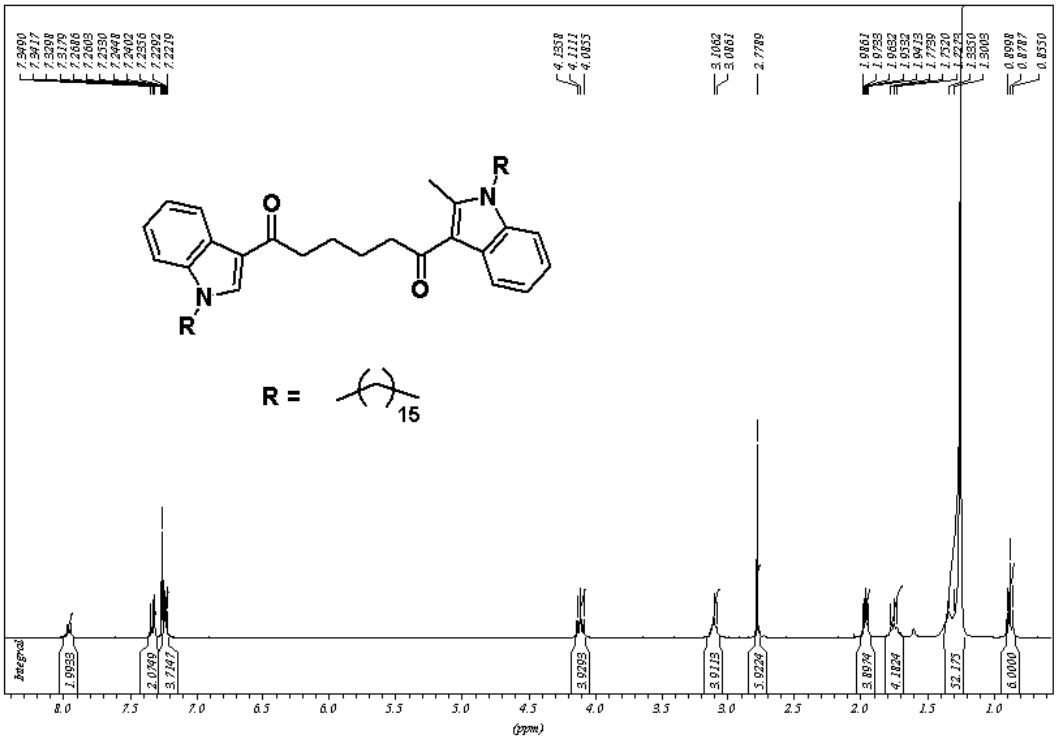

Compound 1o

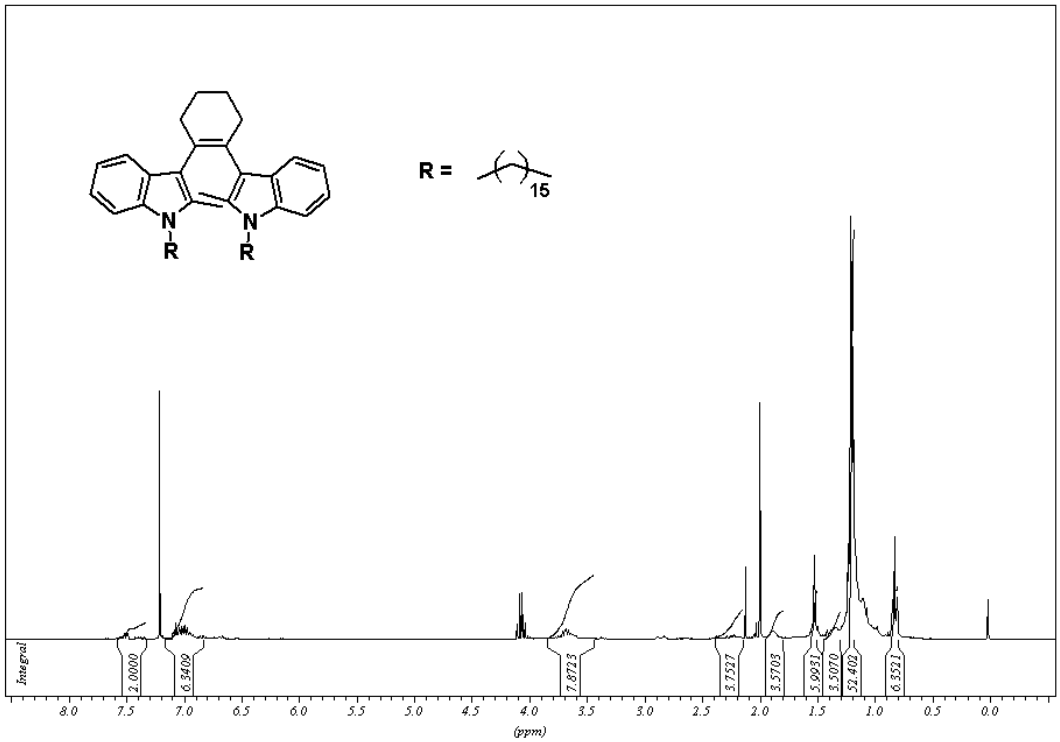
R =
15
N
R
N
R
Integral
2.0000
6.3409
7.8723
3.7527
3.5703
5.9931
3.5070
52.402
6.3521
8.0
7.5
7.0
6.5
6.0
5.5
5.0
4.5
4.0
3.5
3.0
2.5
2.0
1.5
1.0
0.5
0.0
(ppm)

V.5 References

(1) Irie, M. *Chem. Rev.* **2000**, *100*, 1685-1716.

(2) Irie, M.; Fukaminato, T.; Sasaki, T.; Tamai, N.; Kawai, T. *Nature* **2002**, *420*, 759-760.

(3) Morimitsu, K.; Shibata, K.; Kobatake, S.; Irie, M. *J. Org. Chem.* **2002**, *67*, 4574-4578.

(4) Peters, A.; McDonald, R.; Branda, N. R. *Chem. Commun.* **2002**, 2274-2275.

(5) Kawai, T.; Iseda, T.; Irie, M. *Chem. Commun.* **2004**, 72-73.

(6) Tian, H.; Yang, S. *Chem. Soc. Rev.* **2004**, *33*, 85-97.

(7) Giordano, L.; Vermeij, R. J.; Jares-Erijman, E. A. *ARKIVOC* **2005**, 268-281.

(8) Lemieux, V.; Branda, N. R. *Org. Lett.* **2005**, *7*, 2969-2972.

(9) Ohsumi, M.; Fukaminato, T.; Irie, M. *Chem. Commun.* **2005**, 3921-3923.

(10) Samachetty, H. D.; Branda, N. R. *Chem. Commun.* **2005**, 2840-2842.

(11) Tanifuji, N.; Irie, M.; Matsuda, K. *J. Am. Chem. Soc.* **2005**, *127*, 13344-13353.

(12) Lemieux, V.; Spantulescu, M. D.; Baldridge, K. K.; Branda, N. R. *Angew. Chem. Int. Ed.* **2008**, *47*, 5034-5037.

(13) Kawai, S. H.; Gilat, S. L.; Ponsinet, R.; Lehn, J.-M. *Chem. Eur. J.* **1995**, *1*, 285-293.

(14) Takeshita, M.; Irie, M. *Chem. Lett.* **1998**, 1123-1124.

(15) Fernandez-Acebes, A.; Lehn, J.-M. *Chem. Eur. J.* **1999**, *5*, 3285-3292.

(16) Endtner, J. M.; Effenberger, F.; Hartschuh, A.; Port, H. *J. Am. Chem. Soc.* **2000**, *122*, 3037-3046.

(17) Matsuda, K.; Irie, M. *Chemistry* **2001**, *7*, 3466-3473.

(18) Matsuda, K.; Matsuo, M.; Mizoguti, S.; Higashiguchi, K.; Irie, M. *J. Phys. Chem. B* **2002**, *106*, 11218-11225.

(19) Vomasta, D.; Högner, C.; Branda Neil, R.; König, B. *Angew. Chem. Int. Ed.* **2008**, *47*, 7644-7647.

(20) Peters, M. V.; Stoll, R. S.; Kuehn, A.; Hecht, S. *Angew. Chem. Int. Ed.* **2008**, *47*, 5968-5972.

(21) Kawai, S. H.; Gilat, S. L.; Lehn, J.-M. *Eur. J. Org. Chem.* **1999**, 2359-2366.

(22) Odo, Y.; Matsuda, K.; Irie, M. *Chem. Eur. J.* **2006**, *12*, 4283-4288.

(23) Huang, Z.-N.; Jin, S.; Ming, Y.; Fan, M. *Mol. Crys. Liq. Crys.* **1997**, *297*, 99-106.

(24) Mehta, G.; Padma, S. *J. Org. Chem.* **2009**, *53*, 4890-4892.

(25) Stas, S.; Tehrani, K.A.; Laus, G. *Tetrahedron*, **2008**, *64*, 3457-3463.

(26) Aron, Z.D.; Overman, L.E. *Org. Lett.*, **2009**, *7*, 913-916.

(27) Hsueh, P.; Lukowski, M.; Lindsay, H.A.; Milletti, M.C. *Theochem*, **2007**, *806*, 223-230.

(28) Ruan, H.L.; Yin, W.B.; Wu, J.Z.; Li, S.M. *ChemBioChem*, **2008**, *9*, 1044-1047.

(29) Bishop, L.M; Barbarow, J.E.; Bergmann, R.G.; Trauner, D. *Angew. Chem. Int. Ed.* **2008**, *47*, 8100-8103.

(30) Guner, V.A.; Houk, K.N.; Davies, I.W. *J. Org. Chem.*, **2004**, *69*, 8024-8028.

(31) Yu, T.-Q.; Fu, L.; Liu, L.; Guo, Q.-X. *J. Org. Chem.* **2006**, *71*, 6157-6164.

(32) Marshall, H.P.; Grunwald, E. *J. Am. Chem. Soc.* **1954**, *76*, 2000-2004.

Salen metal complexes and their use in amino acid recognition

This chapter deals with the well-known salen molecules and their ability in molecular recognition. In this chapter some basic investigations have been done and discussed.

The Ti-salophen complex **3** was synthesized by Julia Sauerwein, under the supervision of Daniel Vomasta (F-Praktikum).All the measurements as well as the synthesis of the other molecules have been done by Daniel Vomasta.

VI. Salen metal complexes and their use in amino acid recognition

VI.1 Introduction

The development of peptide chemosensors and the specific recognition of peptides by synthetic receptors under physiological conditions still remains a challenging task. Recently reported approaches used porphyrines, helix mimics, crown ethers or short peptides with guanidiniocarbonyl pyrroles as binding sites to specifically recognize peptidic structures.[1] So far, salen complexes have not been used for the molecular recognition of peptidic structures, which is surprising as some salen complexes are Lewis-acidic binding sites and the compound class is well-studied within the field of homogeneous catalysis.[2] Salen complexes have been used as catalytic species in numerous organic transformations including epoxidation of olefins, lactide polymerization, asymmetric ring opening epoxides, and Michael reactions,[3,4] as well as for construction of coordinative frameworks.[2] A chiral cobalt(II)-salen complex has been used to separate D- and L-amino acids by the simultaneous coordination of the C- and N-terminus of only one of the amino acid enantiomers. The Salen complex - amino acid aggregate is separated from the remaining amino acid enantiomer. Dissociation of the salen-amino acid complex deliberates the enantiomerically pure amino acid.[5] Metal-salen complexes are easily prepared in one step from aldehydes and diamines. Some salen metal complexes show luminescent emission upon excitation by light of 330 - 360 nm. The luminescent properties can be used to directly monitor guest binding and an additional labelling by a fluorescent reporter group, as it is necessary for other metal complex binding sites, such as M(II)-IDA (iminodiacetic acid), M(II)-NTA (nitrilotriacetic acid) or M(II)-cyclen (1,4,7,10-tetraazacyclodecane)[6] is avoided. Overall, their simple and cheap synthesis, ease of further derivatization, interesting luminescent properties and the ability to reversibly coordinate guest molecules renders metal-salen complexes interesting molecular building blocks for new chemosensors. [7-10]

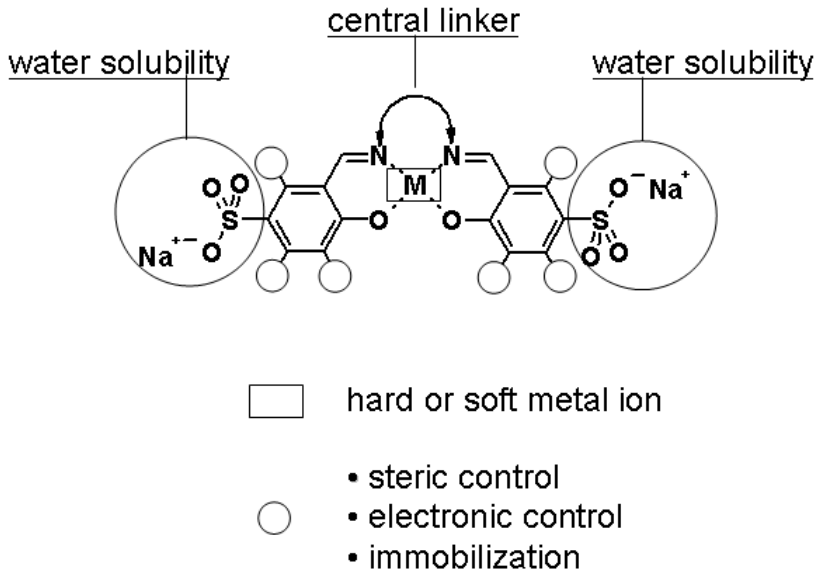

Figure 37. General structure of a symmetric metal-salen complex. The metal ion can be used to change the recognition properties of the complex using either hard or soft metal ions. The substitution at the aryl rings may be used for control of the ligand and complex properties.[3]

Encouraged by the discussed properties some preliminary investigations of selected metal-salen complexes containing Ti(IV), Ni(II), and Fe(III) as the metal ions were performed to explore their ability to recognize peptidic structures.

VI.2 Results and disucussion

Synthesis of achiral salophen and chiral salen metal-complexes

The synthesis of metal complexes **1** and **2** starts from commercially available salicylic aldehyde **6** by formation of imine **7**, sulfonation and removal of the imine protection group to yield compound **8.**[11] Schiff base formation and simultaneous metal ion coordination gives the salen metal complexes **1**[12], **2**[11] and **3** in good yields (Figure 38).

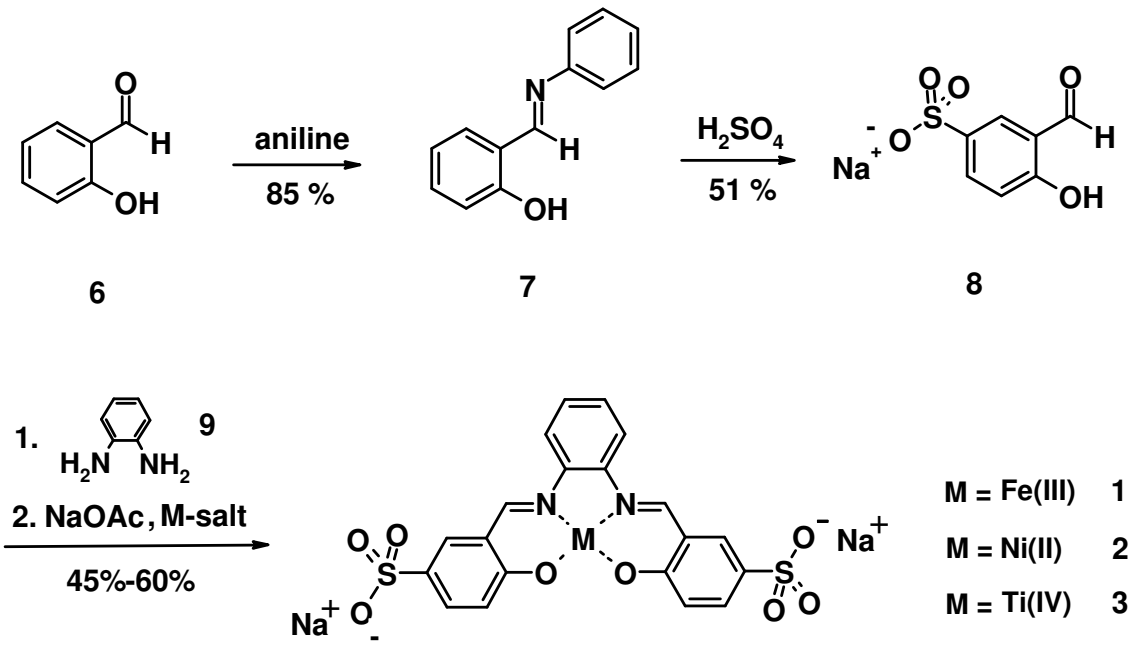

Figure 38. Synthesis of water soluble and Fe(III)[12], Ni(II)[11] and Ti(IV) salophen-complexes **1**, **2** and **3.**

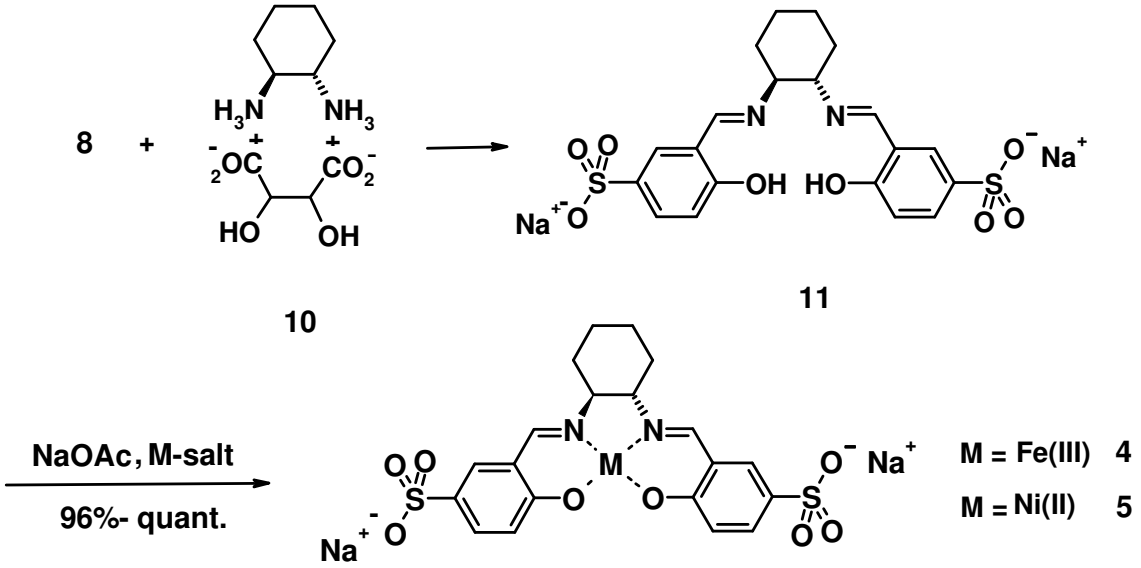

Figure 39. Synthesis of chiral and water soluble Fe(III) and Ni(II) salen-complexes **4**[23] and **5**[24]

The synthesis (Figure 39) of chiral metal-salen complexes **4** and **5** starts from chiral ligand **11**, which was synthesized by condensation of modified salicylic aldehyde **8** with *trans*-1,2-diamino-cyclohexane (**10**). The ligand was then allowed to react with metal-salts under basic conditions to form complexes **4** and **5**.

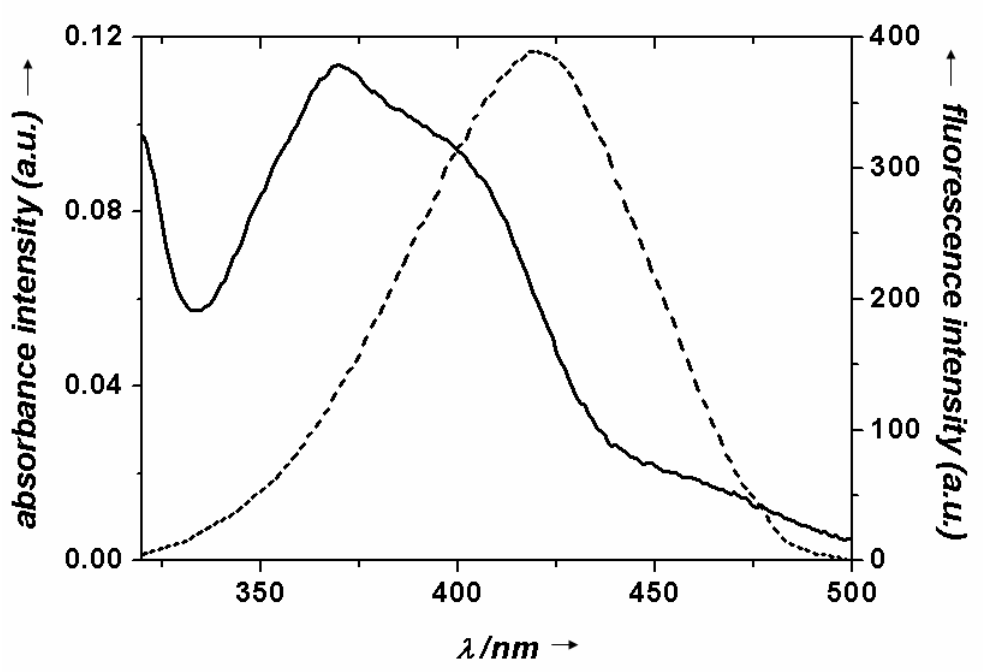

Figure 40. Representative absorbance (solid black line) and fluorescence (dotted black line) spectra of Ni(II)-salophen complex **2** (33 µM, HEPES buffer).

Salophen complexes **1** and **2** show emission with λ_{max} = 428 nm when excited at λ_{ex} = 330 nm. The fluorescence spectrum and the UV-absorption overlap significantly (Stokes shift ~ 60 nm).

Fe(III)-salophen complex **1**

The synthesis of iron(III) – salen complexes results always in the formation of an oxy- bridged binuclear dimer.[12-13] Mass experiments showed the presence of a dimeric structure as well as a monomeric structure. Three different recrystallization steps from water, ethanol or acetonitrile did not produce the pure monomeric or dimeric species. Therefore, the contents of monomeric and dimeric complexes in the mixture is unknown, because from the mass experiment no conclusion about quantities can be made.

Binding studies

The ability of complex **1** to bind amino acids or phosphates was investigated in aqueous HEPES buffer [HEPES: 2-(4-(2-hydroxyethyl)-1-piperazinyl)-ethan-sulfonsäure), 50 mM, 154 mM NaCl at pH = 7.4.

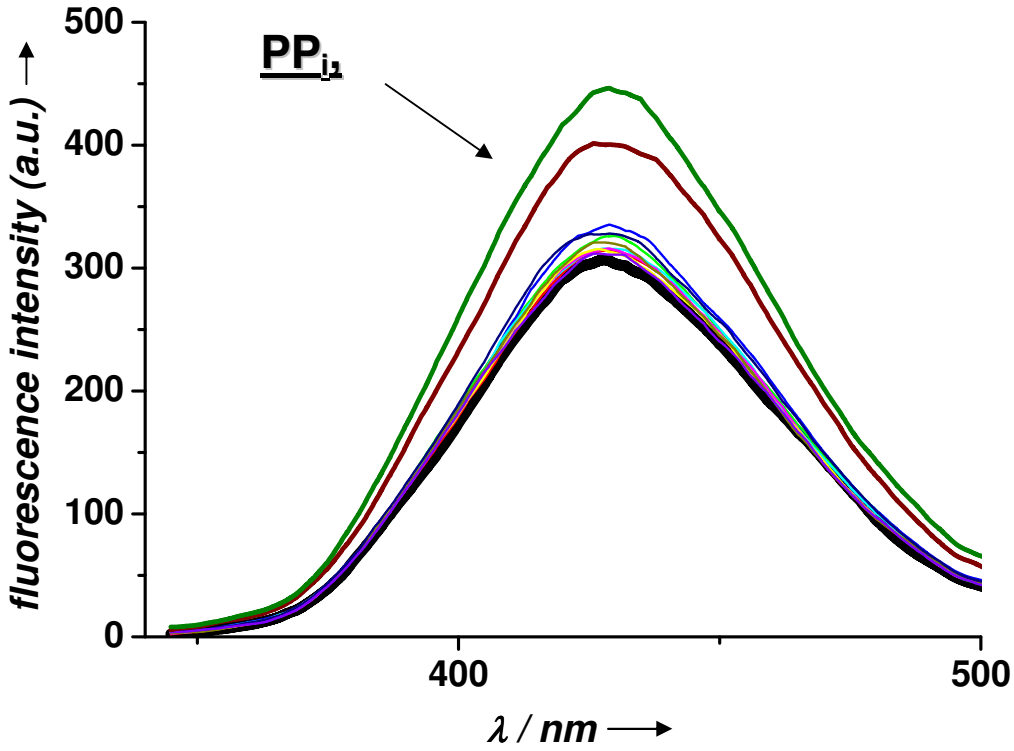

Figure 41. Fluorescence intensity change upon addition of amino acids and phosphate derivatives (1mM, 10 eq) (green line = PP_i, brown line = ATP) to Fe(III)-salophen **1** (thick black line = emission without added analyte) using the well-plate technique (33 µM, 25 °C, λ_{ex} = 330 nm, λ_{ex} = 428 nm).

Only phosphates PP_i and ATP lead to an increase of fluorescence intensity of Fe(III)-salophen **1** (Figure 41), whereas the addition of side chain functionalized unprotected amino acid, such as aspartic acid, histidine methylester and serine caused no change in fluorescence intensity.

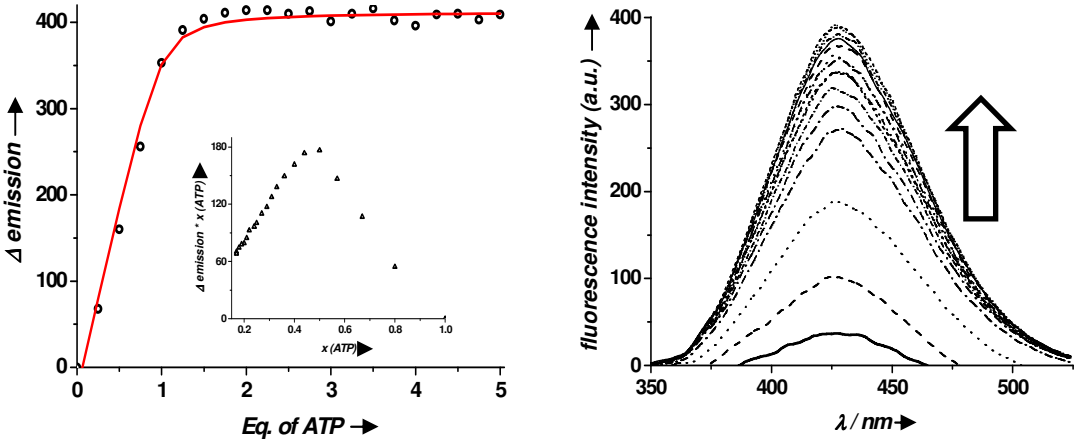

Figure 42. *Left*: Fluorescence titration of Fe(III)-salophen complex (1 µM) **1** with ATP (10 µM). The changes in fluorescence intensity were plotted against equivalents of ATP. The inset shows a Job's plot analysis. *Right*: Changes in fluorescence emission intensity upon addition of increasing aliquots of ATP.

The fluorescence titration of the Fe(III)-salophen against ATP showed a distinct binding stoichiometry of 1 : 1 and a binding constant of lg K = 7.7 was derived from the measurement. This high affinity towards ATP is attributed to the high negative charge of ATP, its ability to act as a bidentate ligand and to the oxophilicity of the Fe(III) – ion.

The poor water solubility of the compound prevented ITC measurements.

Ni(II)-salophen complex **2.**

Water soluble aromatic Ni(II)-salophen complexes are rarely described in literature. They are used for the epoxidation of sytrenes[14] and as singlet oxygen quenchers.[11] The X-ray structure analysis of the parent complex is not known, only the structure of the ethylene-diamine complex was reported (Figure 9). Mass spectrometric analysis of complex **2** gave no indication of the formation of dimeric complexes.

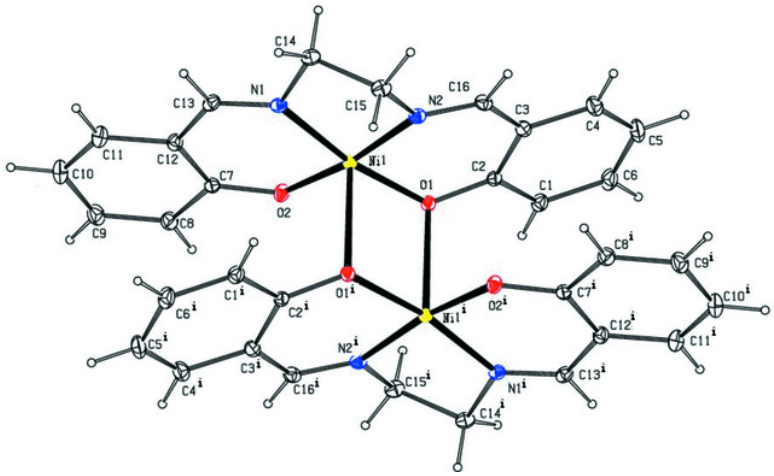

Figure 43. Crystal structure of a possible Ni(II)-salen-dimer (ethylendiamine bridging ligand).[3,15]

Binding studies

The binding properties of complex **2** towards amino acids and phosphates were investigated by a well-plate screening in aqueous HEPES buffer, 50 mM, at pH = 7.4 and 25 °C.

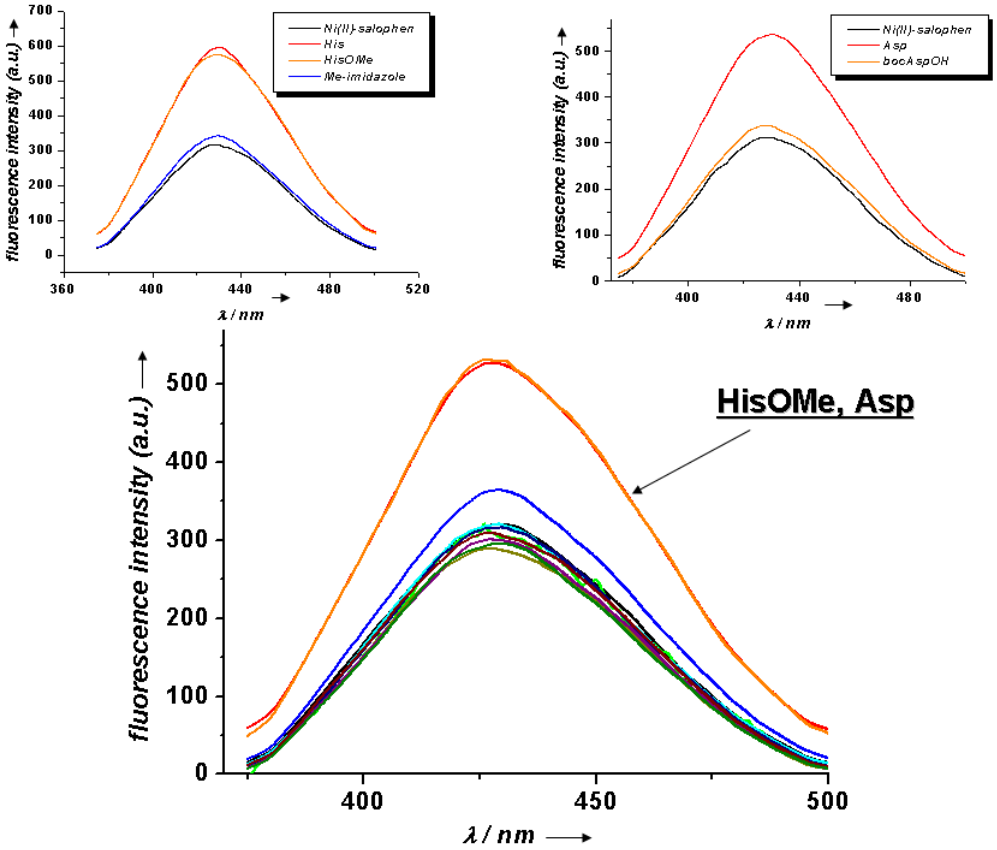

Figure 44. *Upper left:* Fluorescence response of Ni(II)-salophen **2** against histidine derivatives (1mM, 10 eq). *Upper right:* Fluorescence response of Ni(II)-salophen **2** against aspartic acid (1mM, 10 eq) and N-terminal protected aspartic acid (1 mM, 10 eq). *Lower:* Fluorescence intensity change upon the addition of amino acids with functional groups in the side chain (1 mM, 10 eq) to Ni-salen-complex **2** using the well-plate technique (Ni(II)-salophen = 33 µM, 25°C, HEPES buffer 50 mM, 154 mM NaCl, λ_{ex} = 330 nm, λ_{em} = 428 nm).

The amino acid screening revealed an increase in fluorescence intensity upon addition of histidine and aspartic acid (Figure 37 lower part). Other amino acids like serine, cysteine, lysine, and others with a functional group in their side chain, induced no increase of the fluorescence intensity. Changes in fluorescence intensity can be ascribed to the binding of the respective amino acid to the Ni(II)-salophen complex **2** the complex shows selectivity for histidine and aspartic acid. This result is quite surprising, as Gennari and co-workers[5] proposed a simultaneous binding of the C- and N-terminus of the amino acid to a chiral cobalt(II)-salen complex and therefore no selectivity for any amino acid. For the Ni(II)-complex **2** the binding situation is certainly different. The side chain of the amino acid must be involved in the interaction with the metal complex.

To investigate the histidine binding in more detail we performed a screening experiment with histidine, histidine-methylester (HisOMe) and methyl-imidazole (Figure 44 upper left). We found that only unprotected histidine and histidine-methylester interacts with complex **2**, showing that the free C-terminus is not important for the interaction and that imidazole alone can not interact with the Ni(II)-salophen. Only a combination of the N-terminal amino group and the imidazole side chain functionality results in strong binding to complex **2**.
For the screening experiment with aspartic acid and N-terminal protected aspartic acid (Figure 44 upper right) we found similar results to those obtained for histidine. The N-terminal part of the amino acid is important for the binding. The bidentate ligand interaction requires a certain distance between the donor atoms. This can be concluded from the observation that aspartic acid interacts with complex **2** whereas glutamic acid does not.

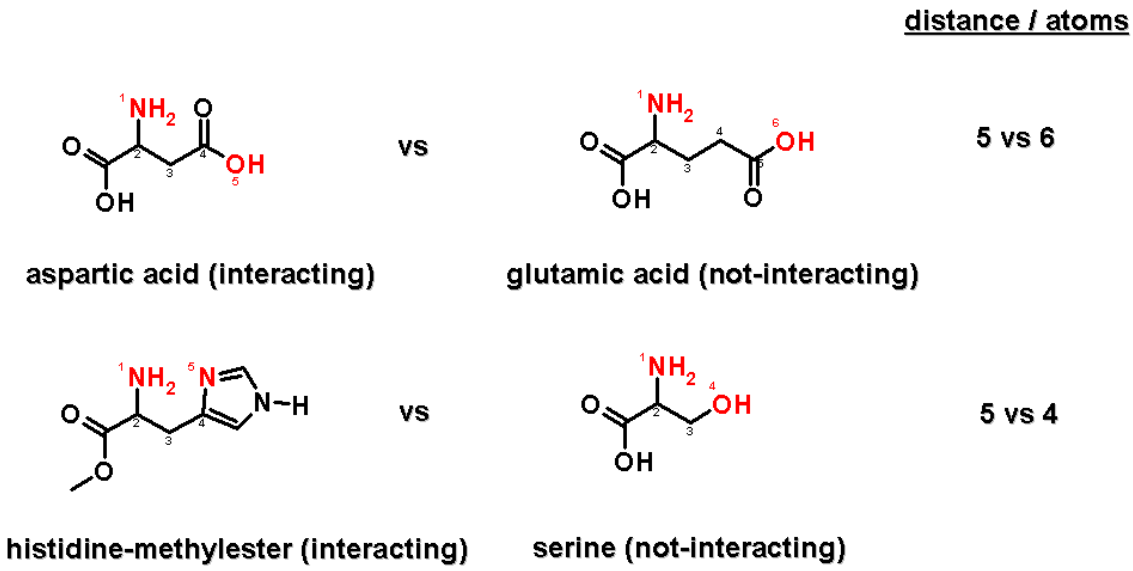

Figure 45. Amino acids and the distance between the coordinating atoms. The coordinating donor atoms are marked in red.

The distance between coordinating donor atoms must be five atoms (Figure 45). If the distance is too large or too small no coordination to complex **2** is observed, as in the case of glutamic acid (six atoms) and serine (four atoms).

However, for the Ni-salophen **2**, no distinct binding constant as well as binding stoichiometry could be obtained for the interaction with histidine and aspartic acid using fluorescence measurements. In every case two coordination aggregates were observed, which was confirmed by ITC measurements. Due to this observation, interpretations about the present structures and therefore determination of the corresponding binding constants are rather difficult. Investigations with different equivalents of the analyte showed that the stoichiometry and the binding constant is dependant on the concentration of the complex **2** (for more information see experimental part). In contrast during ITC measurements this behaviour was not observed, however two different coordination aggregates were obtained one with larger error value. The main difference between these two methods is that fluorescence measurements were done at micro molar concentration (1 µM), the concentration had to be increased to 100 µM for ITC investigations as the method is less sensitive.

To investigate, whether π-π-interactions can explain the differences in stoichiometries, UV spectra of complex **2** at different concentrations were recorded (Figure 46).

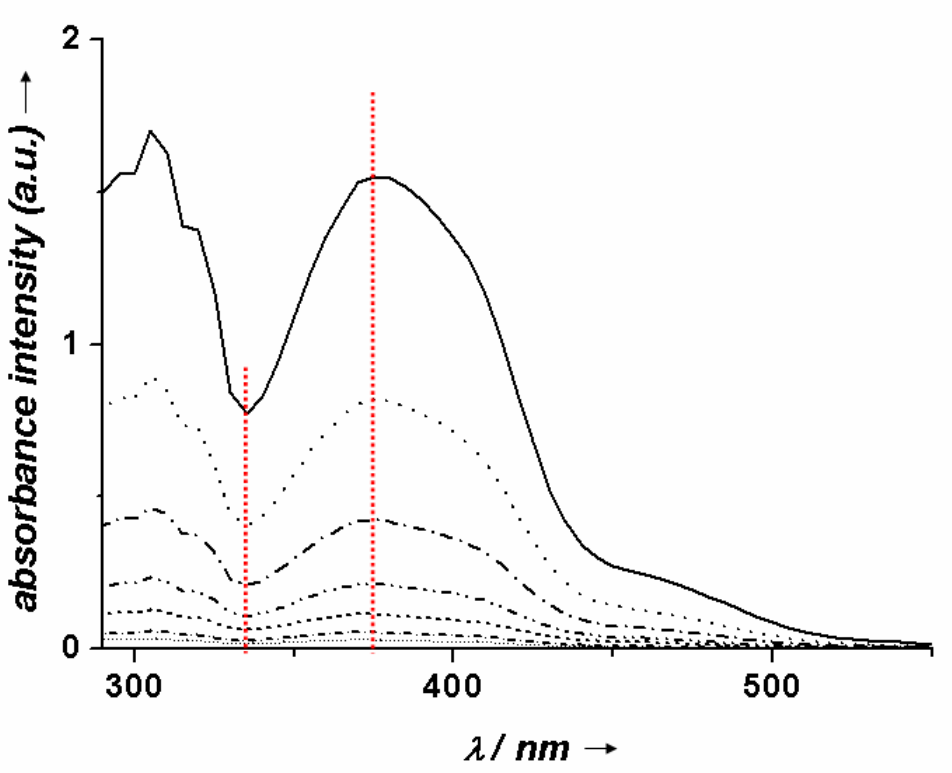

Figure 46. UV-spectra of complex **2** (HEPES buffer) at different concentrations. Concentrations were 100, 50, 10, 5, 1, 0.5 and 0.1 µM. The red line indicates the UV-maximum and UV-minimum, respectively.

The concentration dependent UV measurements did not indicate aggregate formation for compound **2** at the investigated concentrations. From UV measurements at different concentrations no clear indication on aggregate formation by π-π-stacking of the compounds could be derived.

Ti(IV)-salen complex **3**.

The complex **2** was investigated by a well-plate screening under physiological pH (7.4) in HEPES (2-(4-(2-Hydroxyethyl) - 1-piperazinyl)-ethansulfonic acid, 50 mM, 25 °C) buffer solution.

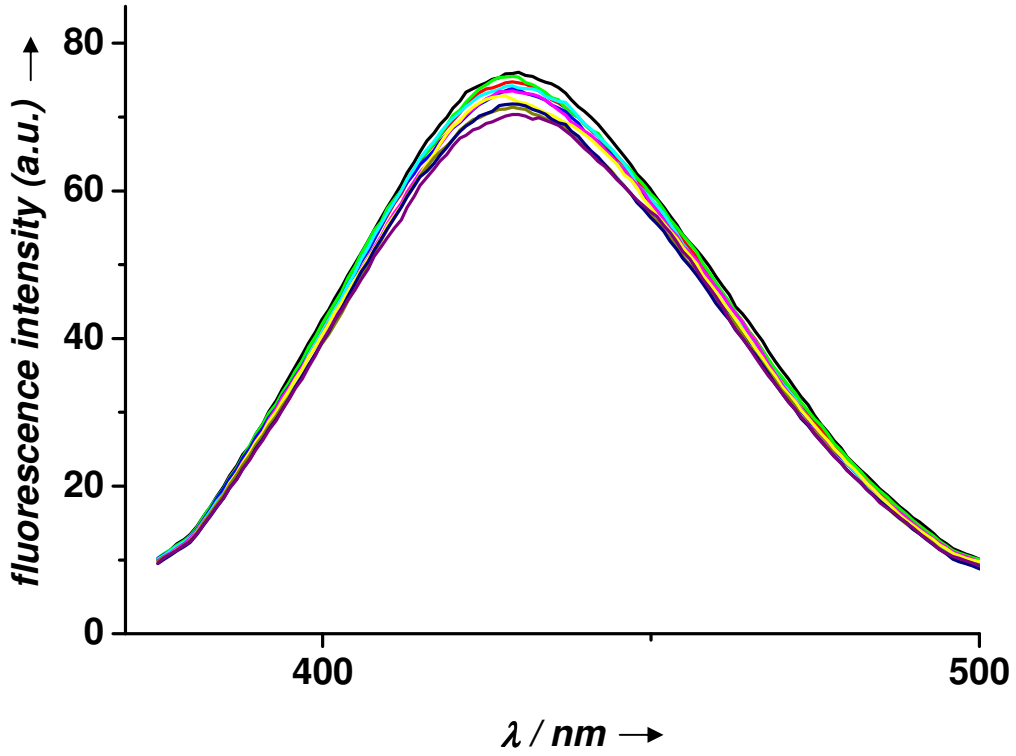

Figure 47. Fluorescence intensity change upon amino acid addition for Ti(IV)-salophen complex using the well-plate technique (33 µM, 25 °C, λ_{ex} = 330 nm, λ_{em} = 428 nm) of amino acids with functional groups in the side chain.

Figure 47 shows that with Ti(IV)-salophen complex **3** no changes in fluorescence intensity are detectable upon addition of different amino acids with functionality in the side chain, such as histidine methylester, serine or aspartic acid. No affinity of complex **3** towards the added amino acids is observed.

Chiral salen complexes **4** and **5**.

Chiral Fe(III) complex **4** is known to interact with catechols and was previously used as a dioxygenase model.[16,17] As this chiral salen complex is not fluorescent like its aromatic analogues, an indicator displacement assay was used to screen compound **4** for binding partners.

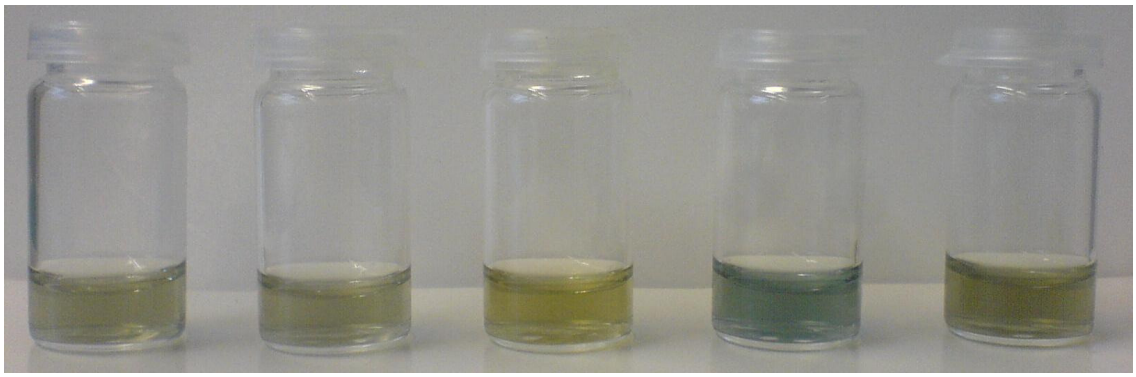

PV **+ Ni-salen** **+ Ni-salophen** **+ Fe-salen** **+ Fe-salophen**

Figure 48. Salophen (**1**, **2**) and salen (**4**, **5**) – screening for binding to pyrocatechol violet (PV, indicator)

Pyrocatechol violet **12** is a catechol-type pH-sensitive dye. It is known that the green colour at neutral pH (7.4) changes to blue when the catechol interacts as a ligand with a metal complex.[18] Figure 48 shows the PV response to the four different metal-salen complexes **1**, **2**, **4** and **5**. As can be seen by the naked-eye, only the chiral Fe(III)-salen binds to the indicator. All the other complexes do not interact with the catechol-type dye **12**.

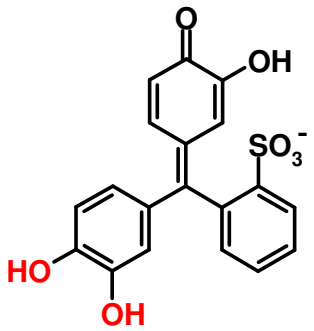

12

Figure 49. Pyrocatechol violet indicator **12**. Groups which are involved in the interaction with the complex are marked in red.

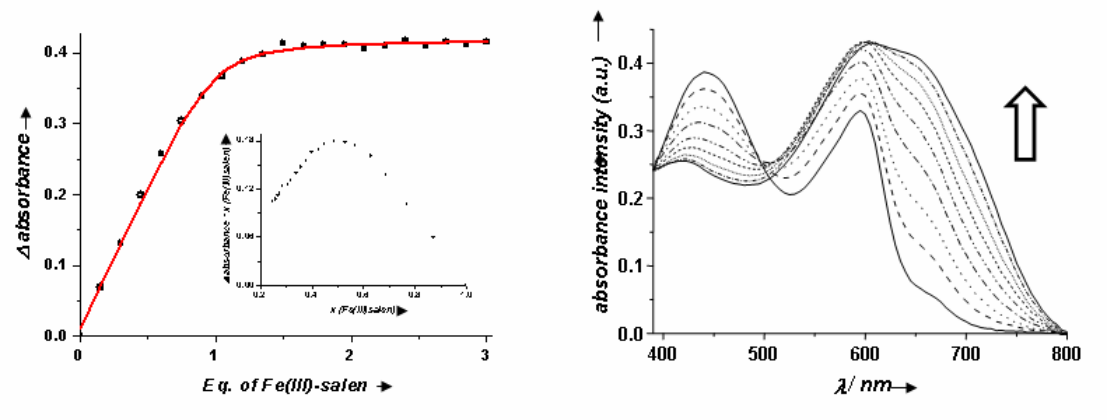

Figure 50. *Left*: UV-titration of Fe(III)-salen **4** (500 µM, HEPES, 50 mM, 25 °C, pH = 7.4) against pyrocatechol violet (50 µM, HEPES, 50 mM, 25 °C, pH = 7.4). The changes in absorbance intensity were plotted against equivalents of Fe(III)-salen. The inset shows the Job's Plot analysis. *Right*: Changes in absorbance upon addition of aliquots of Fe(III)-salen.

The Fe(III)-salen complex **4** shows a binding stoichiometry of 1:1 and a rather high binding constant (lg K = 6.0) to pyrocatechol violet. The other tested salen complexes (**1**, **2** and **5**) are not interacting with catechols. The observation that Ni(II)-complexes **1** and **2** are not binding to pyrocatechol violet is in accordance to literature reports stating that only Fe(III)-complexes binde to catechols.[16,17] However, it is surprising that the aromatic Fe(III)-salophen **1** is not binding.

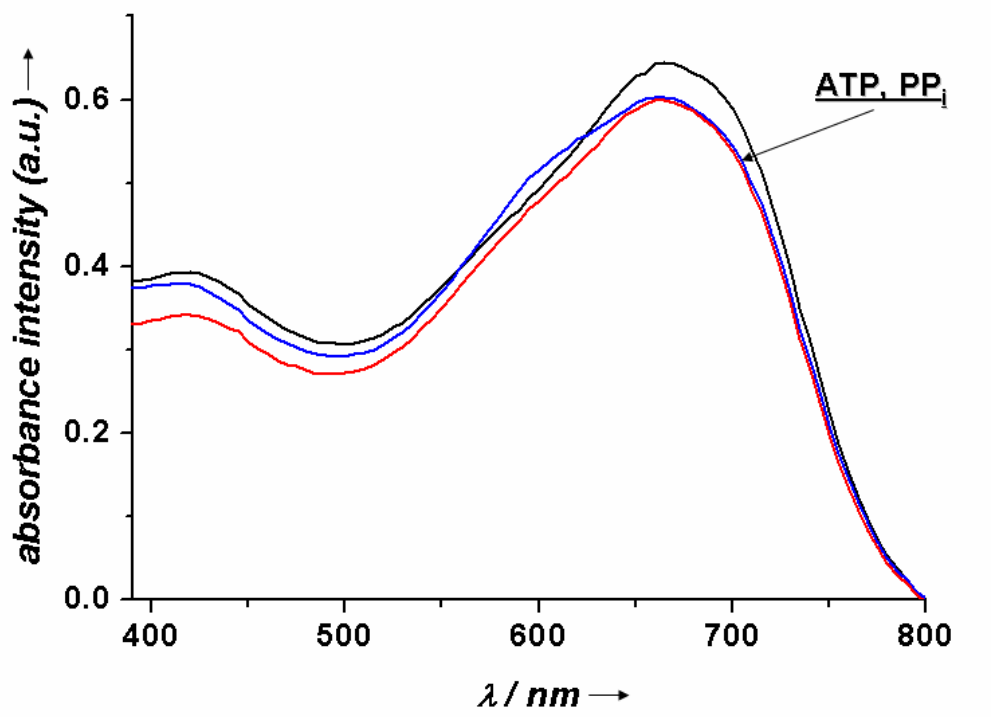

Figure 51. UV-spectra of the titration of a mixture of Fe(III)-salen (100 µM) and PV (100 µM, black line) against ATP (500 µM, 5 eq, blue line) and PP_i (500 µM, 5 eq, red line).

Displacing the indicator by either ATP or PP_i was not successful (Figure 51), which indicates a higher binding affinity for PV (lg K = 6.0) than for the tested analytes ATP and PP_i,. The binding of ATP to complex **3** is therefore weaker than observed for the interaction of Fe(III)-salophen **1** with ATP (lg K = 7.7).

The determination of binding affinities by an indicator displacement method was not possible for the chiral Ni(II)-salen complex **5**. Therefore, ITC measurements for this complex with HisOMe were performed, indicating an affinity in the lower millimolar range. This indicates that the binding affinity to HisOMe is significantly higher for the aromatic Ni(II)-salophen **2** than for its chiral counterpart **5**.

VI.3 Conclusion

A small series of aromatic water-soluble salophen derivates containing Fe(III), Ni(II) and Ti(IV) were synthesized and tested for their ability to recognize amino acids.

In the case of the Fe(III)-salophen derivative no binding could be observed for any of the tested amino acids, only for pyrophosphate (PP_i) and adenosine-triphosphate (ATP). Interaction of this complex with ATP results in a 1:1 stoichiometry and a relatively high binding constant (lg K = 7.7). ITC measurements for this system could not be performed, due to the poor solubility of the complex in HEPES buffer.

For Ni(II)-salophen derivative **2**, interactions with histidine, histidine methylester and aspartic acid could be detected in the well-plate screening. We concluded from the screening results, that for sufficient binding the donor atoms of the amino acid should have a distance of five atoms and the amino acid should act as a bidentate ligand. The C-terminal part of the amino acid is not essential for the interaction. However, fluorescence measurements showed that the binding constant and the stoichiometry seems to be concentration dependant (different binding behaviour upon changing of added equivalents), whereas the ITC measurements do not confirm these observations. Aggregate formation by π-π-interaction was excluded as the origin of the concentration dependency, because the UV spectra remain unchanged at different concentrations (Figure 46).

The salophen-derivative with Ti(IV) as the metal ion showed no affinity to any of the added analytes of this study.

Chiral salen derivatives with an aliphatic bridge between the aromatic moieties show much lower affinities to the same analytes than the non-chiral conjugated salophen-derivatives. However, the Fe(III)-salen complex binds catechols in the µM-range, which allows indicator displacement assays. ITC measurements are prohibited by the poor water solubility of the complex.

Future studies of salophen complexes should focus on extended aromatic systems, like naphthalene, as the central aryl ring. This may prevent aggregation and will shift the excitation wavelength to longer wavelengths making the compounds more suitable for biological applications. Another issue to address is increasing the water solubility, which would then allow the use of ITC measurements to determine binding interactions. Presently, the compounds solubility limits their concentration in binding assays to 50-100 µM, which is not suitable for ITC measurements.

VI.4 Experimental Part

1. Synthesis and characterization of compounds

General. Thin layer chromatography (TLC) was performed on alumina plates coated with silica gel (Merck silica gel 60 F 254, layer thickness 0.2 mm). Column chromatography was performed on silica gel (70–230 mesh) from Merck. Starting materials were purchased from either Acros or Sigma-Aldrich and used without any further purification. Solvents were purchased from Aldrich and used without further purification except for dry THF, which was prepared by distillation from potassium. Complex **1**[12], **2**[11] and water-soluble salicylic aldehyde[11] as well as chiral salen ligand **9**[19] were prepared according to literature known procedures.

Techniques. Melting points (MP) were determined with a Büchi SMP 20. IR-spectra were recorded with a Bio-Rad FTS 2000 MX FT-IR spectrometer. NMR spectra were recorded on a Bruker Avance 300 (1H: 300.1 MHz, 13C: 75.5 MHz, T = 300 K). The spectra are referenced against the NMR-solvent and chemical shifts are reported in ppm. MS-Spectra were determined on a Varian CH-5 (EI), a Finnigan MAT 95 (CI; FAB and FD) or a Finnigan MAT TSQ 7000 (ESI). UV–Vis absorption spectroscopy was performed using a Cary 50 Bio spectrophotometer and fluorescence spectra were recorded using a Varian Cary Eclipse fluorescence spectrophotometer.

Ti(IV)-salen 3.

In a round-bottom flask aldehyde **8** (1 g, 4.3 mmol) and diamine **9** (0.2 g, 2.2 mmol) were dissolved under a N_2-atmosphere in dry THF (20 mL). With stirring NaOAc (0.8 g, 9.8 mmol) and 0.3 mL TiCl4 (3 mmol) were added and the mixture was stirred at reflux for 22 h. The orange precipitate was collected by vacuum filtration and washed with THF (20 mL). The solid was washed with EtOH (3 x 10 mL), petroleum ether (3 x 10 mL) and dried in *vacuo*. The product was obtained as an orange solid (0.8 g, 1.8 mmol, 83%).

Due to its very poor solubility in organic solvents and water no NMR spectrum could be recorded.

ES-MS (H_2O/CH_3OH + 10 mM NH_4OAc): m/z (%) = 557.8 $[MH+Cl]^-$ (100) , 261.2 $[M-2H^+]^{2-}$ (29), 522.3 $[M-H^+]^-$ (11), **FT-IR** = 3364 (w), 3074 (w), 1577 (m), 1146 (m), 1002 (w), 752 (s), 718 (s), 570 (s), 446 (s); **MP** > 300 °C.

Ni(II)-salen 5.[20]

Ligand **11** (0.5 g, 1 mmol) was dissolved in H_2O (8 mL) and NaOAc (0.15 g, 1.8 mmol, 2 eq). $NiCl_2$ (0.2 g, 1 mmol, 1 eq) was added and the mixture was heated to reflux for 16 h. After this period the suspension was allowed to cool to room temperature and the precipitate was collected by centrifugation, washed two times with CH_3CH_2OH (13 mL) and tetrahydrofurane (13 mL). The product was obtained as an orange solid (0.52 g, 1 mmol, 96%).

ES-MS (H_2O/CH_3OH + 10 mM NH_4OAc): m/z (%) = 267.9 $[M-2H^+]^{2-}$ (100), 537.2 $[M-H^+]^-$ (25); **FT-IR** = 3387 (m), 2930 (w), 1581 (s), 1468 (m), 1414 (m), 1383 (w), 1179 (s), 1108 (s), 1034 (s), 932 (w), 829 (m), 746 (w), 688 (m), 614 (s), 574 (m); **MP** > 300 °C.

Fe(III)-salen 4.[19]

Ligand **11** (0.5 g, 1 mmol) was dissolved in H_2O (8 mL) and NaOAc (0.15 g, 1.8 mmol, 2 eq). $FeCl_3$ (0.3 g, 1 mmol, 1 eq) was added and the mixture was heated to reflux for 16 h. After this period the suspension was allowed to cool to room temperature, the precipitate was collected by centrifugation and washed two times with CH_3CH_2OH (13 mL) and tetrahydrofurane (13 mL). The product was obtained as a brown solid (0.55 g, 1 mmol, quant).

ES-MS (H_2O/CH_3OH + 10 mM NH_4OAc): m/z (%) = 268 $[M-2H^+]^{2-}$ (7), 534.8 $[M-H^+]^-$ (4), 284.2 $[M+O_2]^{2-}$ (25), 607.8 $[MH_2+2Cl]^{2-}$ (10), 592.0 $[MH_2+CH_3COO]^-$ (5), 296.4 $[M+CH_3COO]^{2-}$ (100); **FT-IR** = 3504 (m), 2105 (w), 1601 (s), 1422 (w), 1346 (w), 1269 (w), 1141 (s), 1013 (m), 825 (w), 790 (w), 585 (m); **MP** > 300 °C.

Isothermal titration calorimetry (ITC) and fluorescence titration:

*Ni-salophen **2** vs. HisOMe:*

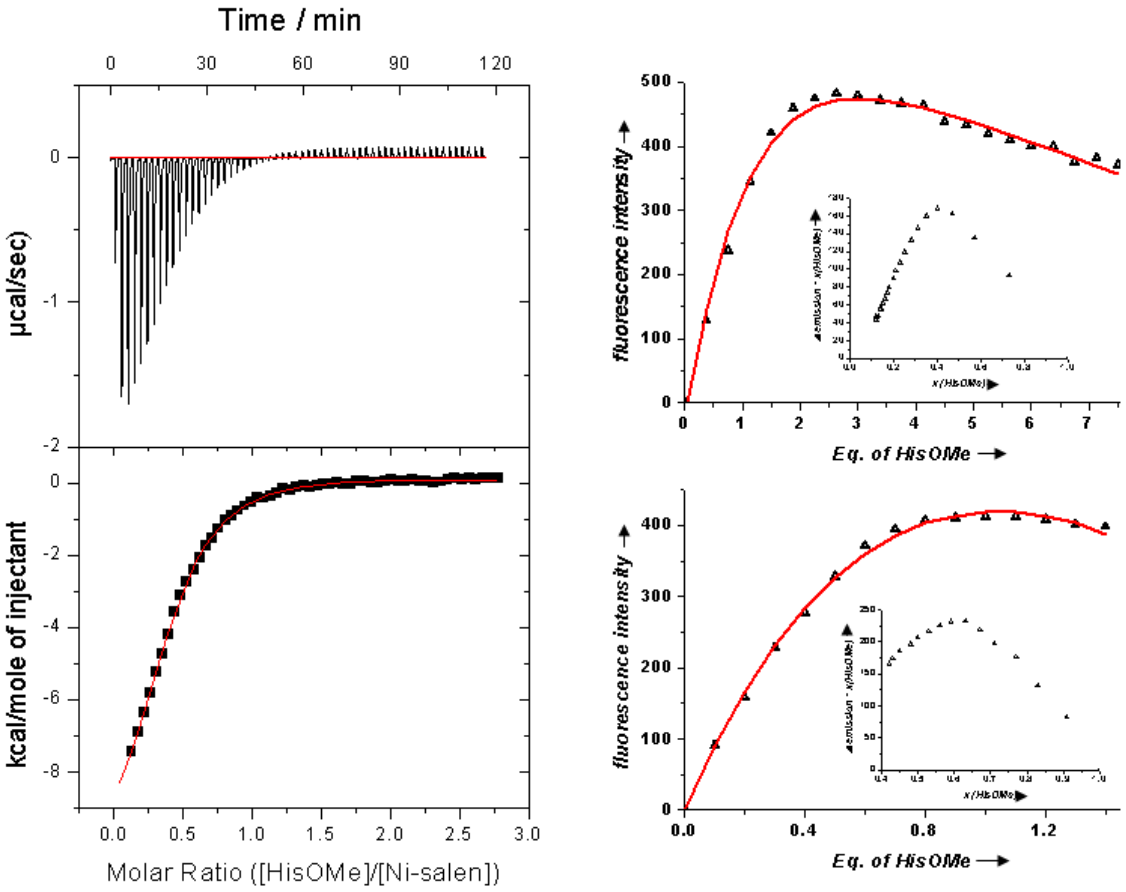

Figure 52. *Left:* Isothermal titration calorimetry (ITC) studies for the binding of complex **2** towards HisOMe. The top panel on the left shows the raw data, generated by titration of 1.43 mL of 0.1 *m*M **2** by 60 injections (5 *µ*L each) of 1.25 *m*M HisOMe. The area under each peak was integrated and plotted against the molar ratio HisOMe to **2** in the left bottom panel. The solid smooth line (left) is the best fit of the data according to the two-binding site model for the following stoichiometries (N_1 and N_2), association constants (K_{a1} and K_{a2}), and enthalpic changes (ΔH°_1 and ΔH°_2). The values of N_1, N_2, K_{a1}, K_{a2}, ΔH°_1, ΔH°_2 were determined to be 1.0 ± 0, 0.4 ± 0.006, (7.4 ± 2.4) x 10^3 M^{-1}, (1.27 ± 0.1) x 10^5 M^{-1}, 1.6 ± 0.1 kcal/mol, and -11 ± 0.03 kcal/mol, respectively. *Upper right:* fluorescence titration of Ni(II)-salophen complex **2** (1 µM) with 7 eq HisOMe 15 µM). The changes in fluorescence intensity were plotted

against equivalents of HisOMe. The inset shows the Job's Plot analysis. *Lower right:* fluorescence titration of Ni(II)-salophen **2** (1 µM) with 1.4 eq HisOMe (5 µM). The changes in fluorescence were plotted against equivalents of HisOMe. The inset shows the Job's plot analysis.

Ni-salophen **2** vs. *Aspartic acid:*

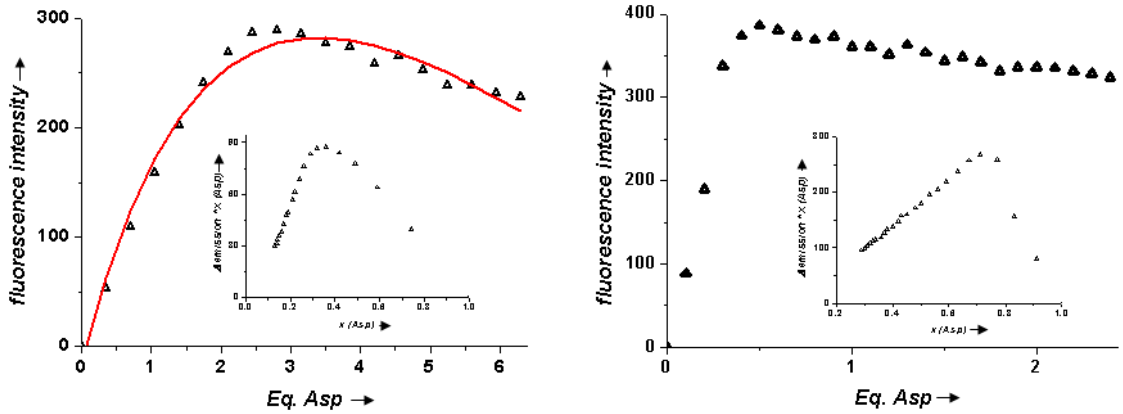

Figure 53. *Left*: fluorescence titration of Ni(II)-salophen complex **2** (1 µM) with 6 eq aspartic acid (20 µM). The changes in fluorescence intensity were plotted against equivalents of aspartic acid. The inset shows Job's Plot analysis. *Right*: fluorescence titration of Ni(II)-salophen complex **2** (1 µM) with 2.4 eq aspartic acid (5 µM). The changes in fluorescence intensity were plotted against equivalents of aspartic acid. The plot could not be fitted with HypNMR and Origin (Hill plot). The inset shows Job's Plot analysis.

Results:

Method		HisOMe lg K (sal : analyte)		aspartic acid lg K (sal : analyte)
fluorescence	1.4 eq	3.9 (1:1)	2.4 eq	no fit possible
		5.1 (2:1)		no fit possible
	7 eq	6.2 (1:1)	6 eq	5.5 (1:1)
		3.3 (1:2)		2.7 (1:2)
ITC	3 eq	3.9±1.9 (1:1)	none	none
		5.1± 0.2 (1:2)		none

sal = Ni(II)-salophen; none = not measured;

Table 6. Result of binding studies showing data from fluorescence titration and ITC.

The obtained binding stoichiometries and binding constants for Ni(II)-salophen complex **2** are not conclusive due to the change in stoichiometry upon addition of various amounts of analyte. The data obtained from ITC measurements do not match with those obtained by fluorescence. While fluorescence measurements were done at micro molar concentration (1 µM) the concentration had to be increased to 100 µM for ITC investigations in order to get reasonable results. Different binding affinities may therefore result from concentration dependant aggregates. Ni(II)-salen aggregates were already mentioned (Figure 43).

VI.5 References

(1) Stadlbauer, S.; Riechers, A.; Späth, A.; König, B. *Chem. Eur. J.* **2008**, *14*, 2536-2541.

(2) Wezenberg Sander, S.; Kleij Arjan, W. *Angew. Chem. Int. Ed.* **2008**, *47*, 2354-2364.

(3) Cozzi, P.G.*Chem. Soc. Rev.* **2004**, *33*, 410-421.

(4) Baleizao, C.; Garcia, H. *Chem. Rev.* **2006**, *106*, 3987-4043.

(5) Dzygiel, P.; Reeve, T.B.; Piarulli, U.; Krupicka, M.; Tvaroska, I.; Gennari, C. *Eur. J. Org. Chem.* **2008**, 1253-1264.

(6) Kruppa, M.; König, B. *Chem. Rev.* **2006**, *106*, 3520-3560.

(7) Larrow, J.F.; Jacobsen, E.N.; Gao, Y.; Hong, Y.; Nie, X.; Zepp, C.M *J. Org. Chem.* **1994**, *59*, 1939-1942.

(8) Hansen, T.V.; Skattebol, J. *Tetrahedron Lett.* **2005**, *46*, 3829-3830.

(9) Kleij, A.W.; Tooke, D.M.; Spek, A.L.; Reek, J.N.H. *Eur. J. Inorg. Chem.* **2005**, 4626-4634.

(10) Holbach, M.; Zheng, X.; Burd, C.; Jones Christopher, W.; Weck, M. *J. Org. Chem.* **2006**, *71*, 2903-2906.

(11) Botsivali, M.; Evans, D.F.; Missen, P.H.; Upton, M.W. *J. Chem. Soc., Dalt. Trans.* **1985**, 1147-1149.

(12) Murray, K.S. *Coord. Chem. Rev.* **1974**, *12*, 1-35.

(13) Lewis, J.; Mabbs, F.E.; Richards, A. *J. Chem. Soc. A* **1967**, 1014-1018.

(14) Wang, S.-G.; Yu, G.-Q. *Shiyou Huagong* **2002**, *31*, 183-186.

(15) Ding, Y.; Ku, Z.; Wang, L.; Hu, Y.; Zhou, Y. *Acta Cryst.* **2008**, *E64*, m173, m173/171-m173/178.

(16) Heistand, R.H.; Roe, A. L.; Que, L. *Inorg. Chem.* **1982**, *21*, 676-681.

(17) Lloret, F.; Moratal, J. Faus, J. *J. Chem. Soc., Dalt. Trans.* **1983**, 1749-1753.

(18) Han, M.S.; Kim, D.H. *Angew. Chem. Int. Ed.* **2002**, *41*, 3809-3811.

(19) Bhattacharjee, S.; Anderson, J.A. *J. Mol. Cat. A* **2006**, *249*, 103-110.

(20) Belokon, Y.N.; Moskalenko, M.A.; Petrosyan, A.A.; Maleev, V.I.; Savel'eva, T.F.; Gagieva, S.C.; Usanov, D.L.; Malfanov, I.L.; Ikonnikov, N.S.; Bulychev, A.G.; Saghiyan, A.S. *Russ. Chem. Bull.* **2004**, *53*, 1126-1129.

VII. Summary

Im ersten Kapitel wurde ein photoaktiver Inhibitor für die menschliche Carboanhydrase I synthetisiert. Dieser basiert auf eine Dithienylethen-Einheit und enthält auf der einen Seite, einen Cu(II)-Komplex, der selektiv Imidazol der Hisitidinseitenketten erkennt. Auf der anderen Seite wurde eine Sulfonamid Einheit angebracht, die ein seit Jahrzehnten benutzter Hemmstoff für Carboanhydrasen ist. Es konnte gezeigt werden, dass durch licht-induzierte Konformationsänderungen des Inhibitors, die Inhibitorwirkung, sowie die Aktivität des Enzyms verändert werden kann. Wird der Inhibitor mit sichtbaren Licht (Wellenlängen größer als 420 nm) bestrahlt, wird er in seine aktivste Form überführt. In dieser Form ist die Aktivität des Enzyms ca. eine Zehnerpotenz geringer als wäre die geschlossene Form präsent. Somit konnte gezeigt werden, dass es mit Hilfe photochromer Verbindungen biologische Reaktionen mit Licht zu beeinflussen.

Im zweiten Kapitel wurden die im ersten Kapitel hergestellten Substanzen auf ihre Selektivität innerhalb der menschlichen Carboanhydrase-Familie getestet. Diese waren die Isoformen I, II, IX, XII und XIV. Dabei wurde herausgefunden, dass für die Isoform I die symmetrisch aufgebauen Inhibitoren am wirkungsvollsten waren (zwei Sulfonamid-Einheiten und zwei Cu(II)-ida Einheiten), diese aber auch nur in ihrer offen Form. Das Molekül mit zwei Sulfonamide Einheiten war auch für die Isoform II der beste Inhibitor, hier konnte jedoch kein Unterschied zwischen der offen und der geschlossenen Form beobachtet werden. Die Isoform IX wurde nur schwach von allen Verbindungen inhibiert, wohingegen alle Verbindungen die Isoformen XII und XIV gar nicht inhibieren konnten.

Photoaktive Verbindung, die symmetrisch und flexibel mit Zn(II)-cyclen Einheiten verknüpft wurden, wurden im dritten Kapitel auf ihre Eigenschaft untersucht, die Erkennung von Phosphat-anionen reversibel zu verändern (schalten). Die Messungen wurden mit Hilfe eines Indicator Displacement Assays durchgeführt. Dabei wurde beobachet, dass der Unterschied zwischen dem offenen und geschlossenen Isomer nur ca. eine Zehnerpotenz beträgt.

Auch die Bindungsaggregate, die in Lösung gebildet werden, konnten nicht eindeutig indentifiziert werden. Schlussfolgernd kann man sagen, dass für eine solche Art der Anwendung, Moleküle benutzt werden müssen, die vollkommen starr sind und nur durch die licht-induzierten Konformationsänderungen des Schalters abhängig sind.

Im vierten Kapitel wurde eine Klasse von Diarylethenen untersucht, die in der Literatur eher wenig Bedeutung findet: Di-indolylethene. Diese enthalten statt der Thiophen-Einheiten zwei Indol-Einheiten. Durch diese Veränderung wird die geschlossene Form dieses Moleküls thermisch reversibel, was für Anwendungen ein schlechtes Charakteristikum ist. Mit Hilfe geeigneter (literaturbekannten) Veränderungen, ist die Verbindung für eine gewisse Zeit (bis zu 48 h) thermisch stabil. Es wurde beobachtet, dass in der geschlossenen Form die Stickstoffatome der Indol-Einheit basisch werden. Protoniert man diese basischen Stickstoffe durch protische Säuren (HOAc, Ameisensäure und Phosphorsäure), was abhängig von der Säurestärke ist, wird wahrscheinlich eine elektrocyklische Rückreaktion zur offenen Form katalysiert (Diese Theorie von der Arbeitsgruppe Prof. Dr. M. Schütz zur Zeit durch Berechnungen geprüft). Die offene Form zeigt keine Reaktion auf Säuren.

Im fünften Kapitel wurde untersucht, inwiefern Metall-salen Komplexe zur selektiven Erkennung von Aminosäuren, sowie von Phosphat-anionen verwendet werden kann. Dabei wurde gefunden, dass achirale Ni(II)-Komplexe selektiv terminales Histidin, sowie terminale Asparaginsäure bindet. Die Affinität zu Histidin ist dabei höher als zu Asparaginsäure. Achirale Fe-salen Komplexe binden selektiv nur Phosphat-anionen und innerhalb der getesten Verbindungen auch nur Pyrophosphat (PP_i) und ATP (lg K = 7.7). Chirale Salen Komplexe haben um ein vielfaches geringere Affinitäten als die achiralen Komlexe, wobei chirale Fe-salen Komplexe mit einer hohen Affinität Catechole binden. Alles in allem, wurde durch diese Voruntersuchungen gezeigt, dass diese Moleküle Potenzial zur Erkennung von Aminosäuren und Phosphat-anionen haben.

VIII. Abbreviations

A	anion
Asp	aspartic acid
aq	aqueous
Boc	*tert*-Butoxycarbonyl
Bu	butyl
^{t}BuOH	*tert*-butanol
c	concentration
calc	calculated
CC	column chromatography
d	days
DCM	dichloromethane
DMAP	4-(dimethylamino) pyridine
DMF	dimethylformamide
DMSO	dimethyl sulfoxide
EA	elemental analysis
EDTA	ethylenediaminetetraacetic acid disodium salt
EE	ethyl acetate
EI	electronic ionisation
eq	equivalents
ESI	electronic spray ionisation
Et	ethyl
Et_2O	diethyl ether
EtOAc	ethyl acetate
EtOH	ethanol
FAB	fast atom bombardment
fig	figure
FI	fluorescence
h	hour
Hepes	4-(2-hydroxyethyl)-piperazine-1-ethane sulfonic acid
His	histidine
HOBt	1-Hydroxybenzotriazole
HPLC	high performance liquid chromatography
HR	high resolution
IDA	iminodiacetic acid
IR	infrared spectroscopy

J	coupling constant
K	cation
LC	liquid chromatography
Lys	lysine
M	molecule
Me	methyl
MeCN	acetonitrile
MeOH	methanol
min	minutes
Mp	melting point
MS	mass spectroscopy
MW	molecular weight
NEt_3	triethyl amine
NIR	near infrared
NMR	nuclear magnetic resonance
NTA	nitrilotriacetic acid
OAc	acetate
PE	petrol ether
Ph	phenyl
Phe	phenylalanine
R_f	retention factor
r.t.	room temperature
sat	saturated
Ser	serine
S_N	nucleophilic substitution
TFA	trifluoroacetic acid
THF	tetrahydrofurane
TLC	thin layer chromatography
TMS	trimethylsilyl
TPP	tetraphenyl porphyrin
UV	ultraviolet
VIS	visible
x	mole fraction

XI. Appendix

PUBLICATIONS

- Synthesis of 6-Chloro-N,N,N',N'-tetrakis-pyridin-2-ylmethyl-[1,3,5]triazine-2,4-diamine; Daniel Vomasta, Manfred Zabel, Burkhard König, *Molbank* **2007**, *4*, M556

- Synthesis of ({8-[4,6-Bis-(bis-pyridin-2-ylmethyl-amino)-[1,3,5]triazine-2-ylamino]-octyl}-ethoxycarbonylmethyl-amino)-acetic acid ethyl ester; Daniel Vomasta, Burkhard König, *Molbank* **2007**, *4*, M557

- Regulation of Human Carbonic Anhydrase (hCAI) Activity by a Photochromic Inhibitor; Daniel Vomasta, Christina Hoegner, Neil R. Branda, Burkhard König, *Angew. Chem.* **2008**, *120*, 7756-7759; *Angew. Chem., Int.Ed.Engl.* **2008**, *47*, 7644 – 7647

- Carbonic anhydrase inhibitors: Two-prong versus mono-prong inhibitors of isoforms I, II, IX and XII exemplified by photochromic 1,2-dithienylethene derivatives, *Bioorg. Med. Chem. Lett. submitted*

Conferences and Posters

- Daniel Vomasta, Michael C. Kruppa, Burkhard König; **Molecular Recognition**; *Summer School Medicinal Chemistry, Asia Link*, in Shanghai, China, September **2005**

- Daniel Vomasta, Neil R. Branda, Burkhard König; **Light-Induced control of binding affinity**; International Conference *Central European Conference On Photochemistry* in Bad Hofgastein, Österreich, März **2006**

- Daniel Vomasta, Neil R. Branda, Burkhard König; **Control of enzyme activity by light**; *International Photochemistry Congress (ICP) 2007*, Köln, Juli **2007**

- Daniel Vomasta, Neil R. Branda, Burkhard König; **Light-induced control of enzyme acitivity**; *Frontiers in Medicinal Chemistry*, Regensburg, März **2008**

- Daniel Vomasta, Christina Hoegner, Neil R. Branda, Burkhard König; **Regulation of Human Carbonic Anhydrase (hCAI) Activity by a Photochromic Inhibitor**; *Orchem*, Weimar, September **2008**.

Curriculum Vitae

Personal Details

Name:	Daniel Vomasta
Date of birth:	22.09.1980
Place of Birth:	Regensburg

Tertiary Education

10.2005 – 03.2009	PhD in Organic Chemistry under Prof. Dr. Burkhard König at the University of Regensburg.
01.2005 – 09.2005	Diploma-Thesis in Organic Chemistry under Prof. Dr. Burkhard König at the University of Regensburg, thesis on the “coordinative Recognition of peptides containing N-terminal histidine and phosphorylated tyrosine”.
11.2000 – 12.2004	Chemistry studies at the University of Regensburg.

School Education

05.2000	Abitur (A levels), majors in Chemistry and economics.
09.1991 – 06.2000	Gymnasium (grammar school) in Neutraubling.
09.1987 – 07.1991	Volksschule (primary school) in Obertraubling.

Stay Abroad

07.2006 – 10.2006	Research at the Simon Fraser University (SFU) in Vancouver/Canada in the working group of Dr. Neil R. Branda.